ABSTRACT

BAKER, ELLEN ELIZABETH. Mechanisms of the Pulmonary Immunological Response to Nickel Nanoparticles in Allergic Airway Remodeling and Pleural Inflammation. (Under the direction of Dr. James Bonner.)

Pulmonary diseases, such as fibrosis, cancer, and mesothelioma, are a major concern for individuals and susceptible populations with pre-existing allergic lung inflammation exposed by inhalation to certain types of particles, metals, and fibers. Inhalation of newly developed engineered nanomaterials (ENMs), especially metal-based nanomaterials, have also been posed as a risk for the development of pulmonary diseases since the novel properties they possess alters their reactivity and toxicity. Exposure to nickel nanoparticles (NiNPs) has been demonstrated to cause greater toxicity in the lung than their larger particle counterparts by inducing more severe inflammation and injury. Therefore, the effects that NiNP exposures have on chronic airway remodeling and pleural fibrosis were addressed using both *in vivo* and *in vitro* rodent studies.

Asthma is a heterogeneous disease of the airways that is characterized by chronic inflammation and airway remodeling, and regulated by a complex interaction of environmental and genetic factors. While most research focuses on how environmental factors influence the development of asthma, candidate genes involved in the pathogenesis of the disease must also be studied in order to better understand the genes that regulate asthma. Therefore, the role of the T-box transcription factor TBX21 (T-bet), which is involved in maintaining T helper 1 cell differentiation in the lung, was analyzed in regards to asthma pathogenesis and NiNP exposure. The absence of T-bet causes naïve, mature T cells to differentiation into T helper 2 cells, which have been classically defined as the T helper cell subset that mediates the development of allergic airway remodeling. In mice, T-bet

deficiency causes the development of spontaneous Th2-mediated allergic lung inflammation, similar to that of human asthma. Thus, we sought to determine if T-bet-deficient (T-bet$^{-/-}$) mice are susceptible to the exacerbation of allergic airway inflammation induced by NiNPs. It was determined that NiNP exposure significantly enhanced airway fibrosis and inflammation in both wild-type (WT) and T-bet$^{-/-}$ mice. Furthermore, NiNP-induced mucous cell metaplasia, interstitial fibrosis, and CCL2 expression were further exacerbated in T-bet$^{-/-}$ mice. We observed that treatment of T-bet$^{-/-}$ mice with a monoclonal anti-CCL2 antibody significantly enhanced NiNP-induced mucous cell metaplasia. Therefore, CCL2 is a potentially important T-bet-regulated chemokine that appears to play a protective role in selectively suppressing nanoparticle-induced mucous production in the lungs during allergic inflammation. Additionally, our results suggest that the presence of T-bet protects the lung from NiNP-induced CCL2 expression, mucin production, and fibrogenesis, thereby identifying T-bet as a potentially important gene that could further regulate lung injury induced by NiNP exposure.

Based on previous studies, which have demonstrated that larger micron-sized nickel particles and MWCNTs containing residual nickel impurities induced pleural fibrosis in rodents *in vivo*, we decided to evaluate how NiNPs interact with platelet-derived growth factor (PDGF)-BB, a pro-fibrotic growth factor, to alter cellular signaling in cultured rat pleural mesothelial cells *in vitro*. Co-exposure of mesothelial cells to NiNPs and PDGF synergistically increased expression of CCL2 and CXCL10, two chemokines induced by injury that have pro-fibrotic or anti-fibrotic activity, respectively. Moreover, pharmacologic inhibition of the mitogen-activated protein kinase (MAPK) pathway determined that extracellular signal-regulated kinases (ERK)1,2 and hypoxia inducible factor (HIF)-1α were

involved in intracellular regulation of CCL2 and CXCL10 induced by NiNPs and PDGF. These data indicate that NiNPs enhance the activity of PDGF in pleural mesothelial cells by regulating chemokine production through a mechanism involving ROS generation and prolonged activation of ERK1,2. Collectively, these results distinguish potentially important susceptibility factors for regulating NiNP-induced pulmonary diseases and suggests that individuals with pre-existing lung inflammation are at a higher risk for environmental and occupational exposures to ENMs.

Mechanisms of the Pulmonary Immunological Response to Nickel Nanoparticles in Allergic Airway Remodeling and Pleural Inflammation

by
Ellen Elizabeth Baker

A dissertation submitted to the Graduate Faculty of
North Carolina State University
in partial fulfillment of the
requirements for the degree of
Doctor of Philosophy

Toxicology

Raleigh, North Carolina

2013

APPROVED BY:

_____	_____
James C. Bonner Committee Chair	Kenneth B. Adler
_____	_____
Jun Ninomiya-Tsuji	Robert C. Smart

DEDICATION

I would like to dedicate my dissertation to my parents, Frank and Eileen Glista, as well as my husband, Sean Baker, for their continual love and support. My parents taught me from an early age that it takes hard work and dedication to achieve your goals. In Sean I found a companion who shares the same passion and dedication in pursing his dreams as I do.

BIOGRAPHY

Ellen Elizabeth Baker was born on June 2, 1985 in Ravenna, Ohio. She graduated high school in 2003 and began her undergraduate studies at the University of Mount Union in Alliance, Ohio to pursue a Bachelor of Science in Biochemistry. During her senior year, when researching ideas on where to take her career, she stumbled upon a Toxicology textbook. After reading more on the subject and interviewing local Toxicologists around the area, Ellen thought that it was an interesting area of science that would be able to provide a wide range of opportunities for her in the future. However, before she continued her education, she wanted to take some time away from school to experience a different aspect of life first. Ellen finished her undergraduate degree in May of 2007 and began searching for a job.

After an unsuccessful job search in Ohio, Ellen moved to Cary, North Carolina where she almost immediately found a position in Research Triangle Park. She began working for a small pharmaceutical company and was quickly reminded as to why she wanted to continue her education. While a great experience, she felt that the company she worked for did not give her enough of a chance to learn and grow as a scientist. Ellen knew, after a few months from graduating college, that she needed to go back to school, sooner rather than later, in order to be around scientists who wanted to teach. She applied and was accepted into the PhD program in Environmental and Molecular Toxicology at North Carolina State University in 2008. It was here, under the guidance of her mentor, Dr. James C. Bonner, that Ellen found her passion for pulmonary research.

ACKNOWLEDGMENTS

I would like to begin by thanking my advisor, Dr. James C. Bonner. I was very young when I joined his lab but he had shown me nothing but patience and support as he taught me how to become the scientist I am today. In his teachings, Dr. Bonner also stressed the importance of a good work/life balance and gave valuable advice on life outside of the lab. I am so very grateful for his guidance in addition to the opportunities he gave me; I simply could not have imagined a better mentor for myself. I will greatly cherish both the scientific and life lessons that I have learned from him and will take them with me throughout the rest of my life and career.

I would also like to thank my committee members, Dr. Kenneth Adler, Dr. Jun Ninomiya-Tsuji, and Dr. Robert Smart, for their help and guidance. They have taken time away from their own busy schedules to provide mentorship and I appreciate all that they have done. Additionally, I would like to thank the members of my lab, Dr. Elizabeth Anderson Thompson, Dr. Brian Sayers, Kelly Shipkowski, Alexia Taylor, and Phillip Bost. They have generously supported me and made my time spent as a graduate student much more enjoyable. Also, I would like to thank Janet Roe, Jeanne Burr, and Jackie Broughton for making sure deadlines were met, the program ran smoothly, but most importantly, for providing comfort when it was greatly needed.

Finally, much appreciation and gratitude goes to my family: my parents, my brother, and sister, my in-laws, as well as my friends. However, I could not have made this journey alone without the support of my husband, Sean. He was always there for me with loving words of encouragement.

TABLE OF CONTENTS

LIST OF FIGURES

CHAPTER 1: The T-box Transcription Factor, TBX21 (T-bet), Inhibits Airway Mucous Cell Metaplasia and Interstitial Pneumonitis in Mice Induced by Nickel Nanoparticles

CHAPTER 2: Nickel Nanoparticles Enhance PDGF-Induced Chemokine Expression by Mesothelial Cells via Prolonged MAP Kinase Activation

GENERAL INTRODUCTION

1. Pulmonary Effects of Nanomaterial Exposure

Nanotechnology is a rapidly growing, diverse field used in many medical, consumer, and industrial applications that is estimated to become a $1 trillion market by 2015 (1, 2). Nanomaterials can be manufactured, created as a by-product, or naturally occur in the environment and are defined as having at least one nanosized dimension that is < 100nm. Engineered nanomaterials (ENMs) are manufactured structures that are manipulated at a molecular level for the fabrication of larger products (3). They have been increasingly gaining popularity because their nanosize allows them to possess novel physical and chemical properties when compared to bulk counterparts that are composed of the same material and the same shape (4). The ability to manipulate these ENMs allows for changes in physical and chemical properties including altered solubility, color, electrical conductivity, strength, and mobility thus making them even more attractive for use in a variety of products. However, each property change affects the chemical and biological reactivity of ENMs, therefore preventing the ability to predict how they will affect human health and the environment (5).

Inhalation is the major route of entry during occupational or environmental exposure to ENMs. Therefore, the toxicity of nanomaterials on the respiratory system is of great concern yet remains relatively unknown (2). Carbon nanotubes (CNTs) are a class of prototypical ENMs that are increasingly used for a variety of purposes in structural engineering, electronics, and medicine. CNTs are made using an allotrope of carbon rolled into a cylindrical shape using either one layer for single walled carbon nanotube (SWCNT)

or two or more layers for multi-walled carbon nanotubes (MWCNT) (6). The fiber-like shape and high length to width (aspect) ratio of CNTs makes them comparable to asbestos fibers and therefore raises concern that they will cause similar injuries (2, 7, 8). While there is currently no epidemiologic data that directly supports the hypothesis that CNTs cause injury to the lung in humans, a variety of studies show that CNTs cause lung inflammation and fibrosis (tissue scarring) when delivered to the lungs of mice or rats by inhalation, oropharyngeal aspiration, or instillation (2, 9). Since the production of CNTs and other nanomaterials is so recent, it could take years to see disease outcomes like fibrosis and cancer. For instance, asbestos-induced mesothelioma and lung cancer is a prime example of how a single exposure can have a long latency period (10-20 years) before it is clinically seen in humans (8). Therefore, studies have been performed in rodents *in vivo* and in cultured rodent or human cells *in vitro* to preemptively analyze the toxicity of CNTs.

Researchers have found that CNTs administered to the lungs, by many routes of exposure including but not limited to inhalation exposure, caused acute inflammation as well as chronic interstitial and pleural fibrosis (2, 10-17). It has been suggested that the development of inflammation and fibrosis in response to CNT exposure is a result of frustrated macrophage phagocytosis that occurs when long fibers, such as CNTs or asbestos, are engulfed by macrophages. Frustrated phagocytosis causes biopersistence of CNTs in the lung and increases generation of reactive oxygen species (ROS) and expression of various cytokines, chemokines, and growth factors that affect surrounding cells (18). Additionally, inhaled CNTs have been found to induce systemic effects on the immune system in mice such as splenic immunosuppression (15). Other organ systems can also be adversely affected

by pulmonary exposure to CNTs, including heart, liver, and vasculature, due to changes in gene expression involved with inflammation and oxidative stress (8, 12, 15, 19, 20). Even though CNTs are categorized together as one type of nanomaterial, there are a variety of different types (e.g., single-walled vs. multi-walled) that can be manufactured using different metal catalysts (e.g. Ni, Co, Fe). Therefore, it is important to note that any response to CNTs is dependent on the material's properties, such as length, surface configuration, and chemical composition, in addition to how they are administered to the lung (21).

Nanoparticles are considered a greater risk for lung disease compared to larger particles due to their large surface area per unit mass, which creates a greater potential for ROS generation. They are also more likely to remain suspended in the air for longer periods of time compared to larger particles, reach the distal regions of the lung once inhaled, and thereby pose a greater inhalation risk during manufacturing, production, and distribution in occupational settings (2, 22). While some larger, micron-sized particles (e.g. TiO_2) are inert and do not cause toxicity, nanosized particles composed from the same material as their bulk counterparts have been shown to exhibit inflammatory responses in the lung (1). Together, the combination of their small size and large surface area allows for increased generation of ROS, which has been linked to the development of inflammation and fibrosis. ROS production, combined with the ability of nanoparticles to reach more distal areas of the lung than larger particles, increases the potential to induce greater lung injury therefore suggesting that pulmonary toxicity increases as particle size decreases (1, 23-25).

Unlike CNTs, pulmonary health effects resulting from exposure to ambient nanoparticles in air pollution (i.e., ultrafine particulate matter, PM) has been documented and

investigated extensively in humans (22). Air pollution PM contains a wide range of particle sizes and has been extensively studied because of the adverse health effects they cause, including exacerbation of asthma and increased risk of cardiovascular disease (26). Ultrafine particles (i.e. nanoparticles) contribute more to PM-induced toxicity than the larger sized particles because they absorb greater amounts of pollutants and oxidative gases and can travel longer distances (27, 28). Upon inhalation, they can cause a greater inflammatory response in the lung, exacerbate pre-existing pulmonary diseases like asthma and chronic obstructive pulmonary disorder (COPD), as well as induce diseases such as pulmonary fibrosis, lung cancer, emphysema, and even cardiovascular disease since the respiratory system receives the entire cardiac output (2, 29). Furthermore, nanoparticles can also more readily translocate from the airspaces in the lung through type I epithelial barriers to enter the circulatory system and, like CNTs, have the ability to systemically affect other organ systems (3).

As previously mentioned, the effects produced by ENMs on the respiratory system are dependent on the physiochemical properties of each ENM, especially metal content. Exposure to airborne metal fumes or particles, in their pure form, is relatively uncommon except in some occupational settings such as welding; however that is currently changing due to the development of ENMs. CNTs and nanoparticles manufactured using a metal catalyst or composed entirely of a metal or metal oxide compound represent a greater risk when inhaled since they have the ability to produce even more ROS and are more likely to be carcinogenic (3, 4, 30, 31). MWCNT and SWCNT are mainly composed of carbon but are manufactured using metal catalysts such as iron, nickel, and cobalt, amongst others. The catalyst used

during the manufacturing process is often left behind as a residual metal and embedded within the CNT, even after washing the CNT with acid (32). While residual metals constitute a small percentage of the CNT, some researchers believe that these residue metal catalysts significantly contribute to the potential adverse health effects that might arise from CNT exposure (1, 17, 33). Additionally, occupational exposure from manufacturing these catalysts in their raw form or the manufacture of metal-based nanoparticles used for other applications does occur and exposure levels can be very high (28). Exposure to nanoparticle metals, especially transition metals such as nickel, vanadium, and chromium, are known to cause respiratory illness, cancer, and workplace-induced asthma (34, 35).

Of importance to this study are the respiratory effects induced by nickel nanoparticles (NiNPs). Micron-sized nickel is already known to cause a variety of pulmonary diseases, including fibrosis and cancer (36). Therefore, the International Agency for Research on Cancer (IARC) has classified nickel and nickel-based compounds as group 1: carcinogenic to humans. However, NiNPs are new products that have different characteristics than their bulk counterparts such as high magnetism, high surface energy and area, low melting point, and low burning point (37). While likely to have some characteristics as bulk nickel, it is important to consider the unique properties NiNPs possess in order determine their impact on human health. Two research groups have compared the effects of NiNPs with larger sized particles composed of the same material. They both found that NiNPs have a great toxicity than their larger particle counterparts by generating more free radical activity, more severe pulmonary inflammation, and increased airway collagen deposition (38, 39). Furthermore,

our lab found that MWCNTs manufactured with a NiNP catalyst induced subpleural fibrosis in one study and exacerbated ovalbumin (OVA)-induced airway fibrosis in another (17, 40).

The occupational recommended exposure limit (REL) proposed by the Occupational Safety and Health Administration (OSHA) for nickel exposures are set as 1.0 mg Ni/m^3; however this limit is based on mass of the material only and does not take into consideration nanosized Ni (39). Furthermore, in addition to workplace exposure, a 2001 the *Ninth Report on Carcinogens* from the National Toxicology Program estimated that roughly 720,000 people living near primary nickel-emitting sources (< 12.5 miles away) receive an average ambient exposure of 0.2 μg Ni/m^3 while another 160 million people are exposed to an average of 0.05μg Ni/m^3 (26). Therefore, a combined 170 million people in the United States alone are being exposed to ambient levels of nickel particulates as a component of air pollution released from industrial activity. Since nickel also causes occupational asthma, pleural effusions, and pulmonary fibrosis in the workplace it is likely that there are some adverse effects on human health from environmental exposure. The increasing usage of nanosized Ni for catalytic purposes in industry suggests that a new wave of occupational and environmental exposures is likely (40). Understanding the biological impact of NiNPs is therefore highly significant to human health and the environment.

2. Characteristics and Phenotypes of Allergic Airway Inflammation

Asthma is a chronic inflammatory disease of the airways that currently affects more than 35 million people in the United States and 330 million people worldwide (41). Additionally, work-related asthma is commonly associated with exposure to particulate matter and affects

many adults with asthma annually (42). Furthermore, the rate of incidence and severity of this disease is continually increasing despite the amount of effective therapies available (43). This especially occurs in the United State or more "Westernized" countries where asthma rates are almost 30-fold higher than developing countries (44). While there is not a single contributing factor for the rise in asthma rates, increases in particulate matter exposure (notably ultrafine particulates), immune system development, early life exposures to allergens or asthma-inducing chemicals, indoor air quality, diet, exposure to second-hand smoke, and differences in hygiene are all considered possibilities (45). However, asthma is considered a heterogeneous disease that is not only regulated by environmental exposures but rather a complex interaction of environmental and genetic factors. A review article summarizing results from over thirty genome-wide associated (GWA) studies reported that researchers have found that there are at least 100 candidate genes that could contribute to the development of various asthma phenotypes (46).

Symptoms of asthma often include shortness of breath, wheezing, coughing, and tightness of chest. Diagnosis is performed without a precise test but is based on the reoccurrence of symptoms, family history, responses to triggers such as cold air, exercise and pet dander, in addition to improvement with appropriate therapies (47). Pathogenesis of this chronic inflammatory disease is characterized by airway hyperresponsiveness (AHR) and accompanied by chronic airway remodeling that includes mucus hypersecretion, airway fibrosis, infiltration of inflammatory cells, and airway smooth muscle cell hypertrophy and hyperplasia. These structural changes cause obstruction of airflow in response to stimuli by bronchoconstriction and narrowing of the airway lumen through contraction of smooth

muscles cells surrounding the bronchioles, excess mucus production as a result of mucous cell metaplasia and/or goblet cells hyperplasia, and subepithelial collagen deposition to prevent airway dilation (48, 49). The main cause behind fatal asthma, and the greatest contributor to airflow obstruction, are mucus plugs caused by mucus hypersecretion that occludes an estimated 98% of the airways (50, 51). Classification of asthma is dependent on the severity of the disease and can be ranked as intermittent, mild persistent, moderate persistent, and severe persistent according to symptoms and lung function (52). It is further defined as allergic (extrinsic or atopic) or non-allergic (intrinsic or non-atopic) asthma according to the type of exposure that can trigger exacerbations (53).

Exacerbations of asthma from environmental and occupational exposures are caused by the inhalation of allergens, particulate matter from air pollution, ozone, cigarette smoke, bacterial and viral infections, as well as irritants. As mentioned above, these stimuli promote exaggerated episodes of inflammation and airway obstruction that could lead to increased rates of hospitalizations, morbidity, and mortality. Furthermore, exacerbating agents not only increase the incidence of acute asthma attacks, but also worsen the severity of chronic airway remodeling associated with asthma. While the final pathophysiologic outcome of exacerbations are the same, the cellular mechanisms that cause them differ depending on the exacerbating agent and are not fully understood (54, 55). In addition, mechanisms that control exacerbations also differ amongst asthma phenotypes. For example, individuals with severe asthma are more likely to suffer from more frequent exacerbations but exhibit increased neutrophilic inflammation instead of the classic eosinophilic inflammation (56). It

is therefore critical to understand the different phenotypes of asthma in order to develop better therapies to control and regulate the disease.

Many cells are involved in the pathogenesis of asthma, including immune cells such as mast cells, eosinophils, neutrophils, macrophages, B cells, T cells and structural cells like airway epithelial cells, fibroblasts, and smooth muscle cells. However, $CD4^+$ T cells have emerged as key players in mediating asthma development (57). $CD4^+$ T cells are mature, naïve T helper (Th) cells that express the CD4 surface protein and secrete specific cytokines to signal to other immune cells. The CD4 protein cluster found on these T helper cells helps the T cell receptor (TCR) to communicate to antigen-presenting cells (APC). The naïve, mature T helper cells are then presented with an antigen by APCs to help them differentiate into subsets of effector T helper cells. There are four main types of T helper cells and they are Th1, Th2, Th17, and regulatory T (Treg) cells (58). While this introduction will mainly focus on Th1, Th2, Th17, and Treg cells, it has been discovered that there are more than just these four subsets that could also be involved in the different asthma phenotypes (59).

Th1 cell differentiation typically protects the lung from viruses and bacteria by mediating a delayed type IV hypersensitivity response. However, with regard to asthma pathogenesis, Th1 cells have been implicated in both increasing and decreasing the severity of allergic inflammation (43). Both IL-12 and interferon-gamma (IFN-γ) signal through the T-box transcription factor, TBX21 (T-bet), to regulate Th1 cell differentiation. T-bet transcription is dependent on signal transducer and activator of transcription (STAT)-1 and STAT-4 activation, which further increases IFN-γ expression. The presence of T-bet, Th1 cytokines, and Th1 cells suppress the development of Th2 and Th17 differentiation (60).

However, there is much debate as to whether Th1 cells are fully protective against asthma or whether they also contribute to the progression of the disease. Th1 cells have been found in the lungs of individuals with asthma and *in vivo* studies suggest they could be present for two reasons (61). During adoptive transfer of Th1 cells into OVA exposed mice, inflammation in the lungs is increased and AHR is not reduced (62). Interestingly, a similar study showed that OVA exposed mice injected with Th1 cells had decreased AHR and eosinophilia with increased levels of IFN-γ (63).

Th2 cell-driven inflammation has been one of the main areas of focus in asthma research to better understand the development of the disease. Early studies found increased numbers of Th2 cells in the airways of asthmatics and defined them as the main Th subset involved in regulating allergic lung inflammation (64). In the presence of interleukin (IL)-4 and IL-2, naïve, mature T helper cells differentiate into effector Th2 cells through the IL-4-induced transcription factor, STAT-6 and GATA-3 (65, 66). Once differentiated, Th2 cells produce a variety of cytokines, such as IL-4, IL-5, IL-9, and IL-13 that contribute to the inflammatory response of asthma. These cytokines regulate the hallmark characteristics associated with the progression of asthma and are involved in the recruitment of eosinophils, mucus production, chronic inflammation, and smooth muscle cell contraction. IL-4 plays a role in further promoting Th2 cell differentiation while IL-5 mediates eosinophil differentiation and survival. IL-13 is the most influential of the Th2 cytokines as it is involved in AHR, goblet cell hyperplasia, and airway remodeling, that involves collagen deposition and mucus hypersecretion (67, 68). When IL-13 is overexpressed in the lungs of mice by intranasal administration, it induces an asthma-like phenotype through a STAT-6-

dependent pathway. Additionally, IL-13 acts directly through STAT-6 to regulate mucus production in airway epithelial cells by increasing the mucin gene, MUC5AC (69, 70). Studies in mouse models of asthma have demonstrated that IL-13 neutralizing antibodies administered to the lung prevent eosinophilia, AHR, airway remodeling, and mucus hypersecretion (71-73). If successful in clinical trials, anti-IL-13 would be an effective therapy for those with Th2-mediated asthma (73).

Another subset of T helper cells have emerged and been identified as Th17 cells that produce IL-17A, IL-17F, and IL-22 through the retinoic acid-related orphan receptor γt (RORγt) transcription factor. They mediate chronic airway inflammation through neutrophilic infiltration instead of eosinophilic infiltration that is associated with Th2-mediated asthma. The presence of Th17 cells in the lung has been shown to correlate with the severity of asthma and resistance to corticosteroid treatment, the most common therapy for asthma (74-76). IL-17 promotes the recruitment of macrophages and neutrophils through increased production of a variety of chemokines and growth factors, notably IL-8 and MCP-1/CCL2, respectively (77, 78). Furthermore, IL-17 has been shown to increase the mucin genes, MUC5AC and MUC5B, in human bronchial epithelial cells through an NF-κB-dependent pathway (79, 80). Transgenic mice deficient in IL-17 or its receptor, IL-17R, exhibited decreased eosinophilia, neutrophilia, and AHR in mouse models of OVA-induced allergic asthma. Monoclonal antibodies that neutralize IL-17 also protected against allergic inflammation in the same way IL-17 deficient mice did, suggesting a possible role for anti-IL-17 therapies in patients with severe asthma (73).

Regulatory T cells are thought to play a role in the suppression, not progression, of asthma and allergic inflammation through cell-to-cell interactions and suppressor cytokine signaling (81). The transcription factor FOXP3 is required for development of T cells to differentiate into Treg cells in which they then express or induce IL-10 and transforming growth factor (TGF)-β (82). It is hypothesized that there is less IL-10 expression and therefore fewer Treg cells in the lungs of asthmatics, which allows for the development of Th2 cells (83). However, very little information is known about the mechanisms that regulate Treg cell-induced suppression of allergic airway inflammation.

Many different animal models are currently being used in order to study the mechanisms that mediate the cellular and biochemical processes of chronic allergic inflammation and airway remodeling in humans. Due to the complexity and heterogeneity of asthma, animal models will never be able to fully mimic human asthma in every aspect. However, they are still useful tools to help us better understand specific pathologic features of the disease and elucidate mechanisms of pathogenesis. Mice are the most common animals used to model asthma due to the fact that they develop allergic airway inflammation and airways hyperresponsiveness to a variety of allergens. Additionally, a variety of transgenic strains are available to study the role of specific genes in the disease process (84). Currently, the most common model of allergic asthma is to induce airway remodeling in mice through a series of allergen sensitizations with adjuvant via intraperitoneal injection followed by intranasal or inhalation challenge of the same allergen. Factors such as the strain of mouse, age of the mouse, the sensitization and challenge protocol (acute vs. chronic exposure), as well as the type of allergen used can influence the extent of allergic inflammation achieved.

Ovalbumin (OVA, a protein found in a chicken egg white), house dust mite, and cockroach allergens are the most frequently used allergens to induce allergic airway inflammation in mice. They produce a Th2-mediated phenotype that includes elevated IgE levels, increased airway inflammation and hyperreactivity along with increased mucous cell hyperplasia/metaplasia, subepithelial fibrosis, and eosinophil infiltration (85). While it is important to study allergen-induced Th2-mediated allergic inflammation, it leaves knowledge gaps regarding the other types of asthma phenotypes as well as the gene environment involved in regulating asthma. Therefore, other studies have used bacteria, viruses, or chemicals (e.g., diisocyanate), usually in combination with an allergen, to understand mechanisms of sensitization or exacerbation of allergen-induced effects (54, 86, 87). In addition, transgenic mice offer a way to easily study genes that regulate the disease. Mice with a homozygous deletion of the transcription factor, Tbx21 (T-bet) were generated. Mice deficient in T-bet (T-bet$^{-/-}$) are the first, and to our knowledge the only, transgenic animal model to spontaneously display physical and morphological characteristics of human asthma without the need of allergen exposure (88, 89).

3. Transcription of T-bet for T Cell Differentiation

T-bet has been identified as a novel nuclear transcription factor for the differentiation of Th1 cells and expression of IFN-γ. It was found to belong to the T box gene family of DNA-binding domains and named as *T-b*ox expressed in *T* cells. Expression was originally thought to be only in thymocytes and Th1 cells, however it could promote IFN-γ production in CD4, CD8, and natural killer (NK) cells (90). It has been discovered that B cells, smooth

muscle cells, dendritic cells, Treg cells, and even endometrial epithelial cells also exhibit T-bet (91-94) Furthermore, it was determined that T-bet converts fully polarized Th2 cells into Th1 cells while suppressing any additional Th2 differentiation through IL-4 and IL-5 repression (90). STAT-1 was determined as the primary transcription factor to induce T-bet in response to IL-12-dependent IFN-γ expression, although some studies also showed that STAT-4 transcription could be involved (95, 96). IL-12-mediated IFN-γ is thought to stabilize T-bet so that it can bind to the IFN-γ promoter region and initiate an autocrine pathway for Th1 cell promotion (95). A variety of other mediators have also been shown to induce T-bet while others suppress its expression. For example, IL-27, Notch1, signaling lymphocyte activation molecule (SLAM), Sem4a, IL-21, glucocorticoid-induced tumor necrosis factor receptor-related protein (GITR), and lymphocyte function-associated antigen 1 (LFA-1) have been determined to induce T-bet. However, TGF-β, Vav1, peroxisome proliferator-activated receptor (PPARα) suppress T-bet. While most of these pathways are linked to the immune system, their full effects have yet to be completely understood (97).

In the absence of T-bet, naïve, mature T helper cells are able to differentiate into Th2 or Th17 cells. However, research has shown that T-bet physically interacts with the transcription factors for both subsets when it is present to allow for the development of Th1 cells (98). During Th1 versus Th2 differentiation, a competition to select the "lineage-defining transcription factor" begins when the naïve T helper cell is activated. IL-2-inducible T cell kinase (ITK) phosphorylation of T-bet mediates a tyrosine-kinase interaction with GATA-3 and prevents GATA-3 from binding to its target DNA. This allows for T-bet to indirectly suppress Th2 cytokine expression by rendering GATA-3 inactive (99). For Th17

differentiation, T-bet physically interacts with the transcription factor Runx1 to block Runx1-dependent transactivation of *Rorc*, the gene that encodes for the Th17 transcription factor, RORγt. Similar to Th2 suppression, this happens in the early stages of naïve T helper cell commitment. Therefore, T-bet is able to suppress both Th2 cell and Th17 cell differentiation at the same time while binding to the IFN-γ promoter region for Th1 cell evolution (100).

Furthermore, homozygous T-bet knockout (T-bet$^{-/-}$) mice were developed by disrupting the gene through homologous recombination in order to gain a better understanding of the function of T-bet *in vivo* (88). T-bet$^{-/-}$ mice spontaneously exhibited physiologic and pathologic characteristics that resembled the pathophysiology of a human asthmatic lung without the need of allergen sensitization and challenge. Deletion of T-bet caused the lungs of these mice to undergo chronic airway remodeling and display Th2-mediated AHR, increased infiltration of eosinophils and lymphocytes, deposition of subepithelial type III collagen, and myofibroblast transformation. Mice with a heterozygous deletion of T-bet (T-bet$^{+/-}$) had half the amount of T-bet and demonstrated a phenotype similar to T-bet$^{-/-}$ mice (89). A follow up study determined that IL-13 was the dominant Th2 cytokine that regulated the spontaneous remodeling caused by T-bet deficiency and that it could also be either dependent or independent of TGF-β signaling (101). Another study using BALB/c T-bet$^{-/-}$ mice, found that when these mice were exposed to OVA they did not overproduce Th2 cytokines but instead had an increase in the Th17 cytokine, IL-17 (102). Moreover, a third study revealed that their OVA sensitization and challenge protocol caused both Th2-mediate and Th17-mediated inflammation in BALB/c T-bet$^{-/-}$ mice (103). These results suggest that mouse strain variation and type of protocol also influences the outcome

of transgenic studies. Since T-bet$^{-/-}$ mice spontaneously exhibit a phenotype similar to human asthma, it would be beneficial to utilize them in order to better understand the mechanisms behind the exacerbation of asthma. While a few researchers have taken advantage of this mouse model to further study the effects of bacteria and viruses have on disease progression there has not been, to our knowledge, any studies that have been performed using T-bet$^{-/-}$ mice to analyze the effects of particle inhalation on exacerbation of airway remodeling (104, 105).

Interestingly, the lungs of asthmatics have been shown to have a decreased amount of T-bet expressing CD4+ T cells (89). Likewise, multiple studies have shown that T-bet polymorphisms are associated with clinical asthma phenotypes, the severity of AHR, and altered responses to inhaled corticosteroids (106-108). Researchers therefore suggest that T-bet might be a useful therapy to protect against asthma exacerbations or even reverse progression of the disease. Two studies demonstrated that transgenic mice overexpressing T-bet had reduced AHR, airway collagen deposition, and fewer eosinophil numbers due to a shift in Th2 to Th1 cell differentiation (106, 109). Additionally, when administered through intranasal delivery, a recombinant adeno-associated virus vector carrying the *T-bet* gene diminished OVA-induced airway inflammation through a restored Th1 immune response (110). Not only would T-bet$^{-/-}$ mice serve as a useful model for Th2-mediated allergic lung inflammation but it would also provide important information for the development of different therapeutic approaches for treatment of the disease.

4. Mechanisms Regulating Pleural Disease

The pleura is composed of a thin, elastic membrane that surrounds the lungs. It forms two layers, the visceral pleura and the parietal pleura by folding back onto itself. The inner, visceral pleura covers the lungs while the outer, parietal pleura lines the chest wall forming a space between them called the pleural cavity. The pleura is lined with a thin, monolayer of cells on top of a basement membrane called the mesothelial lining that is supported by the blood and lymphatic vessels, connective tissue, and fibroblasts (9, 111). The function of mesothelial cells is to secrete fluid composed of surfactant-like molecules into the pleural space in order to facilitate the movement of the lungs as well as protect them. The mesothelium also helps move particulates and cells across the pleural space and is involved in a wide variety of immune functions including the secretion of pro- and anti-inflammatory mediators (112, 113).

Injury occurs in response to an imbalance in mesothelial cell signaling in addition to their interaction with other inflammatory cells, which can result in the development of pleural effusion, mesothelioma, and pleural fibrosis (pleural plaques) (114). Pleural effusions are an abnormal accumulation of excess fluid within the pleural cavity that impairs breathing. A few causes of pleural effusions are infection, congestive heart failure, liver cirrhosis, cancer, trauma, autoimmune diseases, and pulmonary embolism (115). Mesothelioma is a rare form of malignant cancer that develops from mesothelial cells that line the pleura. The development of this cancer is commonly associated with the exposure to asbestos fibers. However, fibrous minerals, radiation, and viral infections have also been known to cause mesothelioma (116). Additionally, there are growing concerns that carbon nanotubes, due to

their asbestos-like shape and ability to reach the pleura, could also cause mesothelial cells to become malignant (2, 7, 17). Some researchers suggest that fibrotic scarring of the pleura, caused by recurring injury, increases the probability that mesothelioma will develop (117).

Pleural fibrosis is the formation of localized plaques or diffuse thickening of the pleura through the deposition of extracellular matrix components and collagen. Causes of pleural fibrosis occur from a range of diseases, infections, medications, cancer, and exposures, such as asbestos and particulate matter. Inflammation of the pleural cavity, usually as a result of pleural effusions, initiates the pathogenesis of fibrosis development while mesothelial cells determine the fate of the disease (114, 118). Mesothelial cells are the deciding factor on whether injury is resolved through normal healing or whether it progresses into fibrosis. Repair of the mesothelium is dependent on leukocyte clearance and a decrease in collagen deposition associated with fibroblast proliferation. Exaggeration or disruption of these events could therefore lead to fibrogenesis (113).

In response to injury, pleural mesothelial cells become active, begin to proliferate, and start secreting chemokines to recruit leukocytes, such as macrophages and neutrophils, to the site of inflammation. Common chemokines expressed by injured mesothelial cells include, platelet derived growth factor (PDGF), a potent mesenchymal cell chemoattractant, IL-8, a potent chemoattractant for neutrophils, monocyte chemoattractant protein-1 (CCL2), a pro-fibrotic mediator, interferon gamma-inducible protein-10 (CXCL10), a chemoattractant for T cells and NK cells, vascular endothelial growth factor (VEGF), a growth factor responsible for vascular permeability during pleura effusions, and growth-related oncogene (GRO)-α that has mitogenic activity and is a chemoattractant for neutrophils (114, 119, 120).

In fibrosis, the wound healing to repair the injured mesothelial cells is impaired. As a result, extravascular fibrin, a protein that is involved in wound healing, begins to accrue at the site of injury resulting in excessive matrix formation. Accumulation of fibrin occurs from abnormalities in coagulation or inhibition of fibrinolysis (121). In addition, subpleural fibroblasts also contribute to matrix formation by inducing collagen and fibronectin protein expression through a TGF-β1 dependent mechanism (122).

An important mediator involved in the development of fibrosis is PDGF. In response to injury, PDGF is increased by mesothelial cells and alveolar macrophages to promote the proliferation and chemotaxis of mesenchymal cells (fibroblasts, myofibroblasts, smooth muscle cells) (123). Macrophages, which are initially recruited by mesothelial cells through CCL2 signaling, are identified as the main source of PDGF expression during fibrogenesis (124, 125). In pleural fibrosis, the formation of fibrotic lesions or thickening of the mesothelium occurs through the deposition and accumulation of extracellular matrix proteins. While mesothelial cells contribute to the production of extracellular matrix protein, myofibroblasts are the cells most responsible for the increase in fibronectin, collagen, and glycosaminoglycans. Additionally, PDGF and transforming growth factor (TGF)-β signaling mediates production of the extracellular matrix proteins in these cells (114, 123, 126).

PDGF is a glycoprotein composed of two dimeric chains of either PDGF-A and/or PDGF-B to form PDGF-AA, PDGF-BB, or PDGF-AB. Additionally, there are also PDGF-C and PDGF-D isoforms, which do not form heterodimers, who contribute to the pathogenesis of fibrosis but whose functions are not well understood. There are two receptors that the PDGF family can bind to, PDGF-Rα and PDGF-Rβ. The PDGF-AA dimer has been shown

to primarily bind to PDGF-Rα while the PDGF-B isoforms, PDGF-AB and PDGF-BB, can bind to and dimerize both receptors. Levels of PDGF-Rs are also increased during fibrosis to promote PDGF signaling. PDGF then acts alone or through a TGF-β-depending mechanism to increase expression of extracellular matrix proteins (127). Interestingly, the PDGF-B isoform is considered to be a more potent chemoattractant than PDGF-A and is also the most abundant isoform expressed in macrophages and mesothelial cells (123, 128, 129). Furthermore, individuals with idiopathic pulmonary fibrosis (IPF) have been shown to have increased expression of PDGF-B (127, 130).

5. CCL2 Signaling in Allergic Airway Remodeling and Pleural Inflammation

Monocyte chemoattractant protein-1 (MCP-1/CCL2) belongs to the C-C chemokine family and exhibits chemoattractant properties for a wide range of immune cells that include monocytes, macrophages, T cells, NK cells, basophils, dendritic cells, and mast cells. Furthermore, a variety of cells such as fibroblasts, mesothelial, epithelial, smooth muscle, and endothelial cells produce CCL2 in response to injury and inflammation (131). Mediators that induce CCL2 in these cells include but are not limited to PDGF, IFN-γ, vascular endothelial growth factor (VEGF), IL-1, IL-4, and lipopolysaccharide (LPS) (132). CCL2 binds with high affinity to the CCR2 receptor to mediate its effect. CCR2 is a seven transmembrane G-protein couple receptor that has two isoforms, CCR2A and CCR2B. The two isoforms of CCR2 are expressed on different cells types that have distinctive cell signaling pathways (133). Both CCL2 and CCR2 have been found to play a role in the

pathogenesis of various inflammatory disorders. Moreover, they both are implicated in mediating the development of pulmonary diseases such as asthma and fibrosis (131, 134).

In asthmatic patients, levels of CCL2 are elevated in the bronchoalveolar lavage fluid (BALF) and bronchial epithelium in comparison with individuals who do not have allergic inflammation (135-137). It has been suggested that CCL2 plays a part in regulating airway hyperreactivity (AHR) by recruiting eosinophils and macrophages into the airway and activating basophils and mast cells (138). *In vitro*, CCL2 has been shown to increase MUC5AC and MUC5B mucin expression in normal human bronchial epithelial cells possibly to contribute to mucus hypersecretion, a characteristic of asthma pathogenesis (139). Moreover, *in vivo* research has shown that CCL2 helps drive naïve T cells to differentiate into IL-4 producing Th2 cells suggesting that increased expression of CCL2 promotes Th2-mediated allergic airway remodeling (140). Additionally, expression of CCL2 is increased in response to IL-13 in wild-type mice but prevented in IL-13 treated CCR2 knockout mice ($CCR2^{-/-}$) along with airway fibrosis and mononuclear cell infiltration (141). Another study demonstrated that allergen exposed $CCR2^{-/-}$ mice had diminished AHR while allergic wild-type mice had decreased histamine expression in response to a CCL2 neutralizing antibody (142).

While most of the research implies that an anti-CCL2 therapeutic would beneficial for the prevention of airway fibrosis in allergic airway inflammation, other studies report that blocking CCL2 signaling actually exacerbates another important aspect of the allergic Th2 phenotype. Two other studies report that $CCR2^{-/-}$ mice are more susceptible to fungal infection and allergen-induced exacerbation of Th2-mediated allergic inflammation and

demonstrate increases in mucous cell hyperplasia and subepithelial fibrosis (143, 144). It is therefore important to elucidate the exact effects and mechanisms in which CCL2 and CCR2 have on regulating specific pathological aspects of allergic airway disease for the development of better therapeutic applications.

CCL2 is also an important pro-fibrotic mediator in the progression of interstitial and pleural fibrosis. Similar to asthma, individuals with idiopathic pulmonary fibrosis also have elevated levels of CCL2 in the bronchoalveolar lavage fluid and lung tissue (145). The mechanism of increased collagen deposition comes from CCL2 stimulating TGF-β in fibroblasts to induce collagen production in an autocrine manner (131, 146). Additionally, CCL2 signaling was also studied in bleomycin-induced pulmonary fibrosis *in vivo* with $CCR2^{-/-}$ mice and with mice treated with an anti-CCL2 monoclonal antibody. It as demonstrate that CCR2 deficiency, in response to bleomycin, displays significantly less interstitial fibrosis, as did treating bleomycin-induced fibrosis with a neutralizing CCL2 antibody (147-149). While this research has provided important information regarding the development of interstitial fibrosis, not much is known about the mechanisms that regulate pleural fibrosis. Therefore, asbestos, a known inducer of pleural disease, has been studied *in vivo* and *in vitro* in order to determine if CCL2 is increased in response to exposure. Indeed, pleural lavage fluid from rats exposed to asbestos show an increase in CCL2 expression. Moreover, the same study analyzed mesothelial cells *in vitro* and determined that they were the cells at least partially involved in CCL2 expression. These findings suggest that elevated levels of the pro-fibrotic mediator, CCL2, in mesothelial cells could contribute to the

pathogenesis of pleural fibrosis seen in response to asbestos exposure (150, 151). Further analysis of the pathways that regulate pleural fibrosis needs to be determined.

RESEARCH HYPOTHESIS

The recent development of nanotechnology had led to the production of newly designed engineered nanomaterials (ENMs) that are attractive for use in industrial, biomedical, and consumer applications due to their novel physical and chemical properties. However, the unique features that ENMs possess also have the potential to alter the material's chemical and biological reactivity. Therefore, it is important to determine the effects of ENMs using rodents *in vivo* and cell cultures *in vitro* studies to predict adverse human health effects following exposure (4). Moreover, metal-based ENMs, such as nickel nanoparticles (NiNPs), represent a greater risk to human health since their bulk metal counterparts are more likely to induce fibrogenic and carcinogenic diseases (2). Previous work performed within our laboratory showed that multiwalled carbon nanotubes (MWCNT), manufactured with a NiNP catalyst, exacerbated airway fibrosis and inflammation in allergen-challenged mice (40). Therefore, it is likely that residual nickel in the MWCNTs contributed to the increase in airway remodeling previously observed. We first hypothesized that NiNP-induced lung injury and remodeling would be enhanced in T-bet-deficient mice that display spontaneous allergic lung inflammation (89). Additionally, we also previously showed that inhalation exposure of MWCNTs containing residual nickel induced subpleural fibrotic lesions and pleural inflammation (17). Larger, micron-sized nickel particles have been shown to induce occupational asthma, as well as interstitial and pleural fibrosis, mesothelioma, and lung cancer upon inhalation (36, 37, 152, 153). However, NiNPs have a great surface area per unit mass that makes them more reactive than their bulk counterparts (1). Other investigators have demonstrated that NiNPs induce more severe

pulmonary inflammation and injury by generating more free radical activity, therefore supporting the hypothesis that when a particle size decreases, pulmonary toxicity increases (2, 38, 39). Based on what is known about nickel-induced pleural fibrosis and the increased toxicity of nanoparticles, we sought to evaluate the potential cellular mechanisms that could regulate NiNP-induced injury by analyzing their effects in rat pleural mesothelial cells *in vitro*. We postulated that NiNPs would induce pleural inflammation and fibrosis by enhancing the platelet-derived growth factor (PDGF) signaling in mesothelial cells that would in turn lead to elevated levels of pro-inflammatory chemokines.

CHAPTER 1

The T-box Transcription Factor, TBX21 (T-bet), Inhibits Airway Mucous Cell Metaplasia and Interstitial Pneumonitis in Mice Induced by Nickel Nanoparticles[1]

Ellen E. Glista-Baker, Alexia J. Taylor, Brian C. Sayers, Elizabeth A. Thompson, James C. Bonner*

**Department of Environmental and Molecular Toxicology, North Carolina State University, Raleigh, North Carolina 27695 USA*

Funding: NIH Grants RC2-ES018772 and R01-ES020897. EEG and BCS are supported by NIEHS training grant T32-ES007046.

Abbreviations used: ENM, engineered nanomaterial; NiNP, nickel nanoparticle; Th cell, T helper cell; T-bet, T-box transcription factor TBX21; BALF, bronchoalveolar lavage fluid; ROS, reactive oxygen species; HIF, hypoxia-inducible factor; Ni, nickel; WT, wild-type; AB/PAS, Alcian blue/periodic acid-Schiff.

Running Head: *T-bet regulates lung remodeling by nickel nanoparticles*

Abstract

Engineered nanomaterials (ENMs), including metal nanoparticles, are increasingly being used in many applications in the electronic, engineering and biomedical fields. The human health risks that ENMs pose from environmental and occupational exposure is of growing concern, especially in susceptible populations such as asthmatics. The T-box transcription factor Tbx21 (T-bet) maintains Th1 cell development in the lung. However, loss of T-bet has been associated with the development of allergic airway inflammation and remodeling. In this study, we hypothesize that T-bet-deficient (T-bet$^{-/-}$) mice are susceptible to lung injury caused by nickel nanoparticles (NiNPs). Wild-type (WT) and T-bet$^{-/-}$ mice were exposed to NiNP (4 mg/kg) by oropharyngeal aspiration (OPA). The bronchoalveolar lavage fluid (BALF) was collected to measure differential cell counts and cytokines, IL-13 and CCL2. The left lung tissue was collected at 1 or 21 days for histopathologic analysis. Right lung mRNA was analyzed for expression of cytokines or mucins, MUC5AC and MUC5B. Quantitative morphometry on alcian-blue/periodic acid Schiff (AB/PAS)-stained lung tissue showed that NiNP exposure caused a marginal increase in mucous cell metaplasia in WT mice at 1 or 21 day post-exposure. However, a significant ($p<0.001$) increase was seen in mucous cell metaplasia in response to NiNP in T-bet$^{-/-}$ mice at 21 days as well as a significant ($p<0.05$) increase in MUC5AC and MUC5B mRNAs. Interstitial pneumonitis caused by NiNP exposure was significantly increased in T-bet$^{-/-}$ mice as determined by quantitative morphometry of trichrome-stained lung tissue. IL-13 protein levels and eosinophilic infiltration were elevated ($p<0.001$) after 1 day in the BALF while CCL2 protein levels were significantly increased at both 1 and 21 days ($p<0.001$ and $p<0.05$, respectively).

Treatment of T-bet$^{-/-}$ mice with a monoclonal anti-CCL2 antibody marginally reduced NiNP-induced interstitial pneumonitis and yet significantly enhanced NiNP-induced mucous cell metaplasia and MUC5AC mRNA levels ($p<0.05$). These findings identify T-bet as a potentially important gene for regulating lung injury induced by NiNP exposure and suggest that individuals with pre-existing allergic airway disease are at a higher risk for environmental and occupational exposures to nanomaterials.

Introduction

Asthma is a chronic inflammatory disease of the airways that currently affects more than 25 million people in the United States and 300 million people worldwide (1). It is characterized by periods of acute bronchoconstriction defined by airway hyperresponsiveness, mucus hypersecretion, and airway remodeling that involves eosinophilic inflammation, subepithelial collagen deposition, mucous cell metaplasia, and airway smooth muscle cell hypertrophy and hyperplasia (2). Exposure to allergens, viral infections, and environmental and occupational irritants, such as particulate matter, often trigger asthma exacerbations that lead to airflow obstruction through exaggerated inflammation and increased mucus production (3). Ultrafine particulate matter <100nm (i.e., nanoparticles) are of most concern in the exacerbation of asthma as they can reach more distal areas of the lung (4).

Environmental, occupational, and genetic factors are thought to act together to initiate allergen-mediated airway inflammation through T cell activation (5). Early studies found increased numbers of T helper 2 (Th2) cells in the airways of asthmatics and defined them as the key players in regulating allergic lung inflammation. In turn, Th2 cells secrete elevated levels of the cytokines IL-4, IL-5, and IL-13 through the transcription factor GATA-3 that initiates and maintains the inflammatory response (6, 7). The T-box transcription factor TBX21 (T-bet), maintains Th1 cell differentiation in the lung and regulates the production of IFN-γ while inhibiting the development of Th2 cells (8-10). Mice with a targeted deletion of T-bet (T-bet$^{-/-}$) have decreased amounts of IFN-γ and overproduce Th2 cytokines (8). The lungs of T-bet$^{-/-}$ mice display spontaneous airway remodeling, subepithelial collagen

deposition, and IL-13 mediated AHR and eosinophil infiltration similar to an asthma-like phenotype (9). Interestingly, the airways of asthmatics have been shown to have significantly less T-bet expression when compared to nonasthmatic lungs suggesting that T-bet$^{-/-}$ mice would be a useful Th2-mediated model of asthma (10).

The rapidly growing nanotechnology industry has led to the manufacture of a variety of engineered nanomaterials (ENMs), new materials that possess novel physical and chemical properties. The characteristics that define ENMs include their nano-size dimensions (any one dimension <100nm), highly uniform and conformal shape, and large surface area. These unique properties make ENMs superior in many ways to bulk material of the same elemental composition, and have increased their popularity and usage in a variety of different industrial, biomedical, and consumer applications (11). However, these unique chemical and physical properties also mean that ENMs may interact with biological systems in ways that differ from that of larger products composed of the same material (4). This, combined with the power to manipulate or functionalize ENMs to fit the application of use, prevents the ability to accurately predict the effects that ENMs will have on human health and the environment (11).

The respiratory tract is of particular interest in evaluating the effects of ENMs since inhalation is considered the primary route of entry, especially during occupational exposures (12). Inhalation of larger micron-sized nickel (Ni) particles are known to cause injury to the lungs, such as pulmonary fibrosis and lung cancer, from reactive oxygen species (ROS)

generation and hypoxia-inducible gene activation (13, 14). However, ENMs composed of metals or those that contain metal impurities from residue metal catalysts are considered more hazardous since they have the potential to produce even higher levels of ROS due to increased surface area (4). Our lab has recently demonstrated that nickel nanoparticles (NiNPs) activate and prolong mitogen-activated protein kinases (MAPK) and hypoxia-inducible genes, such as hypoxia-inducible factor (HIF)-1α, through a ROS-dependent mechanism (15). These findings were supported by previous work showing that NiNP and Ni-based nanoparticles were more toxic than micron-sized Ni particles because of their ability to activate and stabilize HIF-1α transcription (16). Moreover, there is evidence that NiNP compounds further increased pulmonary inflammation and toxicity in the lungs of rodents when directly compared to Ni particle counterparts (17-19).

We have previously reported that multi-walled carbon nanotubes manufactured with a NiNP catalyst increased airway fibrosis in mice with pre-existing allergic lung inflammation, suggesting that ENMs pose as a potential health risk for susceptible individuals with asthma (20). Therefore, we analyzed the effects of NiNPs on the exacerbation of allergic lung inflammation in T-bet$^{-/-}$ mice, a genetically modified mouse model of Th2-mediated asthma. We found that NiNPs increased mucous cell metaplasia in T-bet$^{-/-}$ mice 21 days after initial exposure but not in wild-type (WT) mice. Additionally, mediators of mucus regulation, IL-13 and CCL2, as well as eosinophil infiltration, were increased in T-bet$^{-/-}$ mice in response to NiNP. Interestingly, interstitial pneumonitis, a hallmark response of occupational nickel exposure, was enhanced in T-bet$^{-/-}$ mice. Our findings suggest that individuals with T-bet

deficiency are more susceptible to asthma exacerbations or occupational pneumonitis from NiNP exposure.

Materials & Methods

Animals

Pathogen-free adult male wild-type (WT) or T-bet$^{-/-}$ C57BL/6 mice were obtained from Taconic Farms, Inc. (Germantown, NY) at 6 to 11 weeks of age or The Jackson Laboratory (Bar Harbor, ME) at 8 weeks. Mice were housed in a temperature and humidity controlled facility and given food and water *ad libitum*. All procedures involving animal use were approved by the Institutional Animal Care and Use Committee (IACUC) at North Carolina State University.

Nickel Nanoparticles (NiNPs)

Nickel nanoparticles (NiNPs) were purchased from Sun Innovations (Fremont, CA). They are characterized as spherical in shape with a ~20nm diameter, having a specific surface area of 40-60 m^2/g, a metal purity of 99.9%, and insoluble in water. Size and shape have previously been verified by our lab by measuring digitized TEM images with Adobe Photoshop and determining pixel length of >100 NiNPs (15). Furthermore, the oxidation state of these NiNPs are oxidation state (0) zero as characterized by *Choquette, et al.* (21). Prior to exposure, NiNPs were suspended in a sterile, 0.1% pluronic F-68 (Sigma) in phosphate buffer solution and dispersed for two hours using a bath sonicator at room temperature.

Experimental Design

WT and T-bet$^{-/-}$ mice (*n*=49, Taconic Farms, Inc.) were exposed to NiNPs at 4 mg/kg or 0.1% Pluronic (Sigma Aldrich, St. Louis, MO) surfactant solution by oropharyngeal aspiration under an isoflurane anesthetic, as previously described (22). On day 1 or day 21 after initial NiNP exposure, mice were euthanized via intraperitoneal injection of Fatal Plus (Vortech Pharmaceuticals, Dearborn, MI). Lungs were lavaged with Dulbecco's phosphate-buffered saline (DPBS) and bronchoalveolar lavage fluids (BALF) were collected for ELISA and cell differentials. The middle and caudal lobes of the right lung, as well as the heart, spleen, and a section of the liver, were stored in RNAlater®, according to the manufacturer's instructions (Ambion, Austin, TX), and used for TaqMan® quantitative real-time RT-PCR analysis. The cranial lobe of the right lung was flash frozen in liquid nitrogen and stored at −80°C for collagen determination and protein evaluation. The left lung was infused with 10% neutral buffered formalin, fixed for 24 hours, transferred to 70% ethanol, and embedded in paraffin. Three cross-sectional sections of tissue were cut and processed for histopathology with a Masson's trichrome, hematoxylin & eosin (H&E), or Alcian blue/periodic acid-Schiff (AB/PAS) stain.

Monoclonal Antibody Administration

A second group of WT and T-bet$^{-/-}$ mice (*n*=20, The Jackson Laboratory) were treated with either a rat IgG2B Isotype Control antibody (MAB0061, *n*=7, R&D Systems, Minneapolis, MN) or mouse anti-CCL2 mAb (MAB479, *n*=8, R&D Systems) by intraperitoneal (i.p.) injection before and after being exposed to 0.1% pluronic solution of NiNPs as described

above. Mice received either IgG2B (25µg) or anti-CCL2 (25µg) mAb by i.p. injection on days 4, 8, 12, 16, 20, 23, 28, and 32. They were exposed to either the pluronic solution or NiNPs on day 14 and euthanized via intraperitoneal injection of Fatal Plus 21 days after NiNP exposure on day 35. Samples were collected as described in the *Experimental Design*. Mice used in the antibody study were from The Jackson Laboratory (Bar Harbor, ME).

Bronchoalveolar Lavage and Cytology

Lungs were serially lavaged three times with 0.5 mL of DPBS and combined. An aliquot from each sample was immediately used to analyze differential cell count while the remaining sample was stored at −80°C. A Thermo Scientific Cytospin® 4 Cytocentrifuge (Thermo Fisher Scientific, Waltham, MA) was used to plate cells from the BALF of each animal onto glass slides. Samples were then fixed and stained with the Diff-Quik® Stain Set (Dade Behring Inc, Newark, DE). Differential cell counts were performed on at least 500 cells per sample and represented as the mean ± SEM per exposure group.

Semi-Quantitative Morphometric Analysis

Mucous Cell Metaplasia: Airway mucin production was analyzed using a previously established protocol (23). Photomicrographs of AB/PAS stained lung sections were measured and quantified using ImageJ version 1.44o (National Institutes of Health). Cells that were positively stained for AB/PAS were identified by the deconvolution module using a threshold method and then calibrated for measurement in microns. Data was expressed as the

percentage of epithelial area positively stained for AB/PAS divided by the total epithelial area (%PAS+/Total Area).

Whole Lung Inflammation: Photomicrographs of sections of the lung stained with H&E were evaluated for inflammation based on the number of inflammatory cells (polymorphonuclear cells and alveolar macrophages) that were present and the thickness of the airway epithelium. Images were scored by three independent observers using the following scale: 1 – normal lung tissue, 2 – minimal change, 3 – mild change, 4 – moderate change, and 5 – marked change. Data was presented as the mean value ± SEM of the inflammation score of 5-7 animals for each dose group.

Airway Collagen Deposition: Thickness of collagen surrounding airway bronchioles was quantified using Adobe Photoshop CS5 (Adobe Systems, Inc., San Jose, CA) according to a previously published procedure (24). Photomicrographs of trichrome-stained sections were captured using the 10x objective on an Olympus BX41 microscope (Olympus America, Inc., Canter Valley, PA) and digitized. Airway collagen area was measured and corrected for length of basement membrane (area/perimeter ratio) using the lasso tool in Adobe Photoshop as described (25). At least three airways per animal were analyzed in a blinded, random manner and expressed as the mean ± SEM of 5-7 animals per treatment group per time point.

Interstitial Pneumonitis: Photomicrographs of sections of lung stained with trichrome were qualitatively scored based on the number and size of interstitial fibroproliferative lesions. Images of interstitial lesions were scored in a blinded manner by three independent observers using the same scale described for whole lung inflammation above. Data was presented as the mean value ± SEM of the interstitial lesion score of 5-7 animals for each dose group.

ELISA

Quantikine ELISA kits (R&D Systems) were used to assay protein levels of IL-13 or CCL2 in BALF. Samples were assayed according to kit instructions and absorbance values were measured by the Multiskan FC microplate spectrophotometer microplate reader (Thermo Fisher Scientific).

Taqman Quantitative Real-Time RT-PCR

One-step, TaqMan® quantitative real time RT-PCR (qRT-PCR) was performed to quantify gene expression of our target genes in lung tissue 1 and 21 days after NiNP exposure. Total RNA was extracted and purified from the right cranial and caudal lobes of each lung using an RNeasy™ Fibrous Tissue Mini Kit (Qiagen, Valencia, CA). RNA concentrations were determined by the Nanodrop®1000 spectrophotometer and samples were normalized to a final concentration of 25 ng/µl. qRT-PCR was performed using reagents from the SuperScript® III Platinum® One-Step qRT-PCR Kit (Invitrogen, Grand Island, NY) on the StepOne® Plus instrument (Applied Biosystems, Foster City, CA). A comparative C_T method was used to quantify target gene expression for Mucin 5AC (MUC5AC, Mm01276718_m1), Mucin 5B (MUC5B, Mm00466391_m1), CCL2/MCP-1 (Mm00441242_m1), IL-13 (Mm00434204_m1), and col1a2 (Mm00483888_m1), normalized against the endogenous control β-2 Microglobulin (B2M, Mm00437762_m1) and measured relative to the vehicle-treated control groups. Each individual sample was analyzed in duplicate while the StepOne® Plus software calculated relative quantitation values that were expressed as fold-change over controls.

Sircol Assay for Soluble Collagen

Tissue from the right cranial lobe of each mouse lung were weighed between 10-50 mg, suspended in 1 mL of DPBS, and homogenized for 60 seconds with a Tissuemiser® homogenizer (Thermo Fisher Scientific). Soluble collagen was then measured following the Sircol® Soluble Collagen Assay kit (Biocolor Ltd., Carrickfergus, UK) protocol as previously described (20). Additionally, total protein was analyzed, prior to collagen extraction, using a BCA Protein Assay kit (Thermo Fisher Scientific). Data were expressed as μg of soluble collagen per mg of total protein.

Statistics

All graphs were constructed and statistical analysis was performed using GraphPad Prism software version 5.00 (GraphPad Software, Inc., San Diego, CA). Data are the expressed as mean values ± SEM of 5-6 (Control) or 6-7 (NiNP) animals per genotype. Samples were assayed in duplicate for quantitative real-time RT-PCR, triplicate for ELISA, or as mentioned. Groups were compared with one-way ANOVA with a *post hoc* Tukey, unpaired, two-tailed Student's t-test, or two-way ANOVA with a Bonferroni test. A value of $p \leq 0.05$ was considered significant.

Results

Mucous cell metaplasia is amplified in T-bet deficient mice after NiNP exposure

Wild-type (WT) and T-bet knockout (T-bet$^{-/-}$) mice were exposed to nickel nanoparticles (NiNPs) by oropharyngeal aspiration (OPA) and lung tissue was harvested 1 day or 21 days after initial exposure. The effect of NiNPs on mucous cell metaplasia was evaluated first using semi-quantitative scoring of AB/PAS-stained lung sections as described in *Materials & Methods* (%PAS+/Total Area) to identify the relative area of airway epithelium represented by mucin-producing goblet cells. Data from these measurements showed that NiNP exposure increased mucous cell metaplasia in WT or T-bet$^{-/-}$ mice at 1 day, although this increase was not significant compared to controls or between genotypes (Fig. 1*A*). After 21 days, NiNPs caused a robust and highly significant increase in mucous cell metaplasia in T-bet$^{-/-}$ mice, while WT mice exposed to NiNPs showed only a slight increase in mucous cell metaplasia that was not statistically significant (Fig. 1*A*). Photomicrographs of AB/PAS-stained lung sections portraying representative airways at 21 days post exposure showed relatively few numbers of goblet cells in response to NiNPs in WT mice (Fig. 1*B*). However, in T-bet$^{-/-}$ mice goblet cell numbers dramatically increased after NiNP exposure and the airway epithelium displayed severe mucous cell metaplasia (Fig. 1*B*). Higher magnification of the airways revealed alveolar macrophages containing NiNPs in close proximity to goblet cells in both genotypes (Fig. 1*C*).

MUC5AC and MUC5B mRNA levels are increased in T-bet$^{-/-}$ mice in response to NiNP exposure

Since mucous cell metaplasia was increased in T-bet$^{-/-}$ mice in response to NiNPs, we measured MUC5AC and MUC5B mRNA expression levels in whole lung tissue. Levels of MUC5AC mRNA were increased in the lungs of T-bet$^{-/-}$ mice one day after NiNP exposure, albeit not to a significant extent. However, MUC5AC mRNA levels were significantly increased in T-bet$^{-/-}$ mice at 21 days after NiNP exposure compared to NiNP-treated WT mice (Fig. 2*A*). MUC5B mRNA in whole lung tissue was significantly increased at 1 day and 21 days post NiNP exposure in T-bet$^{-/-}$ mice compared to NiNP-treated WT mice (Fig. 2*B*). NiNPs did not have a significant effect on MUC5AC or MUC5B mRNA expression in WT mice at either time point. The qRT-PCR results shown here support the semi-quantitative analysis of mucous cell metaplasia in T-bet$^{-/-}$ mice exposed to NiNPs (Fig. 1).

T-bet$^{-/-}$ mice display spontaneous eosinophilia that is enhanced by NiNPs

At 1 and 21 days, eosinophils were spontaneously increased in the BALF of all T-bet$^{-/-}$ mice compared to WT mice (Fig. 3*A*). Furthermore, NiNP exposure caused an exaggerated and transient increase in eosinophils in T-bet$^{-/-}$ mice 1 day after treatment. Lymphocyte counts were also slightly higher in T-bet$^{-/-}$ mice at 1 day and significantly increased in response to NiNP exposure by 21 days (Fig. 3*B*). However, the overall number of lymphocytes remained low in both WT and T-bet$^{-/-}$ mice in comparison to other inflammatory cell types in the BALF. NiNP exposure stimulated relatively high numbers of neutrophils after 1 day in both WT and T-bet$^{-/-}$ mice. Numbers of neutrophils decreased by 21 days but still remained

significant in NiNP treated WT and T-bet$^{-/-}$ mice (Fig. 3*C*). Conversely, NiNP exposure decreased the relative number of macrophages similarly in WT and T-bet$^{-/-}$ mice (Fig. 3*D*). Representative photomicrographs images of each inflammatory cell type taken from Diff-Quik®-stained cytospins of BALF collected from WT and T-bet$^{-/-}$ mice at 21 days showed that macrophages and neutrophils contained NiNPs, whereas no NiNPs were found in lymphocytes or eosinophils (Fig. 3*E*).

Inflammation is elevated in the lungs of WT and T-bet$^{-/-}$ mice exposed to NiNPs

In addition to mucous cell metaplasia, inflammation of the lungs of WT and T-bet$^{-/-}$ mice were evaluated by semi-quantitative scoring of H&E-stained lung sections. Inflammatory scores revealed a significant increase in both genotypes following NiNP exposure at 1 and 21 days post exposure when compared to their respective controls (Fig. 4*A*). At 1 day, histopathology showed infiltration of inflammatory cells and thickening of alveolar walls and alveolar duct bifurcations (ADB) in response to NiNPs in WT and T-bet$^{-/-}$ mice (Fig. 4*B*). Additionally, these structural changes were also seen at the 21 day time point in NiNP treated mice (data not shown). Upon further evaluation, higher magnification revealed deposition of NiNPs at ADB as well as NiNPs contained within alveolar macrophages (Fig. 4*C*).

Airway fibrosis is increased similarly in WT and T-bet$^{-/-}$ mice exposed to NiNPs, yet interstitial pneumonitis is exaggerated in T-bet$^{-/-}$ mice

Airway fibrosis, another characteristic associated with the pathogenesis of allergic asthma, was measured at 21 days after NiNP exposure by performing a semi-quantitated

morphometric analysis using Adobe Photoshop (Fig. 5*A*). NiNP exposure significantly increased airway collagen deposition in both WT and T-bet$^{-/-}$ mice when compared to their respective controls (Fig. 5*A* and Fig. 5*B*). Both WT and T-bet$^{-/-}$ mice displayed interstitial lesions containing inflammatory cells and extracellular matrix components (i.e., interstitial pneumonitis) that typically surrounded NiNP agglomerates. However, the number and size of interstitial lesions, collectively termed 'interstitial lesion score', were significantly increased in T-bet$^{-/-}$ mice compared to WT after NiNP exposure at 21 days (Fig. 5*C*). The representative images from trichrome-stained lung sections shown in Fig. 5*D* depict the differences in fibrotic lesions seen between WT mice and T-bet$^{-/-}$ mice. Mice that received an OPA dose of 0.1% pluronic solution did not display any interstitial lesions and were scored as a "1". NiNP exposure did not cause a significant increase in whole lung col1a2 mRNA expression measured by Taqman® quantitative RT-PCR or whole lung soluble collagen protein measured by Sircol® Assay in T-bet$^{-/-}$ or WT mice compared to saline controls (see the online supplement Fig. 6).

NiNP-induced CCL2 mRNA and protein expression is enhanced in T-bet-deficient mice

We measured CCL2 expression since it has been implicated in mucin expression as well as lung inflammation and fibrogenesis. CCL2 mRNA expression in whole lung tissue measured by qRT-PCR was slightly increased by NiNP exposure after 1 day in WT mice. However, a significant increase in NiNP-induced CCL2 mRNA levels was observed in T-bet$^{-/-}$ mice compared to WT mice (Fig. 7*A*). By 21 days, overall CCL2 mRNA levels had decreased but were still significant in both genotypes as compared to their time-matched controls (Fig 7*A*).

CCL2 protein levels measured in BALF mirrored that of CCL2 mRNA expression at 1 day post-exposure as T-bet$^{-/-}$ mice had significantly more CCL2 protein than WT mice exposed to NiNPs (Fig. 7*B*). By 21 days, the amount of CCL2 protein dramatically increased (~10-fold) in both WT and T-bet$^{-/-}$ mice in response to NiNPs compared to the amount of protein that was expressed in the BALF at 1 day (Fig. 7*B*). Furthermore, CCL2 protein levels at 21 days were significantly enhanced in T-bet$^{-/-}$ mice compared to WT mice, suggesting that the presence of T-bet not only inhibits mucous cell metaplasia but CCL2 mRNA and protein as well. Additionally, IL-13 levels, a well-known regulator of mucous cell metaplasia and inflammation in Th2-mediated asthma, were measured in whole lung tissue and BALF for mRNA and protein expression, respectively (see online supplement Fig. 8). IL-13 mRNA was increased in response to NiNPs at 1 day post exposure in both WT and T-bet$^{-/-}$ mice (Fig. 8*A*). However, only IL-13 protein was increased in T-bet$^{-/-}$ mice after NiNP exposure at 1 day (Fig. 8*B*).

Anti-CCL2 antibody treatment enhances NiNP-induced mucous cell metaplasia in T-bet$^{-/-}$ mice, but has no significant effect on NiNP-induced interstitial pneunomitis

The role of CCL2 in mediating NiNP-induced mucous cell metaplasia and interstitial pneumonitis was analyzed by blocking CCL2 activity using a monoclonal antibody. This experiment was performed with T-bet$^{-/-}$ mice that were treated with sequential i.p. injections of either an IgG2B isotype control mAb or anti-CCL2 monoclonal neutralizing (mAb) prior to and after exposure to a single dose of NiNPs by oropharyngeal aspiration. Necropsy was performed only at 21 days after NiNP exposure. Lung sections were stained with AB/PAS to

quantified mucous cell metaplasia using the ImageJ method as previously described above. Surprisingly, T-bet$^{-/-}$ mice treated with an anti-CCL2 mAb had exaggerated NiNP-induced mucous cell metaplasia (Fig. 9*A*). Anti-CCL2 mAb treatment also increased NiNP-induced MUC5AC and MUC5B mRNA levels in T-bet$^{-/-}$ mice (Fig. 9*A* and Fig. 9*B*). Additionally, at 21 days interstitial pneumonitis was analyzed since there was a significant difference between genotypes exposed to NiNPs (Fig. 5*C* and Fig. 5*D*). Although not significant, T-bet$^{-/-}$ mice exposed to NiNPs and treated with anti-CCL2 mAb caused a slight reduction in the interstitial lesion score in compared to T-bet$^{-/-}$ mice treated with the IgG2B Isotype Control mAb (Fig. 9*D*). Conversely, soluble collagen measured by the Sircol Assay was not different between isotype and anti-CCL2 mAb treatments (Fig. 9*E*). A small group of WT mice were exposed to either a 0.1% pluronic solution (n=2) or NiNPs (n=3) without any mAb treatments in order to act as a repeat of the initial *in vivo* experiment. All data analyzed with this group was reproducible and matched the previous results (data not shown).

Discussion

Engineered nanoparticles, including metal catalysts, are increasingly being used for industrial purposes and therefore pose a risk to human health. Similar to micron-sized nickel particles, the major route of exposure for NiNPs is through inhalation exposure, which can either occur in an occupational setting or through exposure to industrial by-products released into the environment (13, 26, 27). Therefore, individuals with pre-existing allergic lung disease or individuals that have deficiencies in specific genes, which serve to suppress allergic sensitization, would presumably be at greater risk. In this study, we investigated the effect of nickel nanoparticles (NiNPs) in mice lacking the transcription factor T-bet, which spontaneously develop allergic airway inflammation (8-10). We found that T-bet$^{-/-}$ mice exposed to NiNPs had exaggerated airway mucous cell metaplasia, higher levels of mucin gene mRNAs, and increased levels of IL-13 and CCL2, two cytokines implicated in asthma. Moreover, NiNPs caused more severe interstitial pulmonary pneumonitis in T-bet$^{-/-}$ mice as compared to wild-type mice. These findings indicate that T-bet is an important regulator of NiNP-induced lung injury and exacerbation of allergic airway disease.

Asthma is a complex, heterogeneous disease of the airways that is influenced by a combination of genetic and environmental factors (28). In order to better understand the pathogenesis of the disease, *in vivo* animal models have been developed to mimic the chronic inflammation, persistent airway hyperresponsiveness, and reversible airflow obstruction associated with the development of asthma in humans (29). Currently, the most common model of allergic asthma is to induce airway remodeling in mice through allergen

sensitization and challenge. Ovalbumin, house dust mite, and cockroach allergens are used to produce a Th2-mediated phenotype that elevates IgE levels, increases airway inflammation and hyperreactivity along with mucous cell hyperplasia/metaplasia, subepithelial fibrosis, and eosinophil infiltration (30). While these studies have provided much information on the mechanisms of the disease in response to allergen exposure, there are still knowledge gaps regarding the genes that regulate the pathogenesis of asthma (28). Although there is "no single gene for asthma" it is important to determine the role that individual genes have with regard to the pathogenesis of the disease or exacerbation of disease by environmental factors such as NiNPs in order to develop effective therapeutic approaches and determine potential risk factors for exposure (31).

T-bet-deficient (T-bet$^{-/-}$) mice spontaneously exhibit physiologic and histopathologic characteristics resembling the pathophysiology seen in a human asthmatic lung without the need for allergen sensitization and challenge (9, 32). The absence of T-bet allows naïve Th cells to differentiate into Th2 cells due to the lack of IFN-γ expression that is produced by CD4^{+} cells when T-bet is present (8). While Th2 cells are not the only subset of Th cells that mediate allergic lung inflammation, they still contribute to roughly 50% of the mechanisms regulating chronic airway remodeling in the asthmatic population (5, 33). Interestingly, multiple studies have shown that T-bet polymorphisms are associated with clinical asthma phenotypes, the severity of AHR, and altered responses to inhaled corticosteroids (32, 34, 35). Given this information, it would be beneficial to utilize T-bet$^{-/-}$ mice to better understand the mechanisms behind the exacerbation of asthma. While a few researchers have taken

advantage of this mouse model to further study the effects bacteria and viruses have on disease progression (36, 37), to our knowledge no studies have been performed using T-bet$^{-/-}$ mice to analyze the effects of engineered nanoparticles on exacerbation of airway remodeling.

Mucus hypersecretion significantly contributes to airflow obstruction during asthma exacerbations that leads to increased rates of morbidity and mortality. It is the major cause behind fatal asthma by occluding roughly 98% of the airways (38, 39). For that reason, it is important to understand how mucous cell metaplasia and mucin regulation is affected in response to NiNP exposure. Mucin granules, detected in goblet cells by an AB/PAS stain, were slightly increased in the airways of T-bet$^{-/-}$ mice 1 day after initial NiNP exposure (Fig. 1). However, examination of epithelial cells by 21 days showed that NiNPs dramatically increased mucous cell metaplasia in T-bet$^{-/-}$ mice but not WT mice. Additionally, we found that mucin mRNA expression for MUC5AC and MUC5B, the two more prominent mucins in the airway, correlated with the amount of mucin protein in T-bet$^{-/-}$ mice that were exposed to NiNPs 21 days post-exposure (Fig. 2). This suggested that the presence of T-bet inhibits NiNP-induced mucous cell metaplasia, thereby reducing mucin production that could lead to airway obstruction. Interestingly, ovalbumin (OVA)-sensitized transgenic mice overexpressing T-bet had significantly reduced goblet cell hyperplasia and mucus hypersecretion that is often increased in an OVA-induce mouse model of asthma (40). Furthermore, another study developed a T cell targeted, tetracycline-inducible T-bet transgenic mouse bred on a T-bet$^{-/-}$ background and sensitized them to OVA. Once T-bet was

induced by doxycycline, goblet cell hyperplasia, as well as AHR, eosinophil infiltration, and airway collagen deposition, was diminished (32). A third study revealed that OVA sensitized mice treated with an intranasal delivery of T-bet also attenuated goblet cell hyperplasia and eosinophilic inflammation (41). While we provided new information about NiNP exacerbating mucin expression in an asthma-like phenotype, our results also support previous studies where T-bet was found to be protective in terms of reducing mucous cell metaplasia.

Exaggerated airway inflammation, in addition to mucus production, can also contribute to airflow obstruction during asthma exacerbations (3). Others have shown that micron-sized nickel, NiNPs, and their related compounds have the ability to cause pulmonary inflammation following exposure (19, 26, 42). Results from our study further support these findings as we have found that inflammation was increased in the lungs of mice exposed to NiNPs (Fig. 4). Our data showed that NiNP-induced inflammation caused infiltration of inflammatory cells as well as inflammation at airway bifurcations where NiNPs accumulated. However, there was not a qualitative difference in lung inflammation between NiNP-exposed WT and T-bet$^{-/-}$ mice as determined by pathology scoring of H&E stained lung sections. Interestingly, we did observe quantitative differences in inflammatory cell profiles from the BALFs between WT and T-bet$^{-/-}$ mice (Fig. 3). For example, control T-bet$^{-/-}$ mice had spontaneous eosinophil infiltration as well as an increased amount of lymphocytes as has been previously reported (9). In response to NiNP exposure, eosinophilic inflammation was further increased after both 1 and 21 days. Additionally, the amount of lymphocytes was also increased after 21 days after NiNP exposure. In contrast, WT mice displayed an

inflammatory response to NiNPs that was comprised primarily of neutrophils and macrophages. Although it was already known that T-bet deficiency causes lymphocytic and eosinophilic inflammation, we have shown that NiNP exposure exaggerates these responses. Moreover, we also observed that neutrophils were prominent in both genotypes in response to NiNPs. While eosinophils are typical in individuals with mild asthma, a mixed neutrophilic and eosinophilic response is indicative of a more severe asthma phenotype often associated with fatal asthma (3).

In addition to the development of chronic inflammation in the lung, inhalation exposure to metallic nickel and nickel-based particles have also been shown to induce pulmonary fibrosis (13, 26, 43-45). In an OVA-induced mouse model of allergic lung inflammation, we have previously reported that multi-walled carbon nanotubes (MWCNT), manufactured with a NiNP catalyst exacerbated pre-existing airway fibrosis (20). In the present study, we hypothesized that NiNPs would exacerbate airway fibrosis in the T-bet$^{-/-}$ mouse model of asthma. However, while our results showed that NiNPs increased airway fibrosis, we did not observe a significant difference between WT and T-bet$^{-/-}$ mice (Fig. 5). Alternatively, a significant difference in interstitial pneumonitis was observed between the two genotypes in response to NiNPs. In the parenchyma of the lungs of T-bet$^{-/-}$ mice, NiNP exposure caused larger and more abundant interstitial lesions, indicating that the presence of T-bet inhibits the progression of these interstitial foci. Previous work has shown that T-bet$^{-/-}$ mice are susceptible to bleomycin-induced pulmonary fibrosis compared to WT mice (46). We did not observe significant increases in lung collagen protein levels using the Sircol Assay (Fig. 6).

Moreover, while the interstitial lesions we defined as 'pneumonitis' contained some trichrome-positive extracellular matrix, these lesions were primarily a mix of inflammatory cells and acellular components. Therefore, these interstitial lesions were most likely not interstitial fibrosis. Also, while airway fibrosis is the type of fibrosis generally associated with asthma physiology, the development of interstitial pneumonitis from exposures such as NiNPs could further limit lung function in an already susceptible population (47).

Monocyte chemoattractant protein-1 (MCP-1/CCL2) is an inflammatory chemokine that has been found to regulate the deposition of collagen, recruitment of immune cells to sites of inflammation, and induction of mucin expression in epithelial cells (48, 49). During pulmonary fibrosis CCL2 stimulates fibroblasts to deposit collagen through a TGF-β1-dependent mechanism while during inflammation acts as a chemoattractant for a variety of immune cells including macrophages, mast cells, eosinophils, and T helper 2 cells (50, 51). Although elevated levels of CCL2 have been found in the BALF and bronchial tissue of individuals with allergic asthma, we did not see a spontaneous increase in either mRNA or protein levels in control T-bet$^{-/-}$ mice (Fig. 7) (52, 53). Additionally, two studies analyzing the effects of nickel oxide nanoparticles *in vivo* found increased amounts of CCL2 protein in the BALF of mice (42, 54). We found that NiNPs increased CCL2 mRNA and protein levels 1 day after exposure in WT mice, which was further enhanced in T-bet$^{-/-}$ mice. By 21 days, both genotypes significantly expressed CCL2 mRNA and protein. However, NiNP exposure caused an exaggerated response of CCL2 protein expression in T-bet$^{-/-}$ mice compared to WT mice.

We hypothesized that NiNP-induced expression of CCL2 protein in the BALF of T-bet$^{-/-}$ mice could be responsible for the increase in inflammatory cell infiltration, mucous cell metaplasia, and interstitial lung lesions seen in T-bet$^{-/-}$ mice exposed to NiNPs. In order to test this hypothesis, T-bet$^{-/-}$ mice were treated with either anti-CCL2 mAb or an IgG2B Isotype Control mAb before and after NiNP exposure. Neutralization of CCL2 in allergen-induced models of asthma has been shown to decrease AHR, inflammation, and macrophage infiltration (55, 56). In the present study however, we did not see a difference in NiNP-induced lung inflammation or inflammatory cell infiltration in mice treated with anti-CCL2 mAb (data not shown). Although CCL2 is neutralized, MCP-5 (CCL12) and MCP-3 (CCL7) could still act through the CCL2 receptor, CCR2, to attract macrophages and eosinophils and regulate inflammation (57, 58). CCR2$^{-/-}$ mice that have decreased amounts of CCL2 from anti-CCL2 gene therapy treatment are protective against bleomycin-induced pulmonary fibrosis (59, 60). While we did not observe significant interstitial fibrosis in T-bet$^{-/-}$ mice treated with NiNPs, we did observe interstitial pneumonitis and found that anti-CCL2 treatment caused a slight decrease in these interstitial lung lesions. The most significant finding was that the anti-CCL2 neutralizing antibody delivered to T-bet$^{-/-}$ mice resulted in enhanced NiNP-induced mucous cell metaplasia as determined by quantitative morphometry of AB/PAS-positive stained epithelial cells (Fig. 9). In addition, the anti-CCL2 neutralizing mAb enhanced NiNP-induced MUC5AC and MUC5B mRNA expression in T-bet$^{-/-}$ mice. These findings are in agreement with previous studies which demonstrated that CCR2$^{-/-}$ mice have exacerbated Th2-mediated allergic airway responses to either OVA or *Asperigillus* fungal infection and demonstrate enhanced goblet cell hyperplasia (61, 62). Therefore, CCL2

signaling appears to be an important protective mechanism in suppressing mucous cell metaplasia to a variety of inhaled agents, including allergens and nanoparticles.

While nickel is already a known allergen and carcinogen, it is still important to analyze their effects at the nanoscale. Currently, occupational exposure limits are based on mass only and do not take into account particle size (19). However, ENMs, such as NiNPs, have a higher surface reactivity and are more likely to reach distal areas of the lung (4). Our results support the hypothesis that NiNPs induce lung injury, such as mucous cell metaplasia, inflammation, and interstitial fibrosis, in a susceptible population with pre-existing allergic lung inflammation. Additionally, we found that the transcription factor T-bet is critical in protecting the lung from these injuries. In conclusion, results from our study suggest that asthmatic individuals deficient in T-bet could be at a great risk of exacerbation when exposed to ENMs such as NiNPs.

Acknowledgements

This work was funded by NIH Grants RC2-ES018772-01 and R01-ES020897-01. EEGB and BCS are supported by NIEHS training grant T32-ES007046-31.

References

1. Centers for Disease Control and Prevention (CDC). 2011. Vital signs: asthma prevalence, disease characteristics, and self-management education: United States, 2001--2009. *MMWR Morb. Mortal. Wkly. Rep.* 60: 547–552.

2. Murphy, D. M., and P. M. O'Byrne. 2010. Recent advances in the pathophysiology of asthma. *Chest* 137: 1417–1426.

3. Wark, P. A. B., and P. G. Gibson. 2006. Asthma exacerbations . 3: Pathogenesis. *Thorax* 61: 909–915.

4. Nel, A., T. Xia, L. Mädler, and N. Li. 2006. Toxic potential of materials at the nanolevel. *Science* 311: 622–627.

5. Lloyd, C. M., and E. M. Hessel. 2010. Functions of T cells in asthma: more than just T(H)2 cells. *Nat Rev Immunol* 10: 838–848.

6. Robinson, D. S., Q. Hamid, S. Ying, A. Tsicopoulos, J. Barkans, A. M. Bentley, C. Corrigan, S. R. Durham, and A. B. Kay. 1992. Predominant TH2-like bronchoalveolar T-lymphocyte population in atopic asthma. *N. Engl. J. Med.* 326: 298–304.

7. Zheng, W., and R. A. Flavell. 1997. The transcription factor GATA-3 is necessary and sufficient for Th2 cytokine gene expression in CD4 T cells. *Cell* 89: 587–596.

8. Szabo, S. J., B. M. Sullivan, C. Stemmann, A. R. Satoskar, B. P. Sleckman, and L. H. Glimcher. 2002. Distinct effects of T-bet in TH1 lineage commitment and IFN-gamma production in CD4 and CD8 T cells. *Science* 295: 338–342.

9. Finotto, S., M. F. Neurath, J. N. Glickman, S. Qin, H. A. Lehr, F. H. Y. Green, K. Ackerman, K. Haley, P. R. Galle, S. J. Szabo, J. M. Drazen, G. T. De Sanctis, and L. H. Glimcher. 2002. Development of spontaneous airway changes consistent with human asthma in mice lacking T-bet. *Science* 295: 336–338.

10. Finotto, S., M. Hausding, A. Doganci, J. H. Maxeiner, H. A. Lehr, C. Luft, P. R. Galle, and L. H. Glimcher. 2005. Asthmatic changes in mice lacking T-bet are mediated by IL-13. *Int. Immunol.* 17: 993–1007.

11. Bonner, J. C. 2010. Nanoparticles as a Potential Cause of Pleural and Interstitial Lung Disease. *Proceedings of the American Thoracic Society* 7: 138–141.

12. Card, J. W., D. C. Zeldin, J. C. Bonner, and E. R. Nestmann. 2008. Pulmonary applications and toxicity of engineered nanoparticles. *AJP: Lung Cellular and Molecular*

Physiology 295: L400–L411.

13. Kasprzak, K., F. Sunderman, and K. Salnikow. 2003. Nickel carcinogenesis. *Mutation Research* 533: 67–97.

14. Salnikow, K., W. Su, M. V. Blagosklonny, and M. Costa. 2000. Carcinogenic metals induce hypoxia-inducible factor-stimulated transcription by reactive oxygen species-independent mechanism. *Cancer Research* 60: 3375–3378.

15. Glista-Baker, E. E., A. J. Taylor, B. C. Sayers, E. A. Thompson, and J. C. Bonner. 2012. Nickel Nanoparticles Enhance Platelet-Derived Growth Factor-Induced Chemokine Expression by Mesothelial Cells via Prolonged Mitogen-Activated Protein Kinase Activation. *American Journal of Respiratory Cell and Molecular Biology* 47: 552–561.

16. Pietruska, J. R., X. Liu, A. Smith, K. McNeil, P. Weston, A. Zhitkovich, R. Hurt, and A. B. Kane. 2011. Bioavailability, intracellular mobilization of nickel, and HIF-1α activation in human lung epithelial cells exposed to metallic nickel and nickel oxide nanoparticles. *Toxicological Sciences* 124: 138–148.

17. Ogami, A., Y. Morimoto, T. Myojo, T. Oyabu, M. Murakami, M. Todoroki, K. Nishi, C. Kadoya, M. Yamamoto, and I. Tanaka. 2009. Pathological features of different sizes of nickel oxide following intratracheal instillation in rats. *Inhalation Toxicology* 21: 812–818.

18. Zhang, Q., Y. Kusaka, K. Sato, K. Nakakuki, N. Kohyama, and K. Donaldson. 1998. Differences in the extent of inflammation caused by intratracheal exposure to three ultrafine metals: role of free radicals. *J. Toxicol. Environ. Health Part A* 53: 423–438.

19. Zhang, Q., Y. Kusaka, X. Zhu, K. Sato, Y. Mo, T. Kluz, and K. Donaldson. 2003. Comparative toxicity of standard nickel and ultrafine nickel in lung after intratracheal instillation. *J Occup Health* 45: 23–30.

20. Ryman-Rasmussen, J. P., E. W. Tewksbury, O. R. Moss, M. F. Cesta, B. A. Wong, and J. C. Bonner. 2008. Inhaled Multiwalled Carbon Nanotubes Potentiate Airway Fibrosis in Murine Allergic Asthma. *American Journal of Respiratory Cell and Molecular Biology* 40: 349–358.

21. Choquette, K. A., D. V. Sadasivam, and R. A. Flowers II. 2011. Catalytic Ni(II) in Reactions of SmI 2: Sm(II)- or Ni(0)-Based Chemistry? *J. Am. Chem. Soc.* 133: 10655–10661.

22. Lakatos, H. F., H. A. Burgess, T. H. Thatcher, M. R. Redonnet, E. Hernady, J. P. Williams, and P. J. Sime. 2006. Oropharyngeal aspiration of a silica suspension produces a superior model of silicosis in the mouse when compared to intratracheal instillation. *Exp.*

Lung Res. 32: 181–199.

23. Ledford, J. G., H. Goto, E. N. Potts, S. Degan, H. W. Chu, D. R. Voelker, M. E. Sunday, G. J. Cianciolo, W. M. Foster, M. Kraft, and J. R. Wright. 2009. SP-A preserves airway homeostasis during Mycoplasma pneumoniae infection in mice. *The Journal of Immunology* 182: 7818–7827.

24. Brass, D. M., J. D. Savov, S. H. Gavett, N. Haykal-Coates, and D. A. Schwartz. 2003. Subchronic endotoxin inhalation causes persistent airway disease. *Am. J. Physiol. Lung Cell Mol. Physiol.* 285: L755–61.

25. Sayers, B. C., A. J. Taylor, E. E. Glista-Baker, J. K. Shipley-Phillips, R. T. Dackor, M. L. Edin, F. B. Lih, K. B. Tomer, D. C. Zeldin, R. Langenbach, and J. C. Bonner. 2013. Role of COX-2 in Exacerbation of Allergen-Induced Airway Remodeling by Multi-Walled Carbon Nanotubes. *American Journal of Respiratory Cell and Molecular Biology*.

26. Magaye, R., and J. Zhao. 2012. Recent progress in studies of metallic nickel and nickel-based nanoparticles' genotoxicity and carcinogenicity. *Environ. Toxicol. Pharmacol.*

27. Phillips, J. I., F. Y. Green, J. C. A. Davies, and J. Murray. Pulmonary and systemic toxicity following exposure to nickel nanoparticles. *Am. J. Ind. Med.* n/a–n/a.

28. Mukherjee, A. B., and Z. Zhang. 2011. Allergic asthma: influence of genetic and environmental factors. *Journal of Biological Chemistry* 286: 32883–32889.

29. Bates, J. H. T., M. Rincon, and C. G. Irvin. 2009. Animal models of asthma. *AJP: Lung Cellular and Molecular Physiology* 297: L401–10.

30. Nials, A. T., and S. Uddin. 2008. Mouse models of allergic asthma: acute and chronic allergen challenge. *Disease Models and Mechanisms* 1: 213–220.

31. Martinez, F. D. 2007. Genes, environments, development and asthma: a reappraisal. *Eur. Respir. J.* 29: 179–184.

32. Park, J. W., H. J. Min, J. H. Sohn, J. Y. Kim, J. H. Hong, K. S. Sigrist, L. H. Glimcher, and E.-S. Hwang. 2009. Restoration of T-box–containing protein expressed in T cells protects against allergen-induced asthma. *J. Allergy Clin. Immunol.* 123: 479–485.e6.

33. Woodruff, P. G., B. Modrek, D. F. Choy, G. Jia, A. R. Abbas, A. Ellwanger, L. L. Koth, J. R. Arron, and J. V. Fahy. 2009. T-helper type 2-driven inflammation defines major subphenotypes of asthma. *Am. J. Respir. Crit. Care Med.* 180: 388–395.

34. Raby, B. A., E.-S. Hwang, K. Van Steen, K. Tantisira, S. Peng, A. Litonjua, R. Lazarus,

C. Giallourakis, J. D. Rioux, D. Sparrow, E. K. Silverman, L. H. Glimcher, and S. T. Weiss. 2006. T-bet polymorphisms are associated with asthma and airway hyperresponsiveness. *Am. J. Respir. Crit. Care Med.* 173: 64–70.

35. Tantisira, K. G., E.-S. Hwang, B. A. Raby, E. S. Silverman, S. L. Lake, B. G. Richter, S. L. Peng, J. M. Drazen, L. H. Glimcher, and S. T. Weiss. 2004. TBX21: a functional variant predicts improvement in asthma with the use of inhaled corticosteroids. *Proc. Natl. Acad. Sci. U.S.A.* 101: 18099–18104.

36. Sullivan, B. M., O. Jobe, V. Lazarevic, K. Vasquez, R. Bronson, L. H. Glimcher, and I. Kramnik. 2005. Increased susceptibility of mice lacking T-bet to infection with Mycobacterium tuberculosis correlates with increased IL-10 and decreased IFN-gamma production. *J. Immunol.* 175: 4593–4602.

37. Bakshi, C. S., M. Malik, P. M. Carrico, and T. J. Sellati. 2006. T-bet deficiency facilitates airway colonization by Mycoplasma pulmonis in a murine model of asthma. *J. Immunol.* 177: 1786–1795.

38. Evans, C. M., K. Kim, M. J. Tuvim, and B. F. Dickey. 2009. Mucus hypersecretion in asthma: causes and effects. *Curr Opin Pulm Med* 15: 4–11.

39. Kuyper, L. M., P. D. Paré, J. C. Hogg, R. K. Lambert, D. Ionescu, R. Woods, and T. R. Bai. 2003. Characterization of airway plugging in fatal asthma. *Am. J. Med.* 115: 6–11.

40. Kiwamoto, T., Y. Ishii, Y. Morishima, K. Yoh, A. Maeda, K. Ishizaki, T. Iizuka, A. E. Hegab, Y. Matsuno, S. Homma, A. Nomura, T. Sakamoto, S. Takahashi, and K. Sekizawa. 2006. Transcription factors T-bet and GATA-3 regulate development of airway remodeling. *Am. J. Respir. Crit. Care Med.* 174: 142–151.

41. Wang, S. Y., M. Yang, X. P. Xu, G. F. Qiu, J. Ma, S. J. Wang, X. X. Huang, and H. X. Xu. 2008. Intranasal delivery of T-bet modulates the profile of helper T cell immune responses in experimental asthma. *J Investig Allergol Clin Immunol* 18: 357–365.

42. Gillespie, P. A., G. S. Kang, A. Elder, R. Gelein, L. Chen, A. L. Moreira, J. Koberstein, K.-M. Tchou-Wong, T. Gordon, and L. C. Chen. 2010. Pulmonary response after exposure to inhaled nickel hydroxide nanoparticles: short and long-term studies in mice. *Nanotoxicology* 4: 106–119.

43. Oller, A. R. 2002. Respiratory carcinogenicity assessment of soluble nickel compounds. *Environ Health Perspect* 110 Suppl 5: 841–844.

44. Zhao, J., X. Shi, V. Castranova, and M. Ding. 2009. Occupational toxicology of nickel and nickel compounds. *J. Environ. Pathol. Toxicol. Oncol.* 28: 177–208.

45. Denkhaus, E., and K. Salnikow. 2002. Nickel essentiality, toxicity, and carcinogenicity. *Crit. Rev. Oncol. Hematol.* 42: 35–56.

46. Xu, J., A. L. Mora, J. LaVoy, K. L. Brigham, and M. Rojas. 2006. Increased bleomycin-induced lung injury in mice deficient in the transcription factor T-bet. *Am. J. Physiol. Lung Cell Mol. Physiol.* 291: L658–67.

47. Bonner, J. C. 2010. Mesenchymal cell survival in airway and interstitial pulmonary fibrosis. *Fibrogenesis Tissue Repair* 3: 15.

48. Gordon, J. R. 2000. Monocyte chemoattractant peptide-1 expression during cutaneous allergic reactions in mice is mast cell dependent and largely mediates the monocyte recruitment response. *J. Allergy Clin. Immunol.* 106: 110–116.

49. Monzon, M. E., R. M. Forteza, and S. M. Casalino-Matsuda. 2011. MCP-1/CCR2B-dependent loop upregulates MUC5AC and MUC5B in human airway epithelium. *AJP: Lung Cellular and Molecular Physiology* 300: L204–15.

50. Gharaee-Kermani, M., E. M. Denholm, and S. H. Phan. 1996. Costimulation of fibroblast collagen and transforming growth factor beta1 gene expression by monocyte chemoattractant protein-1 via specific receptors. *J. Biol. Chem.* 271: 17779–17784.

51. Romagnani, S. 2002. Cytokines and chemoattractants in allergic inflammation. *Mol. Immunol.* 38: 881–885.

52. Sousa, A. R., S. J. Lane, J. A. Nakhosteen, T. Yoshimura, T. H. Lee, and R. N. Poston. 1994. Increased expression of the monocyte chemoattractant protein-1 in bronchial tissue from asthmatic subjects. *American Journal of Respiratory Cell and Molecular Biology* 10: 142–147.

53. Alam, R., J. York, M. Boyars, S. Stafford, J. A. Grant, J. Lee, P. Forsythe, T. Sim, and N. Ida. 1996. Increased MCP-1, RANTES, and MIP-1alpha in bronchoalveolar lavage fluid of allergic asthmatic patients. *Am. J. Respir. Crit. Care Med.* 153: 1398–1404.

54. Cho, W.-S., R. Duffin, M. Bradley, I. L. Megson, W. Macnee, S. E. M. Howie, and K. Donaldson. 2012. NiO and Co3O4 nanoparticles induce lung DTH-like responses and alveolar lipoproteinosis. *European Respiratory Journal* 39: 546–557.

55. Chensue, S. W., K. S. Warmington, J. H. Ruth, P. S. Sanghi, P. Lincoln, and S. L. Kunkel. 1996. Role of monocyte chemoattractant protein-1 (MCP-1) in Th1 (mycobacterial) and Th2 (schistosomal) antigen-induced granuloma formation: relationship to local inflammation, Th cell expression, and IL-12 production. *J. Immunol.* 157: 4602–4608.

56. Gonzalo, J.-A., C. M. Lloyd, D. Wen, J. P. Albar, T. N. C. Wells, A. Proudfoot, C. Martinez-A, M. Dorf, T. Bjerke, A. J. Coyle, and J.-C. Gutierrez-Ramos. 1998. The coordinated action of CC chemokines in the lung orchestrates allergic inflammation and airway hyperresponsiveness. *J. Exp. Med.* 188: 157–167.

57. Sarafi, M. N., E. A. Garcia-Zepeda, J. A. MacLean, I. F. Charo, and A. D. Luster. 1997. Murine monocyte chemoattractant protein (MCP)-5: a novel CC chemokine that is a structural and functional homologue of human MCP-1. *J. Exp. Med.* 185: 99–109.

58. Koth, L. L., M. W. Rodriguez, X. L. Bernstein, S. Chan, X. Huang, I. F. Charo, B. J. Rollins, and D. J. Erle. 2004. Aspergillus antigen induces robust Th2 cytokine production, inflammation, airway hyperreactivity and fibrosis in the absence of MCP-1 or CCR2. *Respir Res* 5: 12.

59. Moore, B. B., R. Paine, P. J. Christensen, T. A. Moore, S. Sitterding, R. Ngan, C. A. Wilke, W. A. Kuziel, and G. B. Toews. 2001. Protection from pulmonary fibrosis in the absence of CCR2 signaling. *J. Immunol.* 167: 4368–4377.

60. Inoshima, I., K. Kuwano, N. Hamada, N. Hagimoto, M. Yoshimi, T. Maeyama, A. Takeshita, S. Kitamoto, K. Egashira, and N. Hara. 2004. Anti-monocyte chemoattractant protein-1 gene therapy attenuates pulmonary fibrosis in mice. *Am. J. Physiol. Lung Cell Mol. Physiol.* 286: L1038–44.

61. Kim, Y., Sung Ss, W. A. Kuziel, S. Feldman, S. M. Fu, and C. E. Rose. 2001. Enhanced airway Th2 response after allergen challenge in mice deficient in CC chemokine receptor-2 (CCR2). *J. Immunol.* 166: 5183–5192.

62. Blease, K., B. Mehrad, T. J. Standiford, N. W. Lukacs, J. Gosling, L. Boring, I. F. Charo, S. L. Kunkel, and C. M. Hogaboam. 2000. Enhanced pulmonary allergic responses to Aspergillus in CCR2−/− mice. *J. Immunol.* 165: 2603–2611.

Figure Legends

FIGURE 1. Mucous cell metaplasia in response to NiNP exposure in WT and T-bet$^{-/-}$ mice. *A*, Quantification of mucus producing cells at 1 or 21 days post-exposure determined using ImageJ analysis software (NIH). Data presented as the percentage of AB/PAS-positive stained area per total area. ***$p < 0.001$ compared to the control group of the same genotype or as indicated. All data represent mean values ± SEM of at least three measurements per lung of 5-7 mice per exposure group. *B*, Low magnification (10X) of AB/PAS stained lung tissue sections (open arrows) at 21 days after WT and T-bet$^{-/-}$ mice were exposed to a 0.1% pluronic solution or NiNP. Asterisk indicates area of fibrosis. *C*, High magnification (40X and 100X) of insert from 10X in (*B*). Black arrows indicate alveolar macrophages containing NiNP agglomerates.

FIGURE 2. MUC5AC and MUC5B mRNA levels at 1 and 21 days after exposure. Taqman quantitative real-time RT-PCR was used to measure changes in whole lung mRNA levels of (*A*) MUC5AC and (*B*) MUC5B. Values are means ± SEM (n = 5-7 animals/group). *$p <$ 0.05, **$p < 0.01$, ***$p < 0.001$ as compared to the control group of the same genotype or as indicated.

FIGURE 3. Differential cell counts in the BALF 1 and 21 day after NiNP exposure. Immune cells numbers for (*A*) eosinophils, (*B*) lymphocytes, (*C*) neutrophils, and (*D*) macrophages are presented as the mean values ± SEM out of a total of 500 cells counted per animal for 5-7 animals per dose group at 20X magnification. *$p < 0.05$, **$p < 0.01$, ***$p < 0.001$ compared

to the time matched control group of the same genotype or as indicated. *E*, Photomicrographs representing each cell type. Macrophages and neutrophils demonstrated phagocytosis of NiNP in both genotypes at both time points in response to exposure (100X).

FIGURE 4. Histopathological analysis of inflammation in the lungs of WT and T-bet$^{-/-}$ mice in response to NiNPs. *A*, Lung pathology was scored in mice for inflammation 1 and 21 days after initial exposure. All data represent mean values ± SEM. *$p < 0.05$, ***$p < 0.001$ compared to the control group of the same genotype (n = 5-7 animals/group). *B*, Representative photomicrographs at low magnification (10X) of H&E stained lung sections at 21 days after mice were exposed. **TB**: Terminal bronchiole, **ADB**: alveolar duct bifurcation, **AD**: alveolar duct. *C*, Higher magnification (40X and 100X) of images from 10X in (*B*).

FIGURE 5. The effects that NiNP have on airway collagen deposition and interstitial fibrosis in WT and T-bet$^{-/-}$ mice. *A*, Cross-sections of airways stained with trichrome were measured for the area to perimeter ratio of collagen deposition. *B*, Representative images of results from (A) of airways stained with trichrome (open arrows) at low magnification (10X) at 21 days post exposure. *C*, Lung pathology was then scored for interstitial fibrosis in WT and T-bet$^{-/-}$ mice. *D*, Low magnification (10X) of trichrome stained lung parenchyma sections (open arrows) at 21 days after WT and T-bet$^{-/-}$ mice were initially exposed. Images are a representation of the data shown in (*C*). Black arrows indicate NiNP agglomerates. Data

are the mean values ± SEM (n = 5-7 animals/group). *$p < 0.05$, ***$p < 0.001$ compared to the control group of the same genotype or as indicated.

FIGURE 6. Total lung col1a2 mRNA and soluble collagen expression in the lungs of WT and T-bet$^{-/-}$ mice in response to NiNP exposure. *A*, Col1a2 mRNA expression levels were measured by qRT-PCR in whole lung tissue at 1 and 21 days after initial exposure (nd, not detectable). *B*, Soluble collagen content, μg/mg of protein, was measured from whole lung homogenates using the Sircol Assay kit. Data are mean values ± SEM (n = 5-7 animals/group). *$p < 0.05$, **$p < 0.01$, ***$p < 0.001$ as compared to the control group of the same genotype or as indicated.

FIGURE 7. CCL2 mRNA and protein levels in the lungs of mice after NiNP exposure. *A*, CCL2 mRNA expression was measured by qRT-PCR in whole lung tissue at 1 and 21 days post exposure while (*B*) CCL2 protein in BALF was analyzed by ELISA after 1 or 21 days of initial exposure (nd, not detectable). *$p < 0.05$, **$p < 0.01$, ***$p < 0.001$ as compared to the control group of the same genotype or as indicated. Data are the mean values ± SEM (n = 5-7 animals/group).

FIGURE 8. IL-13 mRNA and protein expression 1 and 21 day post exposure in the lungs of WT and T-bet$^{-/-}$ mice. *A*, Levels of IL-13 mRNA was measured in whole lung tissue by qRT-PCR at 1 and 21 days after exposure. *B*, Protein expression of IL-13 in the BALF was analyzed by ELISA at 1 or 21 days post exposure. All data represent mean values ± SEM. *p

< 0.05, $^{**}p < 0.01$, $^{***}p < 0.001$ as compared to the control group of the same genotype or as indicated (n = 5-7 animals/group).

FIGURE 9. Mucous cell metaplasia and interstitial pneumonitis in response to anti-CCL2 mAb treatment in T-bet$^{-/-}$ mice 21 days post-exposure. A, Cells stained with AB/PAS were quantitated for mucin protein expression using ImageJ (NIH) analysis for percentage of positive stained area per total area in mice treated with IgG2B Isotype Control or anti-CCL2 mAb and exposed to either a 0.1% pluronic solution or NiNPs. B, MUC5AC and (*C*) MUC5B whole lung mRNA expression were quantitated using qRT-PCR analysis. *D*, Cross sections of lungs stained with trichrome were scored for interstitial fibrosis in WT and T-bet$^{-/-}$ mice 21 days after initial NiNP exposure. Lungs were scored in a blinded manner by three independent reviewers. *E*, Soluble collagen content was measured using the Sircol Assay kit in whole lung homogenates and expressed as μg/mg of protein. *F*, Whole lung col1a2 mRNA expression measured by qRT-PCR. $^{*}p < 0.05$, $^{**}p < 0.01$, $^{***}p < 0.001$ compared to the time matched control group of the same genotype or as indicated. Data are the mean values ± SEM (n = 3-5 animals/group).

Figures

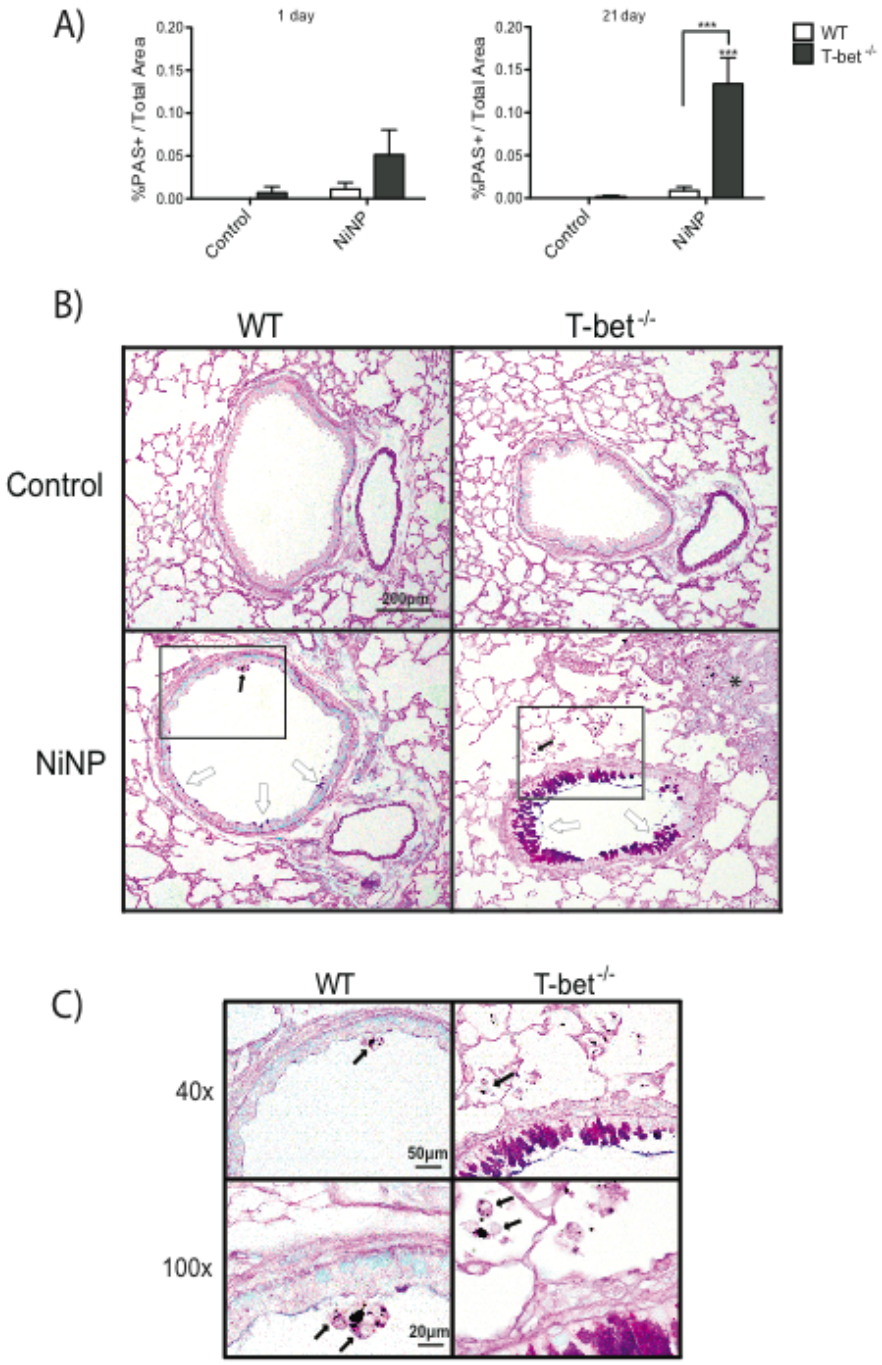

Figure 1. Mucous cell metaplasia in response to NiNP exposure in WT and T-bet-/- mice.

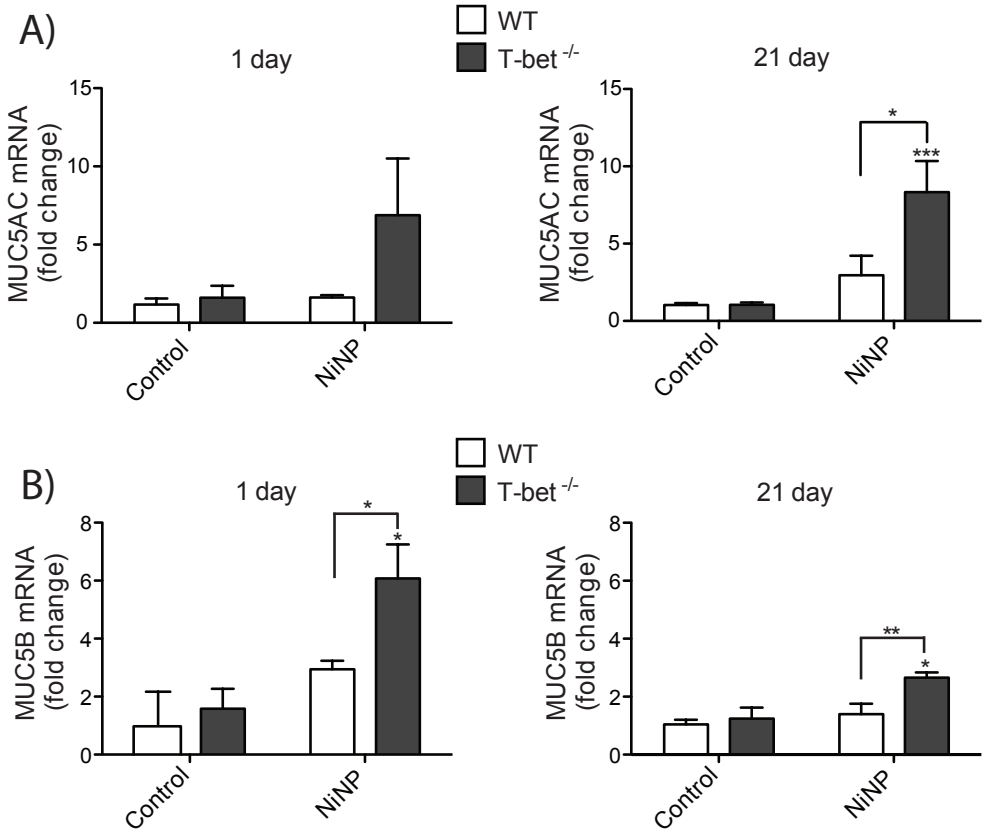

Figure 2. MUC5AC and MUC5B mRNA levels at 1 and 21 days after exposure.

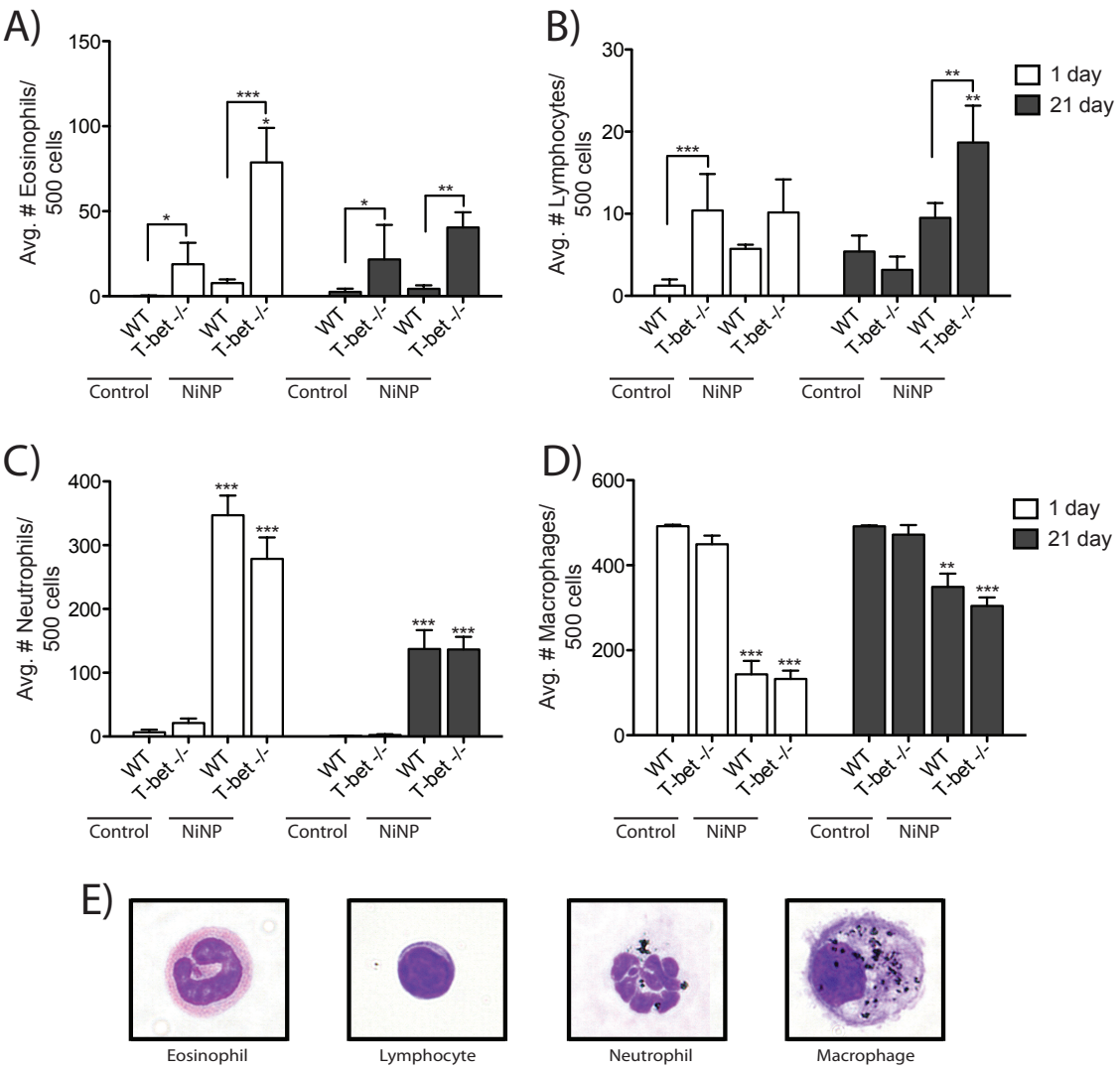

Figure 3. Differential cell counts in the BALF 1 and 21 day after NiNP exposure.

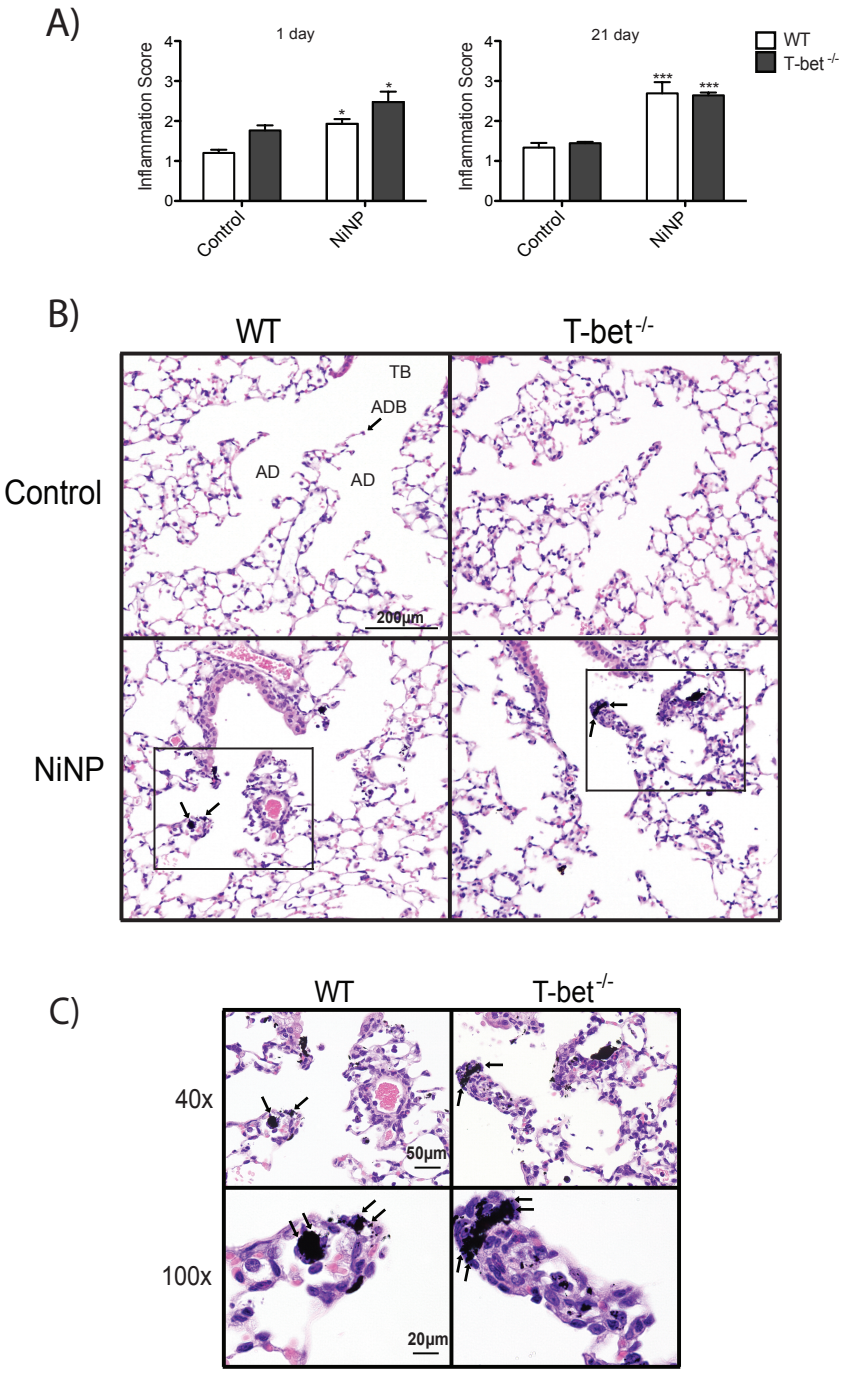

Figure 4. Histopathological analysis of inflammation in the lungs of WT and T-bet$^{-/-}$ mice in response to NiNPs.

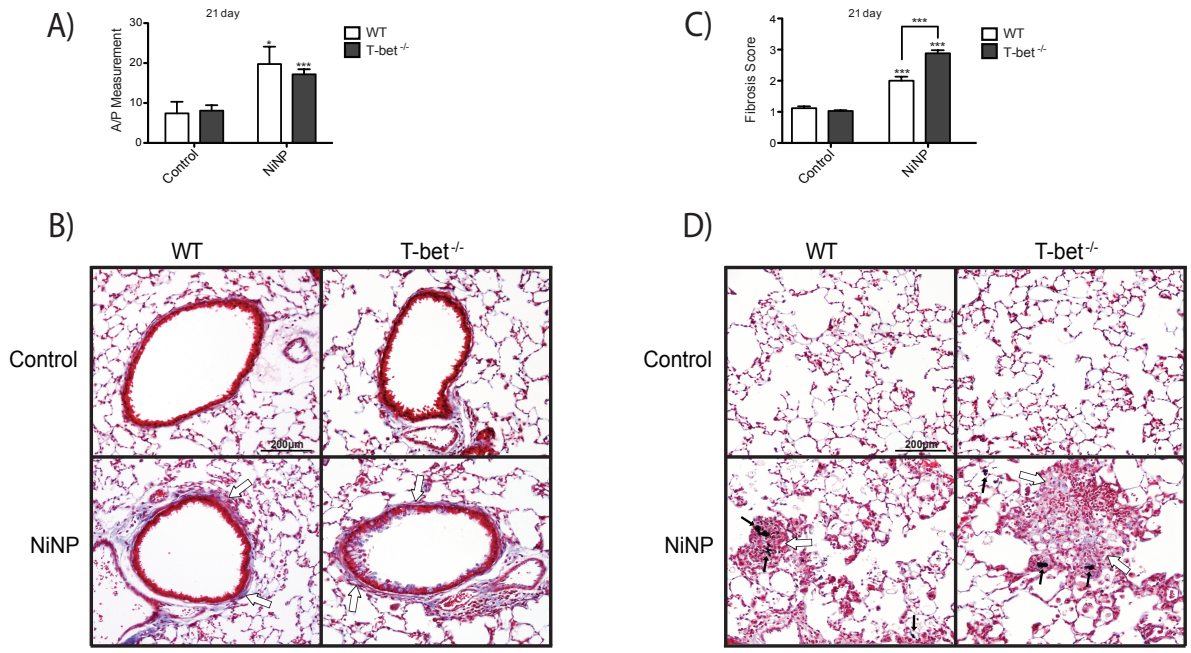

Figure 5. The effects that NiNP have on airway collagen deposition and interstitial pneumonitis in WT and T-bet$^{-/-}$ mice.

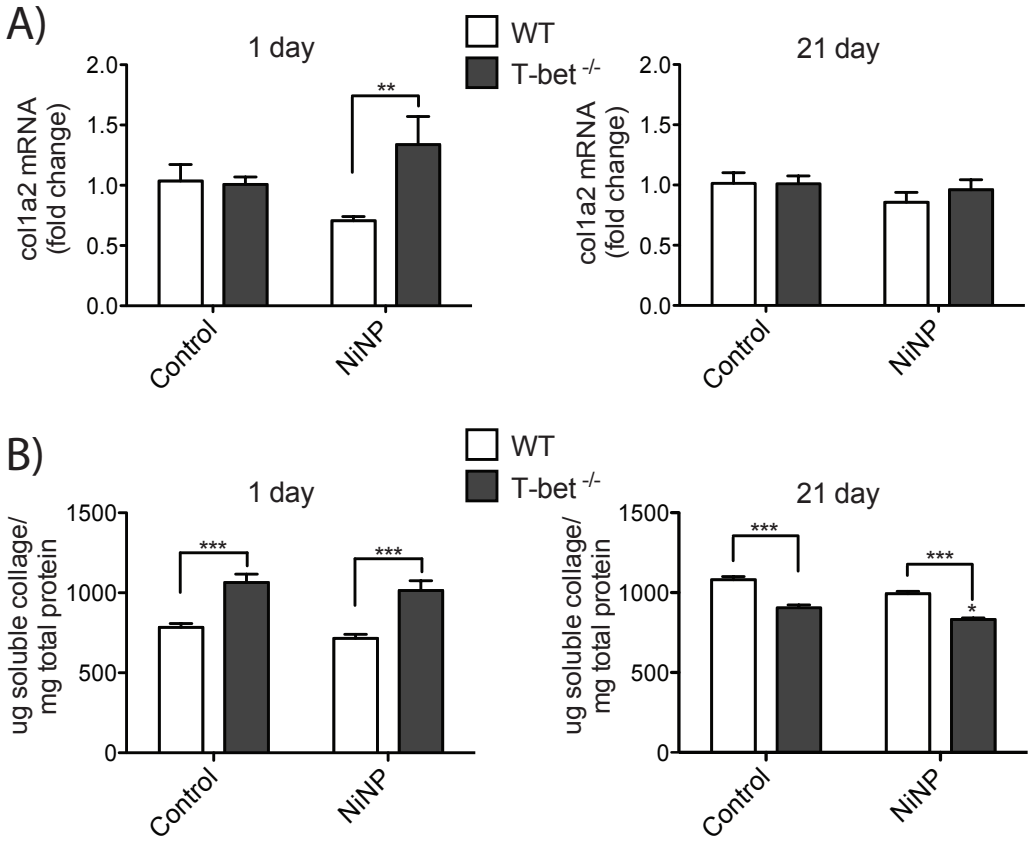

Figure 6. Total lung col1a2 mRNA and soluble collagen expression in the lungs of WT and T-bet$^{-/-}$ mice in response to NiNP exposure.

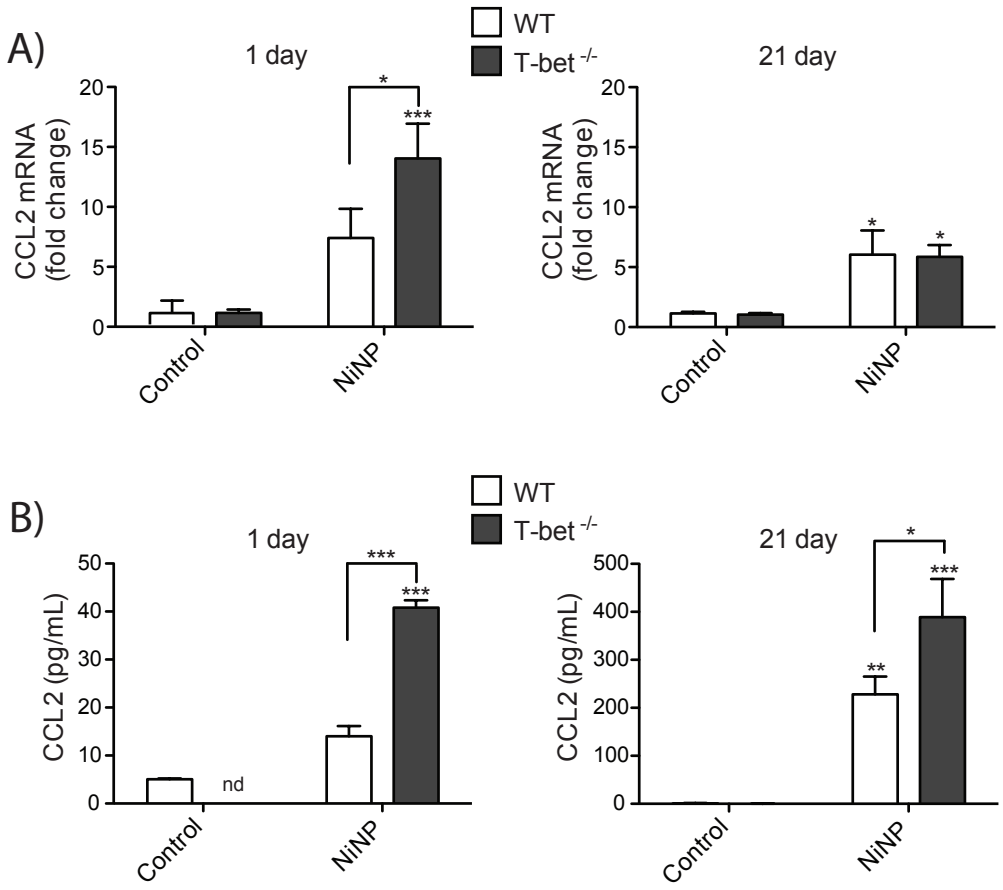

Figure 7. CCL2 mRNA and protein levels in the lungs of mice after NiNP exposure.

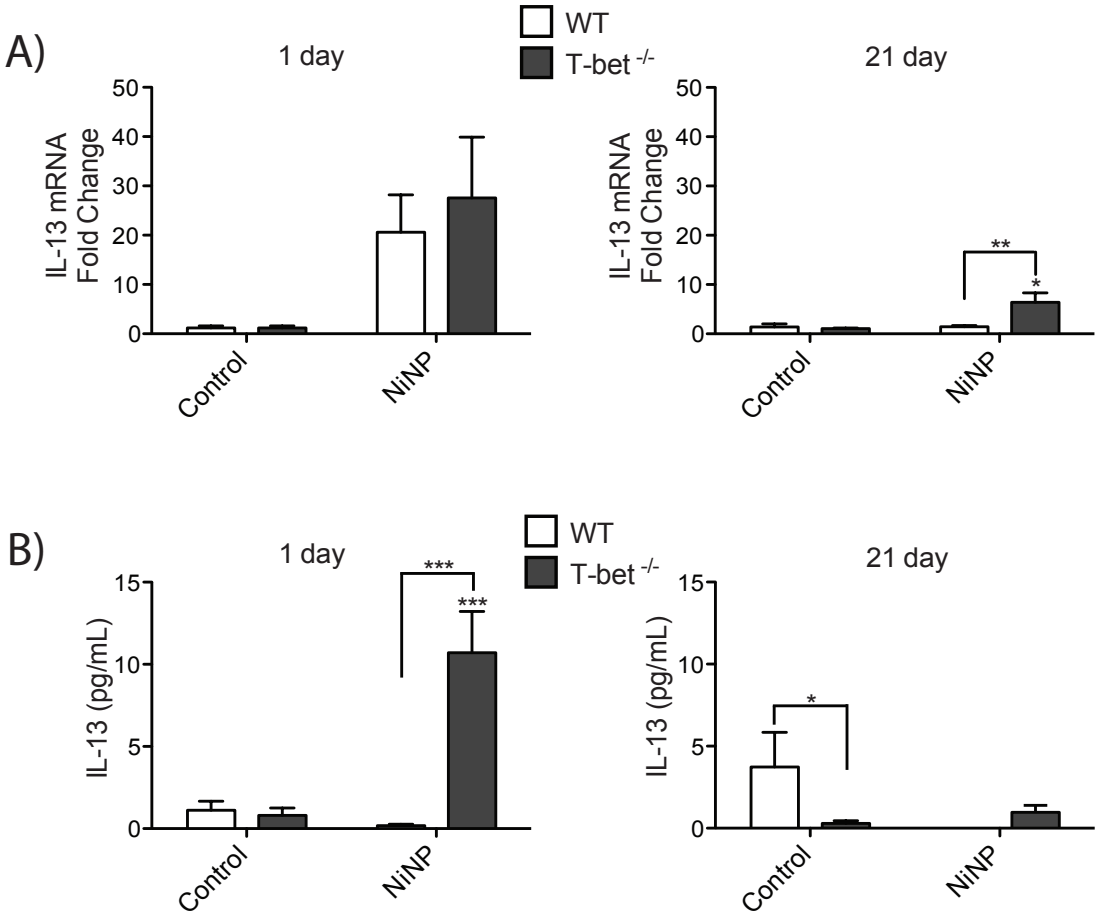

Figure 8. IL-13 mRNA and protein expression 1 and 21 day post exposure in the lungs of WT and T-bet$^{-/-}$ mice.

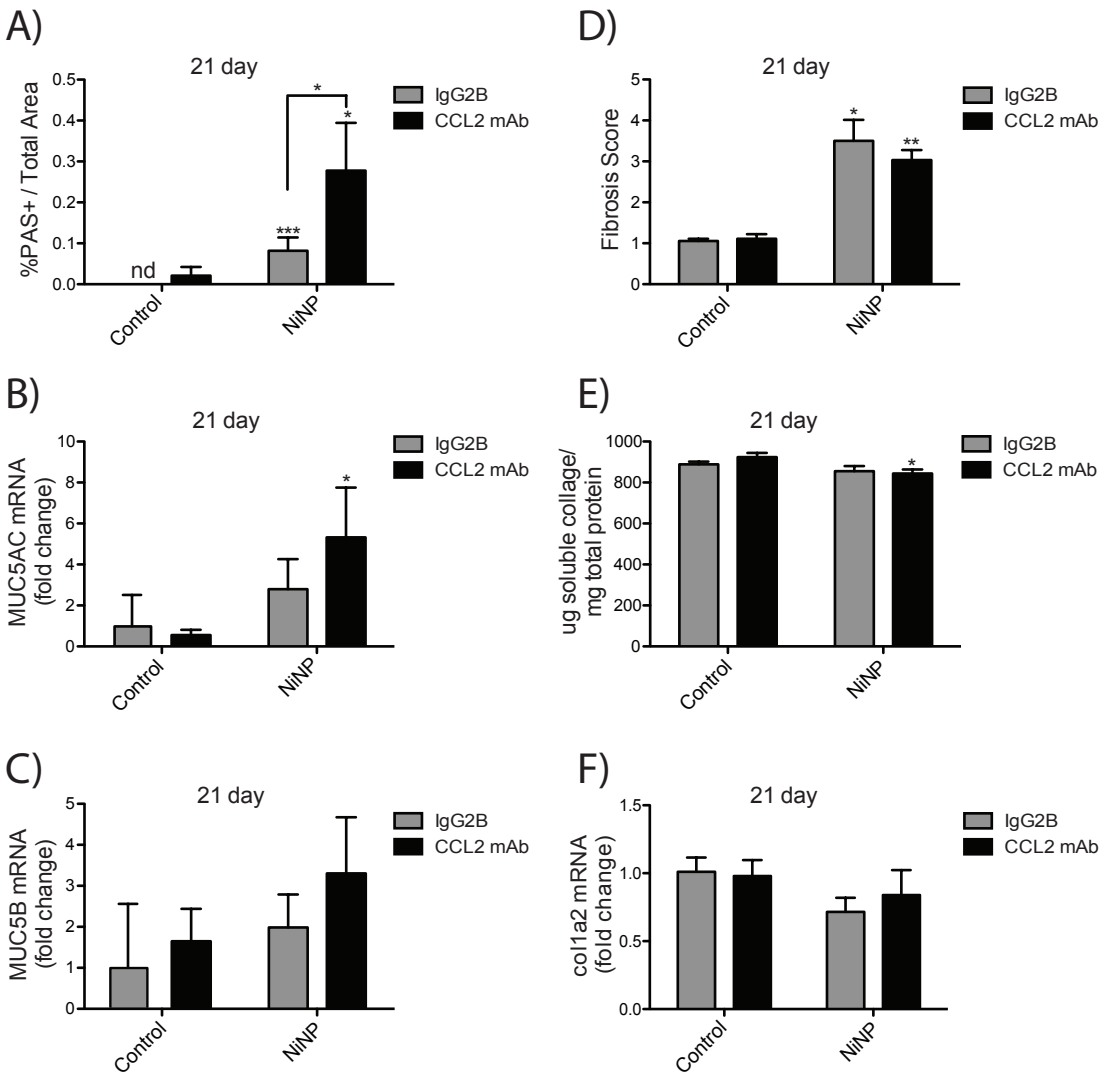

Figure 9. Mucous cell metaplasia and interstitial pneumonitis in response to anti-CCL2 mAb treatment in T-bet$^{-/-}$ mice 21 days post-exposure.

CHAPTER 2

Nickel Nanoparticles Enhance PDGF-Induced Chemokine Expression by Mesothelial Cells via Prolonged MAP Kinase Activation

Ellen E. Glista-Baker, Alexia J. Taylor, Brian C. Sayers, Elizabeth A. Thompson, and James C. Bonner*

**Department of Environmental and Molecular Toxicology, North Carolina State University, Raleigh, North Carolina 27695 USA*

Funding: This work was funded by NIEHS Grant RC2-ES018772. EEG and BCS are supported by NIEHS training grant T32-ES007046.

Abbreviations used: NRM2, normal rat pleural mesothelial cells; MWCNT, multiwalled carbon nanotubes; NiNP, nickel nanoparticles; CBNP, carbon black nanoparticles; PDGF, platelet-derived growth factor; PDGF-R, PDGF receptor; CXCL10, CXC chemokine ligand 10; CCL2, CC chemokine ligand 2; HIF-1α, hypoxia-inducible factor-1α; ERK, extracellular signal-regulated kinase.

Running Head: *PDGF enhances nanoparticle-induced chemokine expression*

Published In: The American Journal of Respiratory Cell and Molecular Biology. 2012 October; Volume 47, Issue 4; Pages 552-61.

Abstract

Pleural diseases (fibrosis and mesothelioma) are a major concern for individuals exposed by inhalation to certain types of particles, metals, and fibers. Increasing attention has focused on the possibility that certain types of engineered nanoparticles (NPs), especially those containing nickel, might also pose a risk for pleural diseases. Platelet-derived growth factor (PDGF) is an important mediator of fibrosis and cancer that has been implicated in the pathogenesis of pleural diseases. In this study we discovered that PDGF synergistically enhanced nickel nanoparticle (NiNP)-induced increases in mRNA and protein levels of the pro-fibrogenic chemokine monocyte chemoattractant protein-1 (MCP-1 or CCL2), and the anti-fibrogenic interferon-inducible CXC chemokine (CXCL10) in normal rat pleural mesothelial (NRM2) cells *in vitro*. Carbon black nanoparticles (CBNP), used as a negative control NP, did not cause a significant increase in CCL2 or CXCL10 in the absence or presence of PDGF. NiNP prolonged PDGF-induced phosphorylation of the mitogen-activated protein kinase (MAPK) family termed extracellular signal-regulated kinases (ERK)-1 and ERK-2 for up to 24 h and NiNP also synergistically increased PDGF-induced hypoxia inducible factor (HIF)-1α protein levels in NRM2 cells. Inhibition of ERK-1,2 phosphorylation (p-ERK-1,2) with the MEK inhibitor PD98059 blocked the synergistic increase in CCL2, CXCL10, and HIF-1α levels induced by PDGF and NiNP. Moreover, the antioxidant L-NAC, significantly reduced HIF-1α, p-ERK-1,2, and CCL2 protein levels that were synergistically increased by the combination of PDGF and NiNP. These data indicate that nickel nanoparticles enhance the activity of PDGF in regulating chemokine production

by pleural mesothelial cells through a mechanism involving ROS generation and prolonged activation of ERK-1,2.

Keywords: Nanoparticles, metals, lung, pleura, chemokines

Introduction

Pleural disease, such as fibrosis and mesothelioma, is a major concern for individuals exposed by inhalation to certain types of fibers, especially asbestos. Increasing attention has focused on the possibility that engineered carbon nanotubes (CNT), a product of emerging nanotechnology, pose a similar risk due to their high aspect ratio, durability and metal catalysts (1). A common catalyst used in the manufacture of multi-walled CNT (MWCNT) is nickel nanoparticles (NiNP) (2). Nickel is known to cause a variety of pulmonary diseases, including fibrosis and cancer, and exposure to nickel particulates can also result in pleural and peritoneal mesothelioma in rodents (3-5). Furthermore, NiNP are more potent inducers of pleural fibrosis compared to micron sized nickel particles (6-7). We recently reported that MWCNT containing residual nickel catalyst reached the pleura of the lungs of mice after inhalation and caused pleural fibrosis and increased immune responses (8).

Platelet derived growth factor (PDGF) is a key mediator of fibrogenesis and is increased in the lungs of mice that are exposed to nickel-containing MWCNT (8-9). PDGF is a family of polypeptides (AA, BB, AB, CC, DD) that bind and dimerize cell-surface receptors termed PDGF-Rα and PDGF-Rβ to form dimeric αα, αβ, or ββ receptors with tyrosine kinase activity. Alveolar macrophages are a rich source of PDGF-BB, while fibroblasts are the central source of PDGF-AA. Additionally, PDGF production by macrophages can be increased in a hypoxic environment stimulated by exposure to nickel (10, 11). PDGF acts as a stimulant of fibroblast growth and chemotaxis through the activation of the mitogen-activated protein (MAP) kinases termed ERK-1 and -2 (collectively referred to as ERK) and plays a major role in fibroblast survival (10, 12). Fibroblasts are

critical to fibrogenesis, as they differentiate into myofibroblasts in response to transforming growth factor (TGF)-β1 to produce collagen, which defines fibrotic lesions (10). Moreover, PDGF is thought to play a role in pleural fibrosis and mesothelioma (13). PDGF-BB is produced by pleural mesothelial cells *in vitro* in an ATF3-dependent manner after exposure to asbestos fibers, and pleural mesothelial cells possess cell surface receptors for PDGF (14-15).

In addition to stimulating the growth, chemotaxis, and survival of mesenchymal cells, PDGF stimulates the production of other cytokines, chemokines, and growth factors that play important roles in angiogenesis and fibrogenesis. For example, PDGF increases the production of CCL2 (monocyte chemoattractant protein-1, MCP-1), a pro-fibrogenic and pro-angiogenic chemokine, via a mechanism involving the activation of phosphoinositide 3-kinase (PI3-K) and NFkB in NIH/3T3 fibroblasts (16-17). Rat pleural mesothelial cells also produce CCL2 in response to asbestos fibers *in vitro*, which in turn serves as a potent chemoattractant for monocytes and macrophages (18-19). CCL2 stimulates fibroblasts to produce TGF-β1 and collagen (20). CCR2, the receptor for CCL2, is required for pulmonary fibrosis mice as CCR2-deficient mice are protected from bleomycin or FITC-induced fibrosis (21-22). In addition to its role in promoting fibrogenesis, CCL2 also stimulates angiogenesis via hypoxia-inducible factor (HIF-1α) and consequent production of vascular endothelial growth factor (VEGF) (23).

While CCL2 promotes fibrogenesis, the interferon-inducible chemokine CXCL10 is anti-fibrogenic. For example, CXCL10 has been demonstrated to reduce bleomycin-induced lung fibrosis in mice and is due, at least in part, to inhibition of angiogenesis (24). In addition

to inhibition of angiogenesis, CXCL10 also mediates chemotaxis of activated T and NK cells, and regulates the expression of adhesion molecules (25-26). CXCL10 mediates its biological effects through its receptor termed CXCR3 and deletion of CXCR3 in mice has been shown to increase bleomycin-induced fibrogenesis (27). We have previously shown that the transition metal, vanadium pentoxide, increases the expression of CXCL10 in human lung fibroblasts through a mechanism involving activation of NADPH-oxidase and autocrine production of IFN-γ (28).

In this study, we hypothesized that PDGF would modify NiNP-induced expression of CCL2 or CXCL10 in rat pleural mesothelial cells. We discovered that NiNP and PDGF-BB synergistically increased CCL2 and CXCL10 in rat pleural mesothelial cells through a mechanism involving the ability of NiNP to prolong ERK phosphorylation that is initially induced by PDGF.

Materials & Methods

Cell Culture

Normal rat pleural mesothelial (NRM2) cells were a kind gift from Edilberto Bermudez at the Hamner Institutes for Health Sciences (Research Triangle Park, NC) and were isolated from the parietal pleura (29). The details of cell culture and treatment with PDGF or NiNP are described in the online supplement.

Nanoparticles

Nickel nanoparticles (NiNP), ~20 nm diameter, were purchased from Sun Innovations (Fremont, CA). We determined NiNP size from digitized TEM images. The diameter of NiNP was measured using Adobe Photoshop by determining pixel length of >100 NiNP and converting pixels to nanometers using a standard magnification bar contained within each TEM image. Carbon black nanoparticles (CBNP), ~8 nm, were from Columbian Chemicals as Raven® 5000 Ultra II Powder (Marietta, GA). Nanoparticles were suspended in a sterile, 0.1% pluronic F-68 (Sigma) in phosphate buffer solution and dispersed for two hr using a bath sonicator at room temperature. Further details on nanoparticle characterization are provided in the Online Supplement.

Taqman Real-Time RT-PCR

One-step, TaqMan quantitative real time RT-PCR (qRT-PCR) was performed to quantify gene expression of our target genes. Total RNA was extracted and purified using an RNeasy Mini Kit (Qiagen). RNA concentrations were determined by the Nanodrop1000

spectrophotometer and samples were normalized to a final concentration of 25 ng/µl. qRT-PCR was performed using reagents from the SuperScript® III Platinum® One-Step qRT-PCR Kit (Invitrogen) on the StepOne Plus instrument (Applied Biosystems). A comparative C_T method was used to quantify target gene expression for CXCL10 (Rn00594648_m1) and CCL2 (Rn00580555_m1) against the endogenous control hypoxanthine phosphoribosyltransferase-1 (HPRT-1) (Rn01527840_m1). Each individual sample was analyzed in duplicate and experiments were repeated at least three times. The StepOne Plus software calculated relative quantitation values and expressed as fold-change.

ELISA

Cell culture supernatants were assayed according to kit instructions for CCL2 (R&D Systems) or CXCL10 (Antigenix America, Inc., Huntington Station, NY) protein secretion. Absorbances were read at 450nm by the Multiskan EX microplate spectrophotometer with a correction wavelength set at 540nm.

Western Blot

Cell lysates were collected at various time points and were separated by SDS-PAGE (Invitrogen), transferred to PVDF membranes, and blocked for 1 hour in 5% non-fat milk in TBST (20 mM Tris, 137 mM NaCl and 0.1% Tween 20). The blot was then incubated at 4°C overnight with primary antibody followed by a 1 h incubation of HRP-conjugated secondary antibody. The immunoblot signal was detected and visualized through enhanced chemiluminescence (ECL, GE Healthcare). Total and phosphorylated PDGF-Rβ primary

antibodies, as well as all secondary antibodies, were purchased from Santa Cruz. Total ERK, phosphorylated ERK and β-actin primary antibodies were purchased from Cell Signaling Technology. HIF-1α antibody was purchased from Novus Biological, Littleton, CO.

Statistical Analysis

Statistical analysis was performed using GraphPad Prism software version 5.00 (San Diego, CA). Two-way ANOVA with a Bonferroni test was used to identify significant differences among multiple treatment groups. One-way ANOVA with a *post hoc* Tukey was used to test significance of treatment groups compared to control. The significance was set at $p < 0.05$ unless stated otherwise. Densitometric analysis was performed on Western Blots using Image J analysis software (NIH).

Results

Nickel nanoparticles (NiNP) form agglomerates in cell culture medium and are internalized by pleural mesothelial cells in vitro. TEM demonstrated that NiNP formed agglomerates when suspended in tissue culture medium (Fig. 1A). The size distribution frequency of individual NiNP was calculated by measuring the diameter of particles from digitized TEM images as described in *Materials & Methods*. The average particle diameter was 25.43 ± 11.62 nm, slightly larger than the 20 nm average diameter provided by the manufacturer (Fig. 1B). Furthermore, greater than 90% of the NiNP were between 10 and 50 nm in diameter. Rat pleural mesothelial cells (NRM2) were treated with NiNP or CBNP and observed by TEM after 24 h of exposure. NiNP agglomerates were identified in contact with the cell membrane and within the cytoplasm of NRM2 cells (Fig. 1C) as were CBNP (Fig. 1E). Higher magnification showed that both NiNP and CBNP agglomerates were contained within membrane-bound vesicles that resembled lysosomes (Fig. 1D, Fig. 1F). NiNP and CBNP both retained their spherical shape and size within cells over a 24 h time period under these experimental conditions.

Nickel nanoparticles synergistically increase PDGF-induced CCL2 and CXCL10 expression in rat pleural mesothelial cells. CCL2 and CXCL10 mRNA and protein were measured using qRT-PCR and ELISA, respectively. The optimal concentrations of PDGF and NiNP used in this study were determined by dose-response relationships. Additionally, time course experiments were also performed to determine temporal expression patterns of CCL2 and CXCL10 (see *Online Supplement*). The induction of CCL2 expression in NRM2 cells was

due to the PDGF-BB isoform, referred to herein simple as 'PDGF', whereas PDGF-AA had no significant effect on the induction of CCL2 levels (data not shown). PDGF or NiNP increased CCL2 mRNA levels by 6 h and maximally increased CCL2 protein levels in cell supernatants at 24 h after exposure (Fig. S1, S2). The combination of PDGF and NiNP synergistically increased CCL2 mRNA and protein levels at 24 h post-treatment (Fig. 2A, B). Similar to CCL2, CXCL10 mRNA and protein levels were synergistically increased in NRM2 cells by a combination of PDGF and NiNP when compared to cells treated with either PDGF or NiNP alone (Fig. 2C, D). The time course of CXCL10 expression was different from CCL2 in that levels of CXCL10 mRNA and protein were maximally induced by NiNP and PDGF at 48 h following exposure (Fig. S3). Treatment of NRM2 cells over all treatments and time points did not result in significant cytotoxicity as determined by LDH assay (data not shown). The synergistic response observed between PDGF and NiNP on increasing chemokine production was observed in two separate isolates of NRM2 cells.

Nickel nanoparticles prolong PDGF-induced phosphorylation of MAPK but do not affect phosphorylation of PDGF-Rβ. PDGF-induced ERK phosphorylation was observed in rat pleural mesothelial cells at 2 h and 24 h after exposure. ERK phosphorylation was measured by Western blot analysis using antibodies against total or phosphorylated ERK protein (Fig. 3A). Densitometric analysis of the ratio of pERK to total ERK was performed for a quantitative evaluation of the different exposure groups (Fig. 3B). At 2 h, treatment of cells with either PDGF or a combination of PDGF and NiNP caused a robust and significant increase in ERK phosphorylation over control and NiNP. However, ERK phosphorylation

induced by PDGF or PDGF plus NiNP were not different from one another at 2 h. In contrast, at 24 h ERK phosphorylation induced by PDGF plus NiNP was significant over all dose groups, while ERK phosphorylation by PDGF alone at 24 h was not significantly different from control (Fig. 3A, B). In order to determine if NiNP acted upstream at the PDGF receptor (PDGF-R) to increase PDGF-induced phosphorylation of ERK at 24 h, Western blot analysis was performed using antibodies specific for phosphorylated PDGF-Rα or PDGF-Rβ or antibodies against total protein levels of these two receptors. Western blot analysis showed that treatment of NRM2 cells with NiNP did not change PDGF-induced phosphorylation of PDGF-Rβ or total protein levels of PDGF-Rβ (Fig. 3C). PDGF-Rα levels were not detectable in NRM2 cells by Western blot analysis but were present in positive control human lung fibroblasts (data not shown).

CXCL10 and CCL2 induction by PDGF and nickel nanoparticles is MEK-dependent. We hypothesized that ERK is an upstream mediator of both CCL2 and CXCL10 since PDGF is known to induce ERK phosphorylation (10). To test this hypothesis, NRM2 cells were treated with 20μM of PD98059 1 h prior to PDGF and NiNP exposure. In order to make sure the inhibitor worked properly, ERK phosphorylation was analyzed by Western Blot. As seen in Fig. 4A, PD98059 significantly reduced ERK signaling in every treatment group including control. Additionally, the MEK inhibitor significantly decreased CXCL10 mRNA and protein expression that was induced by the combination of PDGF and NiNP (Fig. 4B). Similarly, CCL2 mRNA and protein expression induced by the combination of PDGF and NiNP were significantly decreased by PD98059 (Fig. 4C).

PDGF enhances nickel nanoparticle-induced HIF-1α levels via a MAPK-dependent mechanism. NiNP increased HIF-1α levels in NRM2 cells 24 h after exposure as measured by Western blot analysis. PDGF alone did not increase HIF-1α levels, but PDGF synergistically enhanced NiNP-induced HIF-1α expression (Fig. 5A). Quantitative densitometry of HIF-1α were normalized against β-actin in three independent experiments and revealed a statistically significant effect of NiNP on HIF-1α. Furthermore, this effect was significantly enhanced by the addition of PDGF (Fig. 5B). The role of ERK was further investigated as contributory to the additive effect of PDGF and NiNP on HIF-1α expression. Cells were treated with 20μM PD98059 1 h prior to PDGF and/or NiNP exposure. PD98059 blocked PDGF enhancement of NiNP-induced HIF-1α expression, but did not block the induction of HIF-1α by NiNP alone. This indicated that ERK is responsible for only PDGF driven induction of HIF-1α and that there is an additional mediator involved in the induction of HIF-1α by NiNP. HIF-1α mRNA levels were not changed at 24 h after treatment with PDGF, NiNP, or PDGF combined with NiNP (data not shown), suggesting that HIF-1α regulation in response to PDGF and NiNP is regulated at the post-translational level.

Nickel nanoparticle-induced HIF-1α levels and NiNP enhancement of PDGF-induced chemokine expression is reduced by the antioxidant NAC. NRM2 cells were pre-treated with 5mM of *N*-Acetyl-L-cysteine (NAC), an antioxidant, for 1 h prior to treatment with NiNP, PDGF, or the combination of NiNP and PDGF. Treatment with NAC decreased HIF-1α protein levels that were induced after exposure to NiNP or the combination of NiNP and PDGF (Fig. 6A). Quantitative densitometry of HIF-1α Western blots were normalized

against β-actin in three independent experiments and revealed a statistically significant effect of NAC on reducing HIF-1α levels induced by NiNP or the combination of NiNP and PDGF (Fig. 6B). Additionally, NAC significantly reduced ERK-1,2 phosphorylation (p-ERK-1,2) and CCL2 protein levels in NRM2 cell supernatants that were induced by the combination of NiNP and PDGF (Fig. 6C,D). The effect of NAC on CXCL10, which was induced after 48 hr of treatment with NiNP with or without PDGF, was not evaluated since the combination of antioxidant and NiNP or NiNP plus PDGF caused significant cytotoxicity at this time point (data not shown).

Discussion

Nanomaterials have increasingly gained popularity due to the novel physical and chemical properties they possess compared to their bulk counterparts. Their nano-size dimensions, shape, and surface area make them attractive for use in numerous applications, yet the potential risks they pose to human heath remain largely unknown (1). In this study, we investigated the effects of nickel nanoparticles (NiNP) on pleural mesothelial cell signaling and chemokine production. When particle size is decreased to nanoscale proportions, this alters physiochemical properties (e.g. increased surface area and reactivity), and has the potential to change particle interaction with the cellular microenvironment and subcellular structures (30). Nano-sized nickel particles, when compared to larger Ni particles, have greater surface area, higher magnetism, and lower melting point (31). Additionally, nanoparticles cause more lung injury compared to larger particles due to their higher surface area per unit mass and increased potential to generate ROS (30). Previous studies have shown that NiNP cause more inflammation and toxicity in the lungs of rodents after intratracheal instillation when compared to micron-sized Ni particles, demonstrating that pulmonary toxicity increases as particle size decreases (31, 6, 7, 1).

Nanoparticles are more likely to migrate to the distal areas of the lung and reach the pleural mesothelium (1). Previous studies have shown that nickel nanoparticles (NiNP) and Ni-containing nanomaterials can reach the pleura, causing fibrosis and mesothelioma in rodents (5-8). It is therefore important to gain a better understanding of the cellular and molecular mechanisms behind the progression of NiNP-induced pleural diseases. We found that NiNP are taken up by cultured rat pleural mesothelial cells and stimulate marginal

increases in chemokines (CCL2 and CXCL10) and HIF-1α. However, in the presence of PDGF-BB, a fibroblast mitogen and chemoattractant, NiNP-induced chemokine and HIF-1α expression were synergistically increased. Our data support the hypothesis that synergy between NiNP and PDGF involves initiation of ERK phosphorylation by PDGF-BB and prolonged activation of PDGF-induced ERK signaling by NiNP-generated ROS. This hypothetical mechanism is illustrated in Fig. 7.

NiNP are used as a catalyst in the fabrication of MWCNT and there are concerns that they could be a contributing factor to pulmonary fibrosis or mesothelioma (6, 12, 5). We have previously reported a significant fibrotic response in the lungs and pleura of mice after inhalation exposure to MWCNT containing residual Ni (32, 8). It is unknown whether the NiNP used in this study closely represents the residual Ni catalyst found in MWCNT, although TEM photomicrographs coupled with EDX spectroscopy indicate NiNP within MWCNT (8). Moreover, the dose of NiNP used in the *in vitro* studies presented here are likely much higher than doses of Ni that would occur at the pleura of mice after lung exposure to MWCNT. However, aside from exposures to MWCNT that contain residual Ni, it is important to consider that much higher exposures to NiNP alone could occur occupationally where Ni is used for manufacturing or catalytic processes.

Our study also shows that the cellular effects of NiNP are not merely related to the physical size of the nanoparticles, as CBNP also were avidly taken up by NRM2 cells and did not cause significant ERK phosphorylation, induction of HIF-1α, or chemokine expression. These findings suggest that the reactivity of NiNP, in addition to nanometer size, is important for the biological effects observed in NRM2 cells. We observed that NiNP

retained their spherical shape and size within NRM2 cells over a 24 h period with no indication of degradation (Fig. 1). This observation suggests that no dissolution of Ni is necessary to produce the biological responses reported in this study and that surface reactivity of NiNP plays an important role in generating ROS to initiate cell signaling and HIF-1α or chemokine induction. Nevertheless, we cannot rule out the possibility that some Ni ions were generated that could have caused significant effects on biological responses. Finally, it is unclear whether the observed effects reported here might be seen with other types of metal nanoparticles. Therefore, other transition metals used to manufacture engineered nanoparticles should be tested in order to determine whether or not they act synergistically with PDGF to promote HIF-1α and chemokine expression in mesothelial cells.

In our previous work, rats or mice exposed to MWCNT containing residual Ni exhibited increased levels of PDGF (9, 32). PDGF is an important mediator of fibrotic diseases (10) and has been implicated in the pathogenesis of pleural disease (13). During the pathogenesis of fibrosis, PDGF contributes to the production and deposition of collagen by driving myofibroblast proliferation and chemotaxis (33,34). After exposure to MWCNT, mice have increased levels of PDGF throughout the lung that could be available to mesothelial cells *in vivo* (9, 8). Alveolar macrophages are a major source of PDGF-BB in the lungs, while PDGF-AA is mainly produced by fibroblasts and epithelial cells (35, 10). Pleural mesothelial cells are another source for increased levels of PDGF-BB after asbestos exposure and injury. This suggests that PDGF-BB could act in an autocrine fashion to increase CCL2 expression in mesothelial cells (18, 19). We have previously showed that

macrophages engulf inhaled MWCNT and then migrate to the pleura where they accumulate beneath the mesothelium (8). In our experiments, we found that PDGF-BB, but not PDGF-AA, enhanced NiNP-induced chemokine production by rat pleural mesothelial cells. Moreover, we have observed that the majority of NiNP delivered to the lungs of mice by oropharyngeal aspiration are taken up by alveolar macrophages and many of these macrophages are found in the subpleural region of the lungs adjacent to the pleural mesothelium (Glista-Baker and Bonner, unpublished observation). As illustrated in Fig. 7, paracrine signaling between macrophages and mesothelial cells via PDGF-BB could be important to the amplification of NiNP-induced signaling in pleural mesothelial cells *in vivo*. Nevertheless, it is unclear how PDGF-BB produced by macrophages would translocate across the epithelial barrier that separates the subpleural region of the lung from the mesothelial lining. Moreover, cell types other than macrophages cannot be ruled out as a source of PDGF-BB and this issue requires further study.

A key step in the progression of fibrosis is the deposition of collagen, which is stimulated primarily by TGF-β1 (36). CCL2 is considered to be a pro-fibrotic chemokine since it plays a role in stimulating fibroblasts to produce collagen by induction and activation of TGF-β1 (20). Additionally, CCL2 is a potent chemoattractant produced by pleural mesothelial cells that induces the migration of macrophages to an area of inflammation and injury (19). Time course experiments demonstrated that CCL2 mRNA and protein were induced transiently by PDGF-BB, whereas NiNP caused a sustained increase in CCL2 expression (Fig. S1, S2). The combination of PDGF and NiNP caused a synergistic increase in CCL2 mRNA and protein at 24 h (Fig. 2A,B). These data demonstrate a potentially

important interaction between nanoparticle exposure and an endogenous growth factor that could be important in progression of subpleural fibrosis or pleural cancer. We also demonstrated that PDGF and NiNP synergistically increased CXCL10 mRNA and protein levels in mesothelial cells (Fig. 2C, D). The chemokine CXCL10 promotes the recruitment of many inflammatory cells such as T-cells, monocytes, fibroblasts and endothelial cells (24). Additionally, mesothelial cells are a significant source of CXCL10 during inflammation (37). Elevated levels of CXCL10 have been found to be indicative of injury and inflammation associated with pulmonary fibrosis (38). Unlike CCL2, which is pro-fibrogenic, CXCL10 is anti-fibrogenic and transgenic mice that lack CXCL10 or its receptor CXCR3 have exaggerated lung fibrosis (24, 27). Furthermore, CXCL10 is involved in the early stages of peritoneal wound healing by preventing the formation of fibrotic adhesions (39). Therefore, CXCL10 is likely a protective response to injury. While CCL2 and CXCL10 have opposing roles in fibrosis, it is equally important to understand the regulation of both of these chemokines since they likely have important functions in pleural fibrosis and the resolution of pleural fibrosis, respectively.

We identified ERK-1,2 as a key signaling intermediate in the molecular mechanism by which PDGF-BB and NiNP synergistically increased CXCL10 and CCL2. PDGF-BB binds to the extracellular domain of PDGF-Rα and/or PDGF-Rβ transmembrane subunits to form dimeric PDGF-Rαβ or PDGF-Rββ on the cell surface (10). The autophosphorylation on tyrosine residues within the intracellular domain of these dimeric receptors initiates activation of the intracellular ERK-1,2 signaling pathway. ERK-1,2 signaling can regulate multiple processes including cellular proliferation and cell cycle progression depending on

the duration of the signal and cell type (40). Furthermore, prolonged ERK-1,2 phosphorylation leads to differences in the expression of immediate early genes (IEG) which can allow for additional cell growth, differentiation and survival associated with the development of cancer and disease (41). We observed that NiNP caused sustained PDGF-induced ERK-1,2 phosphorylation (Fig. 3A, B), suggesting that this activity could contribute to the increased expression and stabilization of IEGs, which include CCL2 and CXCL10 (17, 42). This was verified upon treatment of NRM2 with the MEK-1/2 inhibitor, PD98059, which blocked ERK-1,2 activity and significantly decreased IEG expression that was induced by the combination of PDGF plus NiNP (Fig. 4A). However, in the absence of NiNP, ERK-1,2 phosphorylation induced by PDGF was not sustained. Moreover, NiNP did not alter phosphorylation at the PDGF receptor (Fig. 3C), suggesting that cross-talk between NiNP and growth factor signaling that occurs downstream of the PDGF receptor.

Nickel is known to cause oxidative stress by generating a variety of intracellular reactive oxygen species (ROS) such as hydrogen peroxide and oxygen radicals while decreasing antioxidants such as glutathione (43). This creates a hypoxic environment in the cell and induces hypoxia-inducible genes, specifically the stabilization and accumulation of the hypoxia-inducible factor-1α protein (HIF-1α), a primary biomarker of oxidative stress (44). The HIF-1 complex consists of two subunits, HIF-1α and HIF-1β that binds to the Hypoxia Response Element (HRE) in the promoter region. While HIF-1β is constitutively expressed, the HIF-1α protein is stabilized by low oxygen levels and becomes resistant to proteasomal degradation (45). Additionally, the transcription of HIF-1 can also be regulated by intracelluar signaling intermediates, including MAPKs, such as ERK (44, 46). Our results

show that PDGF-BB synergistically increased NiNP-induced HIF-1α protein levels in NRM2 cells, but that the combination of PDGF and NiNP had no effect on HIF-1α mRNA levels (data not shown). This suggests that the increase in HIF-1α caused by the combination of PDGF and NiNP was due to HIF-1α protein stabilization. The induction of HIF-1α by the combination of PDGF and NiNP was also significantly reduced by the MEK inhibitor (Fig. 5). However, NiNP-induced HIF-1α levels were not affected by the MEK inhibitor, PD98059. These data indicated that PDGF enhancement of NiNP-induced HIF-1α was ERK-dependent, while NiNP-induced induction of HIF-1α is ERK-independent.

As stated earlier, others have shown that reactive oxygen species (ROS), such as hydrogen peroxide contribute to the stabilization of HIF-1α protein (43, 44). Recent studies have also shown that nano-sized nickel particles can sustain HIF-1α activity in human cell lines (47, 48). Therefore, we hypothesized that ROS mediated the induction of HIF-1α and chemokines that were induced by NiNP or the combination of NiNP and PDGF in NRM2 cells. Our results show that NAC significantly decreased total HIF-1α protein levels after exposure to NiNP alone and also after the combination of PDGF plus NiNP (Fig. 6A, B). Additionally, we observed that NAC treatment also significantly reduced p-ERK-1,2 levels and CCL2 protein levels that were induced by the combination of NiNP and PDGF (Fig. 6C,D). These data suggest that ROS mediate induction of HIF-1α by NiNP and play a role in the synergistic increase in chemokine production stimulated by the combination of NiNP and PDGF. However, NAC had no effect on CCL2 production induced by PDGF alone (Fig. 6D), suggesting that ROS are not required for the PDGF signaling component of this mechanism. Moreover, while HIF-1α induction and ERK-1,2 phosphorylation by NiNP and PDGF were

almost completely inhibited by NAC at 24 hr, the induction of CCL2 by NiNP and PDGF was only partially reduced by NAC, suggested that both ROS-dependent and ROS-independent signaling is involved in the induction of CCL2 by the combination of NiNP and PDGF.

Nickel compounds are classified as carcinogenic in humans causing lung and nasal cancer as well as pulmonary inflammation and fibrosis after chronic exposure (49). Our data demonstrate that PDGF-BB synergistically increased NiNP-induced production of chemokines in rat pleural mesothelial cells via an ERK-1,2-dependent mechanism that appears to be due to NiNP prolonging ERK phosphorylation after initiation by PDGF-BB. In the context of carcinogenesis, others have shown that an ERK-2 survival pathway mediates resistance of human mesothelioma cells to asbestos injury (50). Therefore, it would be important to know whether mesothelioma cells are resistant to NiNP or MWCNT exposure as a consequence of ERK-2 signaling. Additionally, we also found that ERK activation is important for PDGF-BB to increase HIF-1α, typically associated with hypoxia and oxidative stress, while ROS mediated NiNP-induced HIF-1α. These findings are highly relevant to *in vivo* exposures since macrophages have previously been shown to accumulate at the subpleural region after exposure to other nanomaterials that cause pleural fibrosis. Macrophages could influence the biological responses of mesothelial cells by triggering increased expression of pro-fibrotic growth factors such as PDGF-BB when exposed to NiNP (Fig. 7). In summary, our findings suggest that PDGF-BB is a critical co-activator of NiNP-induced chemokine production at the pleural mesothelium that relies on ERK phosphorylation and ROS generation as a central part of the signaling mechanism.

Acknowledgements

We thank Dr. Jeanette Shipley-Phillips at The College of Veterinary Medicine at North Carolina State University for excellent technical expertise in transmission electron microscopy for visualizing nanoparticles in cultured mesothelial cells.

References

1. Donaldson K, Murphy FA, Duffin R, Poland CA. Asbestos, carbon nanotubes and the pleural mesothelium: a review of the hypothesis regarding the role of long fibre retention in the parietal pleura, inflammation and mesothelioma. *Part Fibre Toxicol* 2010;7:5-22.

2. Pumera M. Carbon nanotubes contain residual metal catalyst nanoparticles even after washing with nitric acid at elevated temperature because these metal nanoparticles are sheathed by several graphene sheets. *Langmuir* 2007;23:6453–6458.

3. Jones J, Warner C. Chronic exposure to iron oxide, chromium oxide, and nickel oxide fumes of metal dressers in a steelworks. *Brit J Industr Med* 1972;29:167-177.

4. Kasprzak K, Sunderman F, Salnikow K. Nickel carcinogenesis. *Mutat Res* 2003;533:67–97.

5. Kane AB. Animal models of malignant mesothelioma. *Inhal Toxicol* 2006;18:1001–1004.

6. Ogami A, Morimoto Y, Myojo T, Oyabu T, Murakami M, Todoroki M, Nishi K, Kadoya C, Yamamoto M, Tanaka I. Pathological features of different sizes of nickel oxide following intratracheal instillation in rats. *Inhal Toxicol* 2009;21:812–818.

7. Zhang Q, Kusaka Y, Sato K, Nakakuki K, Kohyama N, Donaldson K. Differences in the extent of inflammation caused by intratracheal exposure to three ultrafine metals: role of free radicals. *J Toxicol Environ Health Part A* 1998;53:423–438.

8. Ryman-Rasmussen JP, Cesta MF, Brody AR, Shipley-Phillips JK, Everitt JI, Tewksbury EW, Moss OR, Wong BA, Dodd DE, Andersen ME, Bonner JC. Inhaled carbon nanotubes reach the subpleural tissue in mice. *Nat Nanotechnol* 2009;4:747–751.

9. Cesta MF, Ryman-Rasmussen JP, Wallace DG, Masinde T, Hurlburt G, Taylor AJ, Bonner JC. Bacterial lipopolysaccharide enhances PDGF signaling and pulmonary fibrosis in rats exposed to carbon nanotubes. *Am J Resp Cell Mol* 2010;43:142–151.

10. Bonner JC. Regulation of PDGF and its receptors in fibrotic diseases. *Cytokine Growth F R* 2004;15:255–273.

11. Kuwabara K, Ogawa S, Matsumoto M, Koga S, Clauss M, Pinsky DJ, Lyn P, Leavy J, Witte L, Joseph-Silverstein J. Hypoxia-mediated induction of acidic/basic fibroblast growth factor and platelet-derived growth factor in mononuclear phagocytes stimulates growth of hypoxic endothelial cells. *Proc Natl Acad Sci USA* 1995;92:4606–4610.

12. Bonner JC. Mesenchymal cell survival in airway and interstitial pulmonary fibrosis.

Fibrogenesis Tissue Repair 2010;3:15-29.

13. Mutsaers SE, Prele CM, Brody AR, Idell S. Pathogenesis of pleural fibrosis. *Respirology* 2004;9:428–440.

14. Shukla A, MacPherson MB, Hillegass J, Ramos-Nino ME, Alexeeva V, Vacek PM, Bond JP, Pass HI, Steele C, Mossman BT. Alterations in Gene Expression in Human Mesothelial Cells Correlate with Mineral Pathogenicity. *Am J Resp Cell Mol* 2009;41:114-123.

15. Walker C, Bermudez E, Stewart W, Bonner J, Molloy CJ, Everitt J. Characterization of platelet-derived growth factor and platelet-derived growth factor receptor expression in asbestos-induced rat mesothelioma. *Cancer Res* 1992;52:301–306.

16. Alberta JA, Auger KR, Batt D, Iannarelli P, Hwang G, Elliott HL, Duke R, Roberts TM, Stiles CD. Platelet-derived growth factor stimulation of monocyte chemoattractant protein-1 gene expression is mediated by transient activation of the phosphoinositide 3-kinase signal transduction pathway. *J Biol Chem* 1999;274:31062–31067.

17. Freter RR, Alberta JA, Hwang GY, Wrentmore AL, Stiles CD. Platelet-derived growth factor induction of the immediate-early gene MCP-1 is mediated by NF-kappaB and a 90-kDa phosphoprotein coactivator. *J Biol Chem* 1996;271:17417–17424.

18. Tanaka S, Choe N, Iwagaki A, Hemenway D, Kagan E. Asbestos exposure induces MCP-1 secretion by pleural mesothelial cells. *Exp Lung Res* 2001;26:241–255.

19. Hill GD, Mangum JB, Moss OR, Everitt JI. Soluble ICAM-1, MCP-1, and MIP-2 protein secretion by rat pleural mesothelial cells following exposure to amosite asbestos. *Exp Lung Res* 2003;29:277–290.

20. Gharaee-Kermani M, Denholm EM, Phan SH. Costimulation of fibroblast collagen and transforming growth factor beta1 gene expression by monocyte chemoattractant protein-1 via specific receptors. *J Biol Chem* 1996;271:17779–17784.

21. Moore BB, Paine R, Christensen PJ, Moore TA, Sitterding S, Ngan R, Wilke CA, Kuziel WA, Toews GB. Protection from pulmonary fibrosis in the absence of CCR2 signaling. *J Immunol* 2001;167:4368–4377.

22. Gharaee-Kermani M. CC-chemokine receptor 2 required for bleomycin-induced pulmonary fibrosis. *Cytokine* 2003;24:266–276.

23. Hong KH. Monocyte chemoattractant protein-1-induced angiogenesis is mediated by vascular endothelial growth factor-A. *Blood* 2005;105:1405–1407.

24. Keane MP, Belperio JA, Arenberg DA, Burdick MD, Xu ZJ, Xue YY, Strieter RM. IFN-gamma-inducible protein-10 attenuates bleomycin-induced pulmonary fibrosis via inhibition of angiogenesis. *J Immunol* 1999;163:5686–5692.

25. Neville LF, Mathiak G, Bagasra O. The immunobiology of interferon-gamma inducible protein 10 kD (IP-10): a novel, pleiotropic member of the C-X-C chemokine superfamily. *Cytokine Growth F R* 1997;8:207–219.

26. Belperio JA, Keane MP, Arenberg DA, Addison CL, Ehlert JE, Burdick MD, Strieter RM. CXC chemokines in angiogenesis. *J Leukoc Biol* 2000;68:1–8.

27. Jiang D, Noble P. Regulation of pulmonary fibrosis by chemokine receptor CXCR3. *J Clin Invest* 2004;114:291–299.

28. Antao-Menezes A, Turpin EA, Bost PC, Ryman-Rasmussen JP, Bonner JC. STAT-1 signaling in human lung fibroblasts is induced by vanadium pentoxide through an IFN-beta autocrine loop. *J Immunol* 2008;180:4200–4207.

29. Bermudez E, Libbus B, Mangum JB. Rat pleural mesothelial cells adapted to serum-free medium as a model for the study of growth factor effects. *Cell Biol Toxicol* 1998;14:243–251.

30. Nel A, Tian X, Mädler L, Li N. Toxic potential of materials at the nanolevel. *Science* 2006: 311:622-627.

31. Zhang Q, Kusaka Y, Zhu X, Sato K, Mo Y, Kluz T, Donaldson K. Comparative toxicity of standard nickel and ultrafine nickel in lung after intratracheal instillation. *J Occup Health* 2003:45:23-30.

32. Ryman-Rasmussen JP, Tewksbury EW, Moss OR, Cesta MF, Wong BA, Bonner JC. Inhaled Multiwalled Carbon Nanotubes Potentiate Airway Fibrosis in Murine Allergic Asthma. *Am J Resp Cell Mol* 2008;40:349–358.

33. Yi ES, Lee H, Yin S, Piguet P, Sarosi I, Kaufmann S, Tarpley J, Wang NS, Ulich TR. Platelet-derived growth factor causes pulmonary cell proliferation and collagen deposition in vivo. *Am J Pathol* 1996;149:539–548.

34. Homma S, Nagaoka I, Abe H, Takahashi K, Seyama K, Nukiwa T, Kira S. Localization of platelet-derived growth factor and insulin-like growth factor I in the fibrotic lung. *Am J Respir Crit Care Med* 1995;152:2084–2089.

35. Nagaoka I, Trapnell BC, Crystal RG. Upregulation of platelet-derived growth factor-A and -B gene expression in alveolar macrophages of individuals with idiopathic

pulmonary fibrosis. *J Clin Invest* 1990;85:2023–2027.

36. Fine A, Goldstein RH. The effect of transforming growth factor-beta on cell proliferation and collagen formation by lung fibroblasts. *J Biol Chem* 1987;262:3897–3902.

37. Visser CE, Tekstra J, Brouwer-Steenbergen JJ, Tuk CW, Boorsma DM, Sampat-Sardjoepersad SC, Meijer S, Krediet RT, Beelen RH. Chemokines produced by mesothelial cells: huGRO-alpha, IP-10, MCP-1 and RANTES. *Clin Exp Immunol* 1998;112:270–275.

38. Tager A, Luster A, Kradin R. T-cell chemokines interferon-inducible protein-10 and monokine induced by interferon-gamma are upregulated in bleomycin-induced lung injury. *Chest* 1999;116:90S.

39. Mrstik M, Kotseos K, Ma C, Chegini N. Increased expression of interferon-inducible protein-10 during surgically induced peritoneal injury. *Wound Repair Regen* 2003;11:120–126.

40. Jurek A, Amagasaki K, Gembarska A, Heldin CH, Lennartsson J. Negative and positive regulation of MAPK phosphatase 3 controls platelet-derived growth factor-induced Erk activation. *J Biol Chem* 2009;284:4626–4634.

41. Murphy L, Blenis J. MAPK signal specificity: the right place at the right time. *Trends Biochem Sci* 2006;31:268–275.

42. Luster AD, Ravetch JV. Biochemical characterization of a gamma interferon-inducible cytokine (IP-10). *J Exp Med* 1987;166:1084–1097.

43. Huang X, Frenkel K, Klein CB, Costa M. Nickel induces increased oxidants in intact cultured mammalian cells as detected by dichlorofluorescein fluorescence. *Toxicol Appl Pharm* 1993;120:29–36.

44 Andrew AS, Klei LR, Barchowsky A. Nickel requires hypoxia-inducible factor-1 alpha, not redox signaling, to induce plasminogen activator inhibitor-1. *Am J Physiol Lung Cell Mol Physiol* 2001;281:L607–615.

45. Jiang BH, Rue E, Wang GL, Roe R, Semenza GL. (1996) Dimerization, DNA binding, and transactivation properties of hypoxia-inducible factor 1. *J Biol Chem* 1996;271:17771–17778.

46. Jimenez LA, Zanella C, Fung H, Janssen YM, Vacek P, Charland C, Goldberg J, Mossman BT. Role of extracellular signal-regulated protein kinases in apoptosis by asbestos and H2O2. *Am J Physiol* 1997;273:L1029–1035.

47. Pietruska JR, Liu X, Smith A, McNeil K, Weston P, Zhitkovich A, Hurt R, Kane AB. Bioavailability, intracellular mobilization of nickel, and HIF-1α activation in human lung epithelial cells exposed to metallic nickel and nickel oxide nanoparticles. *Toxicol Sci* 2011;124:138–148.

48. Wan R, Mo Y, Chien S, Li Y, Tollerud D, Zhang Q. The role of hypoxia inducible factor-1α in the increased MMP-2 and MMP-9 production by human monocytes exposed to nickel nanoparticles. *Nanotoxicology* 2011;5:568–582.

49. Denkhaus E, Salnikow K. Nickel essentiality, toxicity, and carcinogenicity. *Crit Rev Oncol Hematol* 2002;42:35–56.

50. Shukla A, Barrett TF, MacPherson MB, Hillegass JM, Fukagawa NK, Swain WA, O'Byrne KJ, Testa JR, Pass HI, Faux SP, Mossman BT. An extracellular signal-regulated kinase 2 survival pathway mediates resistance of human mesothelioma cells to asbestos-induced injury. *Am J Resp Cell Mol* 2011;45:906-914.

Figure Legends

FIGURE 1. Nickel nanoparticles (NiNP) behave as nanoparticle agglomerates in cell culture medium and are taken up by pleural mesothelial cells *in vitro*. NiNP were dispersed in a bath sonicator for two hours in a 0.1% pluronic F-68 in phosphate buffer solution prior to dosing NRM2 cells as indicated in *Materials & Methods*. NiNP exposed NRM2 cells were collected at 24 h and characterized using transmission electron microscopy (TEM) imaging. (*A*) NiNP agglomerate in control medium. (*B*) Size distribution showing the majority of NiNP had a diameter between 20-50 nm. (*C*) NiNP agglomerates (black arrows) were observed in contact with the cell membrane and within the cytoplasm of a cultured NRM2 cell. (*D*) Higher magnification of the black box in (*C*) showing NiNP agglomerates enclosed within a membrane-bound vesicle in the NRM2 cell. (*E*) CBNP agglomerates (black arrows) were also observed in contact with the cell membrane and within the cytoplasm. (*F*) Higher magnification of the black box in (*E*) showing CBNP agglomerate enclosed within a membrane-bound vesicle. Subcellular structures indicated are nucleus (Nu), microvilli (Mv), mitochondria (Mi) and lysosome (Ly).

FIGURE 2. Nickel nanoparticles (NiNP) synergistically increase PDGF-induced CCL2 and CXCL10 mRNA and protein expression in rat pleural mesothelial cells. NRM2 cells were grown to confluency, serum starved for 24 h and treated with PDGF-BB (50 ng/mL) alone or immediately prior to adding CBNP or NiNP (10 μg/cm^2). Either mRNA or cell culture supernatants were collected for analysis by Taqman quantitative real-time RT-PCR or ELISA, respectively. (*A*) CCL2 mRNA analyzed at 24 h. ***$p < 0.001$ compared to control

determined by one-way ANOVA with post-hoc Tukey test. $^{\#\#}p < 0.01$, between NiNP and PDGF + NiNP or $^{+++}p < 0.001$ between PDGF and PDGF + NiNP as determined by two-way ANOVA with Bonferroni post-test. (*B*) Secreted CCL2 protein at 24 h. $^{***}p < 0.001$ compared to control determined by one-way ANOVA. $^{\#\#}p < 0.01$, between NiNP and PDGF + NiNP or $^{++}p < 0.01$ between PDGF and PDGF + NiNP as determined by two-way ANOVA. (*C*) CXCL10 mRNA levels at 24 h. $^{*}p < 0.05$ compared to control determined by one-way ANOVA. $^{\#}p < 0.05$, between NiNP and PDGF + NiNP or $^{+}p < 0.05$ between PDGF and PDGF + NiNP as determined by two-way ANOVA. (*D*) Secreted CXCL10 protein at 48 h. $^{*}p < 0.01$ or $^{***}p < 0.001$ compared to control. $^{\#\#}p < 0.01$, between NiNP and PDGF + NiNP or $^{+++}p < 0.001$ between PDGF and PDGF + NiNP as determined by two-way ANOVA. All data represent mean values ± SEM of three experiments ran in duplicate.

FIGURE 3. Nickel nanoparticles (NiNP) enhance and prolong PDGF-induced ERK phosphorylation but not PDGF-Rβ in rat pleural mesothelial cells. NRM2 cells were grown to confluency, serum starved and treated with PDGF-BB (50 ng/mL) or PDGF-BB plus NiNP (10 μg/cm^2) and cell lysates were collected at 2 and 24 h post-exposure. (*A*) Western blot analysis showing strong PDGF-induced phosphorylated ERK (p-ERK) at 2 h that is almost completely diminished by 24 h. NiNP co-exposure did not alter PDGF-induced ERK phosphorylation at 2 h, but enhanced PDGF-induced activation at 24 h. Total ERK protein levels were not changed by any of the treatments. (*B*) Densitometry of the blots in (*A*) showed the relative ratio of p-ERK to total ERK protein for each time point. Densitometric analysis was performed using Image J analysis software (NIH) as described in *Materials and*

Methods and represent mean values ± SEM of three experiments. (*C*) Western blot analysis showed PDGF-BB-induced phosphorylation of PDGF-Rβ at 15 min that is not affected by NiNP. PDGF-BB-induced PDGF-Rβ phosphorylation was diminished by 24 h and not affected by NiNP. $^{**}p < 0.01$ compared with untreated (control) and NiNP exposed cells, $^{***}p < 0.001$ compared to cells treated with control or NiNP alone as determined by one-way ANOVA with post-hoc Tukey test and $^{\wedge}p < 0.05$ compared with cells treated with PDGF alone as determined by two-way ANOVA with Bonferroni post-test. Both western blots shown are representative of at least three independent experiments that produced similar results.

FIGURE 4. CXCL10 and CCL2 expression in rat pleural mesothelial cells is regulated by the MEK-ERK signaling pathway. NRM2 cells were grown to confluency, serum starved and then pretreated with 20 μM PD98059 (black bars) for 1 h prior to adding PDGF (50 ng/mL) or NiNP (10 μg/cm^2) alone or in combination for 24 h or 48 h. (*A*) Western blot analysis showing phospho- and total ERK protein levels in cell lysates from NRM2 cells. (*B*) CXCL10 mRNA levels at 24 h and secreted protein levels at 48 h from NRM2 cells were measured using TaqMan quantitative real time RT-PCR or ELISA, respectively. (*C*) CCL2 mRNA and secreted protein levels were measured at 24 h after exposure. Data represent mean values ± SEM of three experiments ran in duplicate. $^{**}p < 0.01$ or $^{***}p < 0.001$ compared to cells in same exposure group treated with MEK inhibitor, PD98059, and determined by two-way ANOVA with Bonferroni post-test.

FIGURE 5. PDGF enhancement of nickel nanoparticle induced HIF-1α is mediated by MAPK signaling. NRM2 cells were grown to confluency, serum starved and then pretreated with 20 μM PD98059 (black bars) for 1 h prior to adding PDGF (50 ng/ml) or NiNP (10 μg/cm^2) alone or in combination for 24 h or 48 h. (*A*) Western blot analysis of HIF-1α protein levels in cell lysates from NRM2 cells showing that PDGF enhancement of NiNP induced HIF-1α is reduced by PD98059. (*B*) Densitometry of Western blots in (*A*) showing the relative ratio of HIF-1α to β-actin protein for each treatment. Densitometric analysis was performed using Image J analysis software (NIH) as described in *Materials and Methods*. All data represent mean values ± SEM of three independent experiments. ***$p < 0.001$ compared to control or PDGF treatment with or without PD98059 as determined by one-way ANOVA with post-hoc Tukey test, $^{###}p < 0.001$ compared NiNP to PDGF + NiNP treatment without PD98059, or $^p < 0.05$ compared to cells in same exposure group treated without MEK inhibitor, PD98059 as determined by two-way ANOVA with Bonferroni post-test. Western blot shown is a representative of at least three independent experiments that produced similar results.

FIGURE 6. HIF-1α and CCL2 expression induced by NiNP and PDGF is reduced by the anti-oxidant, NAC. NRM2 cells were grown to confluency, serum starved and then pretreated with 5 mM NAC for 1 h prior to adding PDGF (50 ng/mL) or NiNP (10 μg/cm^2) alone or in combination for 24 h. (*A*) Representative western blot of HIF-1α protein levels in cell lysates from NRM2 cells showing that induction of HIF-1α levels after treatment with NiNP or NiNP and PDGF-BB were both reduced by NAC. (*B*) Densitometry of three

independent Western blots including the representative blot displayed in (*A*) showing the relative ratio of HIF-1α to β-actin protein for each treatment. Densitometric analysis was performed using Image J analysis software (NIH) as described in *Materials and Methods*. *(C)* Western blot showing increased levels of phosphorylated ERK-1,2 (p-ERK-1,2) after 24 hr treatment with the combination of PDGF and NiNP that were reduced by 1 hr pretreatment with NAC. Note that ERK-1,2 phosphorylation is transiently induced by PDGF alone at 2 hr and returns to basal levels by 24 hr (see Fig. 3). (*D*) ELISA results showing that CCL2 protein induced by the combination of NiNP and PDGF is significantly reduced by pretreatment with NAC. The ELISA data are from a single experiment with samples run in triplicate. *$p < 0.05$ or **$p < 0.01$ compared to cells in same exposure group treated without NAC as determined by two-way ANOVA with Bonferroni post-test.

FIGURE 7. Schematic illustration showing the hypothetical cell signaling mechanism involved in the synergistic induction of HIF-1α and chemokines by NiNP and PDGF in rat pleural mesothelial cells. NiNP are taken up by pleural mesothelial cells to generate ROS, increase HIF-1α and stimulate chemokine production. PDGF-BB, a growth factor produced by activated alveolar macrophages or other cellular sources, binds to PDGF-Rβ on mesothelial cells to stimulate ERK phosphorylation and marginally increase chemokine production. NiNP is postulated to increased the duration of PDGF-induced ERK phosphorylation and thereby synergistically increase the production of CCL2 and CXCL10, which play important roles in the progression and resolution of pleural fibrogenesis, respectively.

Figures

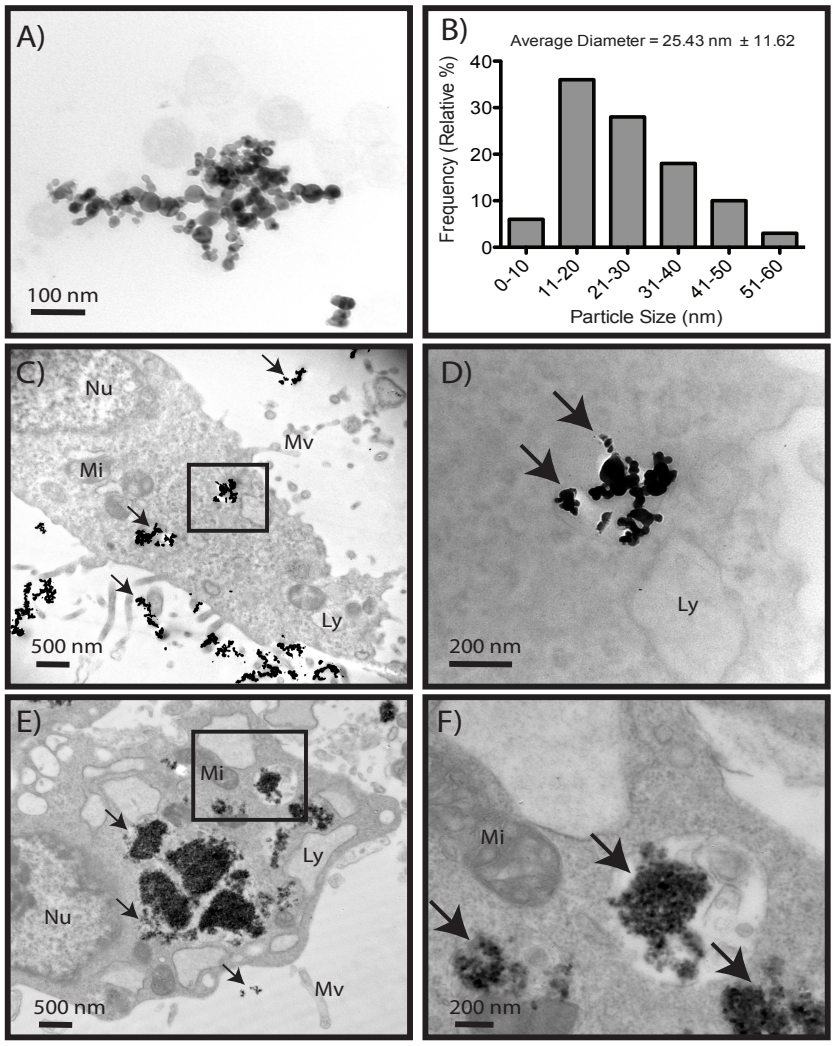

Figure 1. NiNPs behave as nanoparticle agglomerates in cell culture medium and are taken up by pleural mesothelial cells *in vitro*.

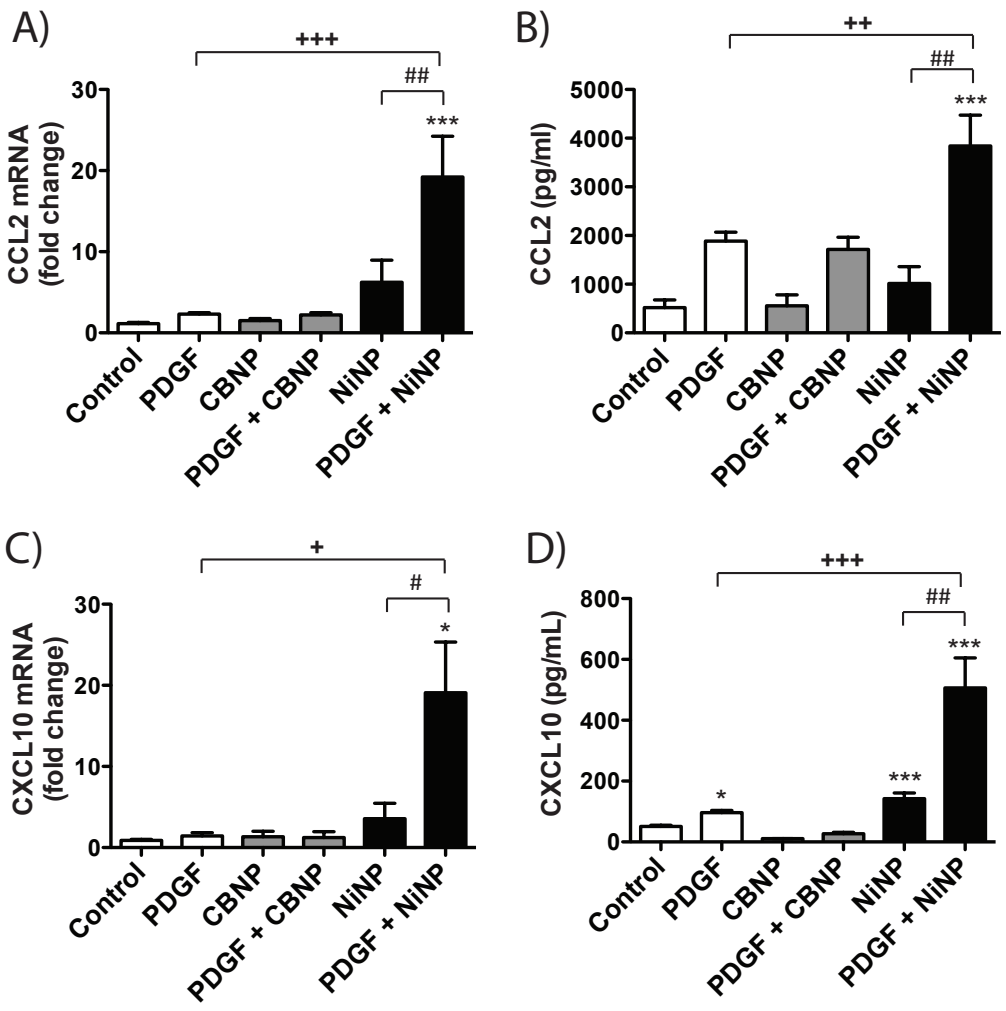

Figure 2. NiNPs synergistically increase PDGF-induced CCL2 and CXCL10 mRNA and protein expression in rat pleural mesothelial cells.

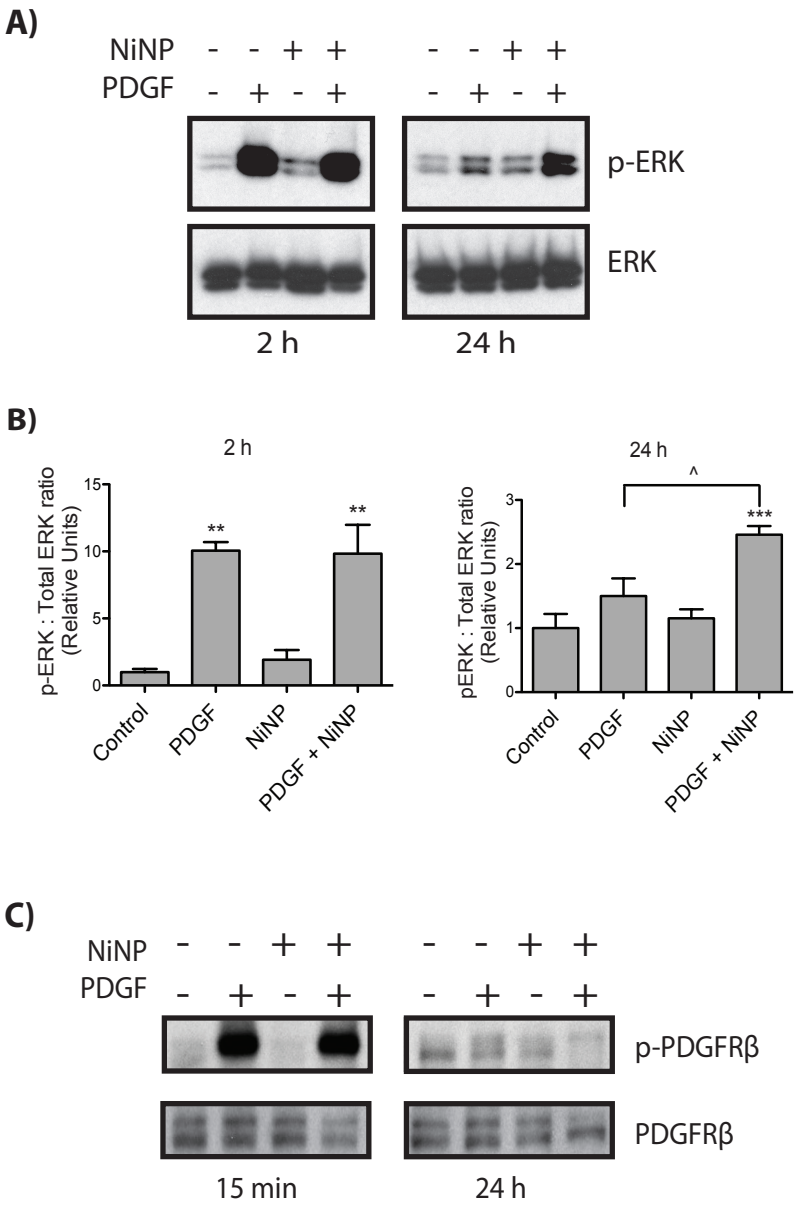

Figure 3. NiNPs enhance and prolong PDGF-induced ERK phosphorylation but not PDGF-Rβ in rat pleural mesothelial cells.

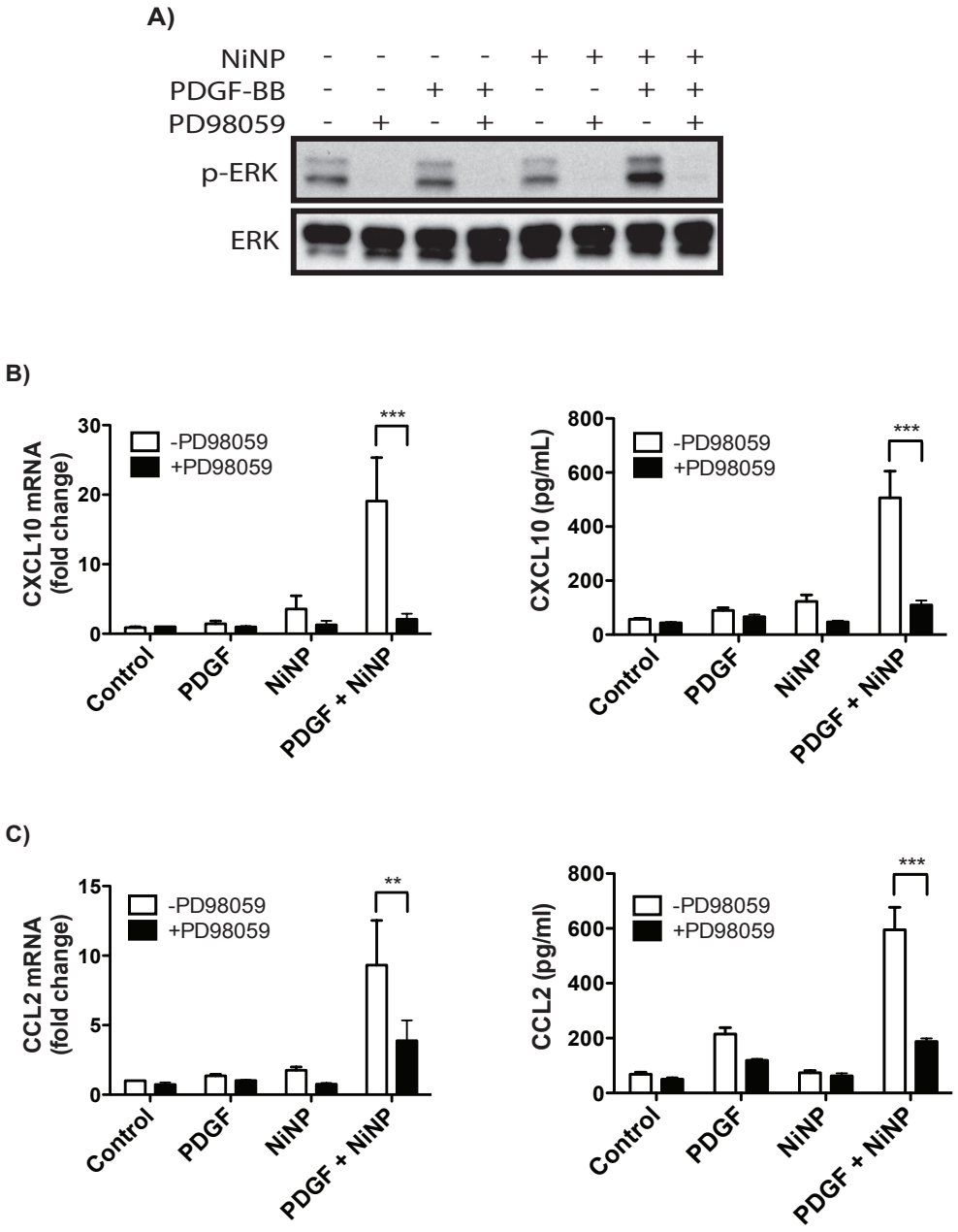

Figure 4. CXCL10 and CCL2 expression in rat pleural mesothelial cells is regulated by the MEK-ERK signaling pathway.

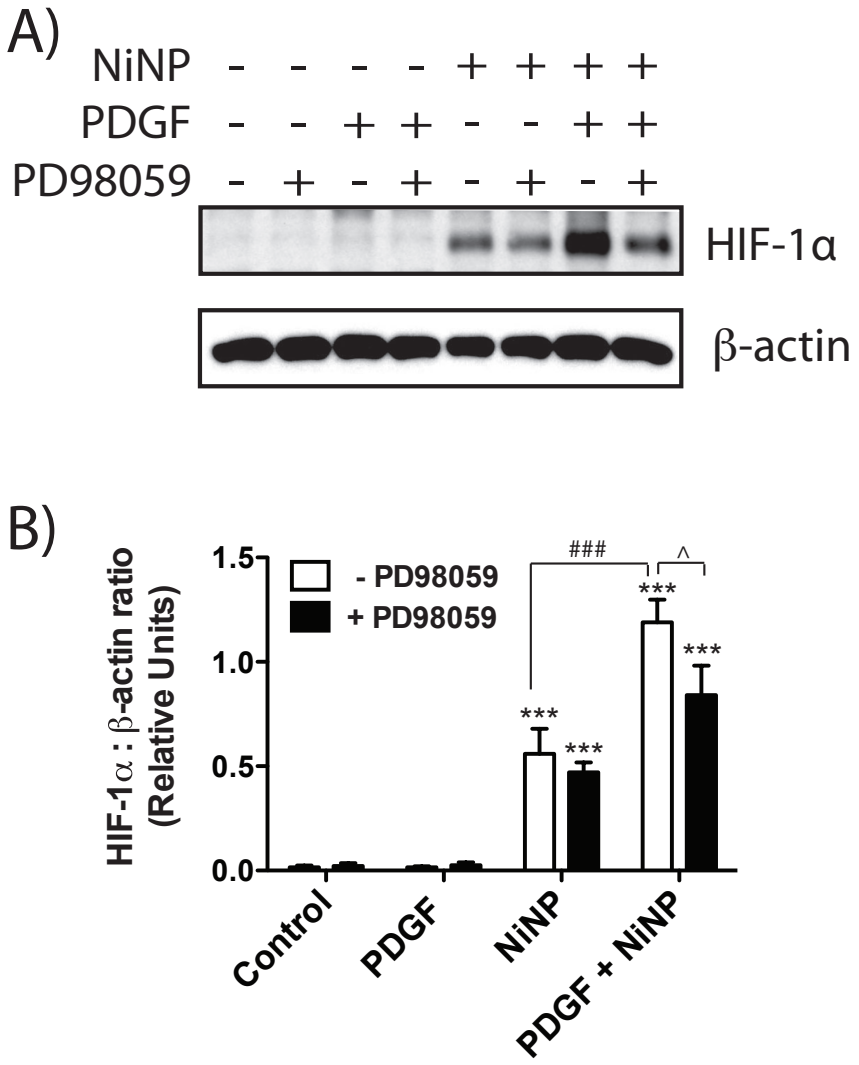

Figure 5. PDGF enhancement of nickel nanoparticle induced HIF-1α is mediated by MAPK signaling.

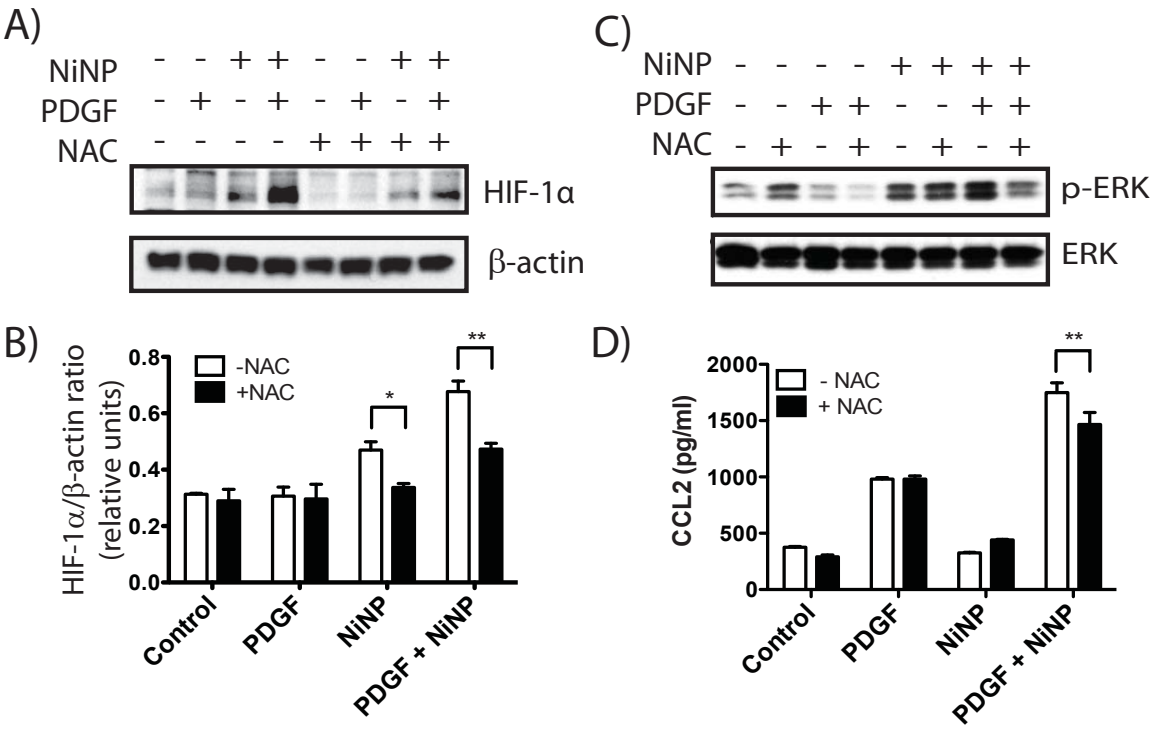

Figure 6. HIF-1α and CCL2 expression induced by NiNP and PDGF is reduced by the anti-oxidant, NAC.

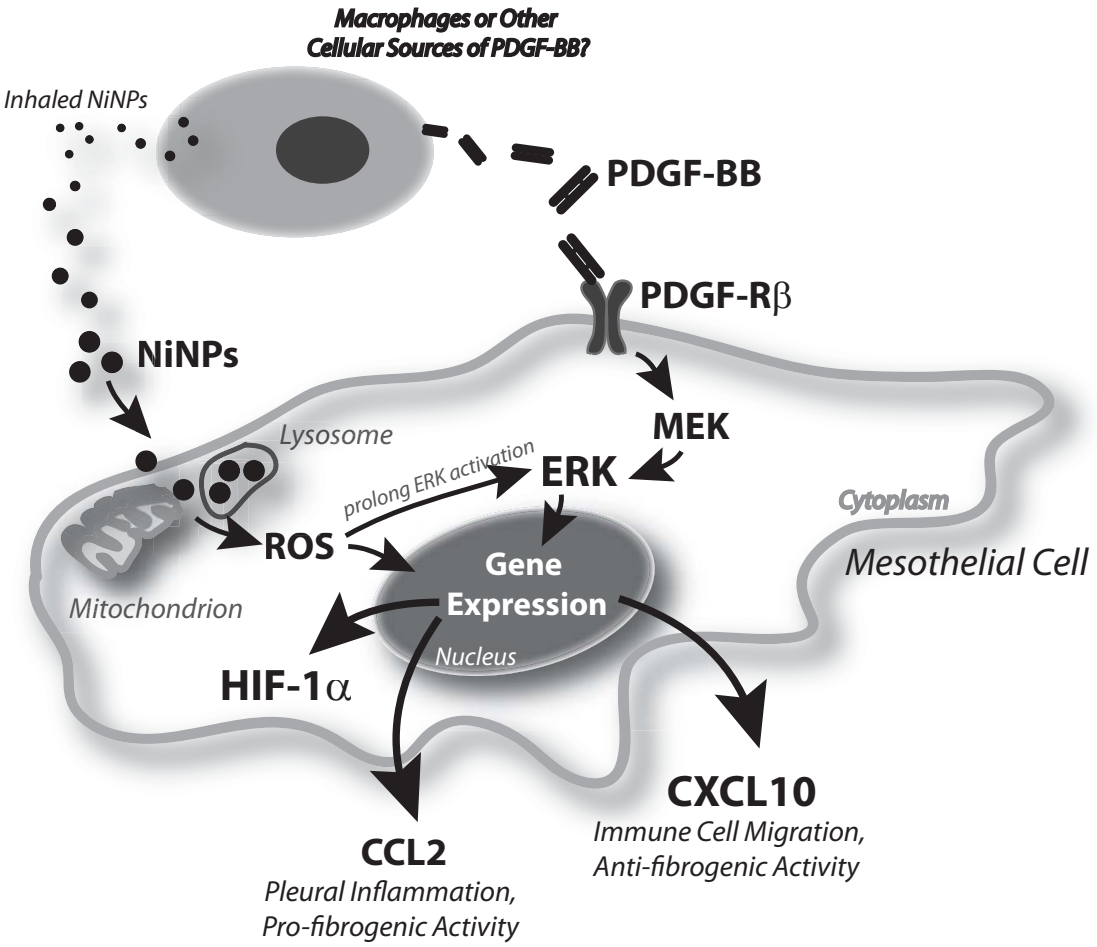

Figure 7. Schematic illustration showing the hypothetical cell signaling mechanism involved in the synergistic induction of HIF-1α and chemokines by NiNP and PDGF in rat pleural mesothelial cells.

Data Supplement

Supplementary Methods

Nanoparticle Characterization. According to the manufacturer, NiNP were spherical and had an average diameter of 20nm, ranging from 2-50nm, with a specific surface area of 40-60 m^2/g, a metal purity of 99.9%, and insolubility in water. They were additionally characterized as a pure metal nanoparticle in oxidation state (0) zero (Choquette *et al*. 2011). Carbon black nanoparticles (CBNP), approximately 100% amorphous carbon, were from Columbian Chemicals as Raven® 5000 Ultra II Powder (Marietta, GA) had a mean diameter of 8nm, an external surface area of 350 m^2/g, and were insoluble in water. NiNP and CBNP were suspended in a sterile, 0.1% pluronic F-68 (Sigma) in phosphate buffer solution at a stock concentration of 10 mg/mL and then dispersed for two hours using a bath sonicator at room temperature prior to dosing.

Cell Culture and Treatment with PDGF, NiNP, and inhibitors. Normal rat pleural mesothelial cells (NRM2) were cultured in a modified 1:1 mixture of F-12 Kaighn's and Dulbecco's Modified Eagle Medium (Invitrogen) containing 10% fetal bovine serum (Gibco), 0.2% Insulin, Transferrin, and Selenium (ITS, Lonza) and 50μM hydrocortisone (Sigma) and exhibited a cobblestone morphology once confluent (37°C, 5% CO_2). NRM2 cells were grown to confluence in 60mm cell culture dishes (BD Biosciences) and rendered quiescent for 24 h in 5mL of serum-free defined medium. NRM2 cells were treated with either NiNP (10 $\mu g/cm^2$) or CBNP (10 $\mu g/cm^2$, negative control) in the absence or presence of PDGF-BB (50 ng/ml) (R&D Systems) while untreated cells were dosed with pluronic

solution alone (control). The MEK inhibitor PD98059 was from (Cell Signaling) and L-NAC was from (Sigma). The final concentration of NiNP or CBNP was determined using the surface area of the cell culture dish since the particles participated out of solution easily. NRM2 cells were viable with all treatments at all time points therefore cell culture supernatants, cell lysates, and total RNA was collected for ELISA, western blot or Taqman real-time RT-PCR analysis, respectively.

Supplementary Reference

Choquette KA, Sadasivam DV, Flowers RA 2nd. Catalytic Ni(II) in reactions of SmI2: Sm(II)- or Ni(0)-based chemistry? *J Am Chem Soc.* 2011 133(27):10655-61.

Supplementary Figure Legends

FIGURE S1. Dose-response relationship and time course of CCL2 mRNA and protein expression by NRM2 cells treated with PDGF-BB. (A) CCL2 mRNA levels in NRM2 cells and (B) CCL2 protein levels in NRM2 supernatants 24 hr after treatment with a PDGF-BB concentration range. (C) Time course of CCL2 mRNA in NRM2 cells and (D) CCL2 protein in NRM2 supernatants after treatment with 50 ng/mL PDGF-BB. Each data set shown is from a representative experiment of two to three independent experiments that produced similar results.

FIGURE S2. Dose-response relationship and time course of CCL2 mRNA and protein expression by NRM2 cells treated with nickel nanoparticles (NiNP). (A) CCL2 mRNA

levels in NRM2 cells 24 hr after treatment with a NiNP concentration range. (B) Time course of CCL2 mRNA in NRM2 cells and (C) CCL2 protein levels in NRM2 supernatants after treatment with 10 mg/cm^2 NiNP. Each data set shown is from a representative experiment of two to three independent experiments that produced similar results.

FIGURE S3. Time course of CXCL10 mRNA and protein expression by NRM2 cells exposed to nickel nanoparticles (NiNP) in the absence or presence of PDGF-BB. (A) CXCL10 mRNA levels in NRM2 cells treated with PDGF-BB (50 ng/ml), NiNP (10 mg/cm^2), or a combination of PDGF-BB and NiNP over a time-course. (B) CXCL10 protein levels in NRM2 cell supernatants at 24 hr or 48 hr following treatment with PDGF-BB, NiNP, or PDGF-BB plus NiNP. Each data set shown is from a representative experiment of two to three independent experiments that produced similar results.

Online Data Supplement Figures

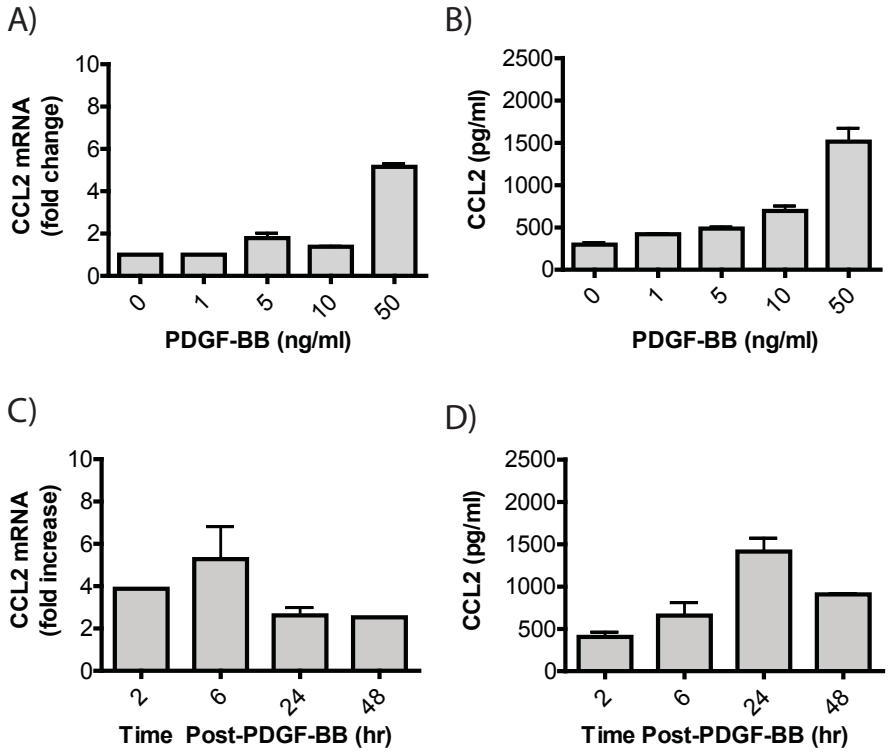

Figure S1. Dose-response relationship and time course of CCL2 mRNA and protein expression by NRM2 cells treated with PDGF-BB.

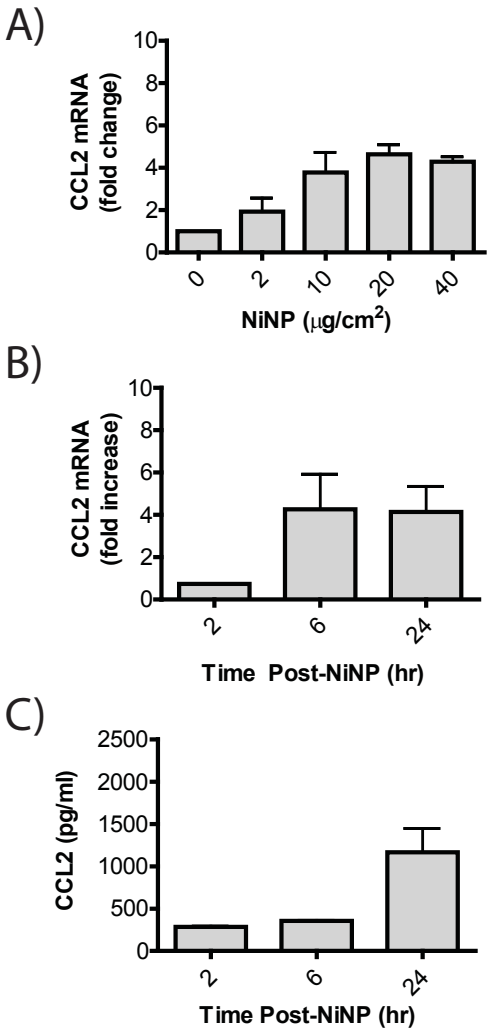

Figure S2. Dose-response relationship and time course of CCL2 mRNA and protein expression by NRM2 cells treated with NiNPs.

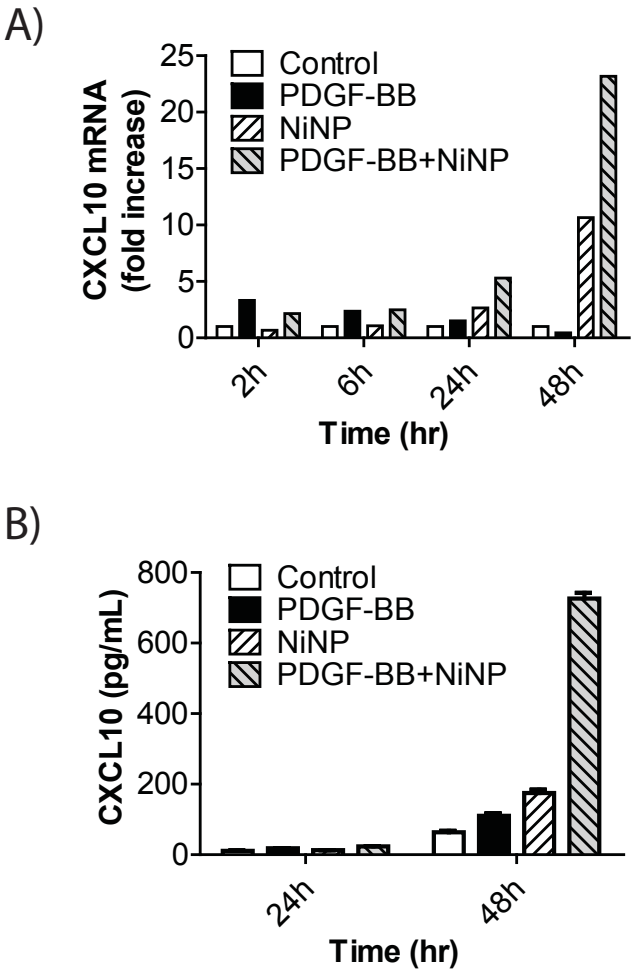

Figure S3. Time course of CXCL10 mRNA and protein expression by NRM2 cells exposed to nickel nanoparticles (NiNP) in the absence or presence of PDGF-BB.

GENERAL DISCUSSION

The growth and expansion of nanotechnology has lead to an increase in the production of a wide spectrum of engineered nanomaterials (ENMs) that possess unique physical and chemical properties. However, while ENMs are beneficial for use in a wide variety of applications, their novel physical and chemical properties along with their small size raise concerns about their potential effects on human health (1). Since inhalation is the major route of exposure, particularly in an occupational setting, our laboratory is interested in how ENMs affect the lung. We previously reported that inhaled multi-walled carbon nanotubes (MWCNT) exacerbate allergen-induced lung inflammation and airway fibrosis in mice therefore suggesting that individuals who have pre-existing lung disease are more susceptible to MWCNT inhalation (40). In another study, we found that the same type of MWCNTs could reach the subpleura of mice after inhalation exposure; a process that was facilitated in part by alveolar macrophage uptake and transport (17). This study also showed that MWCNTs caused inflammatory lesions on the mesothelial surface of the pleura and subpleural fibrotic lesions. Other researchers have also shown that nickel nanoparticles (NiNPs), the catalyst used in the manufacture of the MWCNTs we studied, induced pulmonary inflammation and pleural fibrosis (38, 39, 154). When compared to their micron-size nickel counterparts, NiNPs have a higher surface energy per unit mass that can increase their potential to generate reactive oxygen species and alter their interactions with the surrounding environment. Furthermore, they have also been shown to elicit greater injury in the lung when compared to their bulk counterparts, demonstrating that pulmonary toxicity increases as particle size decreases (1, 39). Therefore, the focus of this study was to gain a

better understanding of the cellular and molecular mechanisms that regulate NiNP-induced lung diseases.

Chapter 1: The T-box Transcription Factor, TBX21 (T-bet), Inhibits Airway Mucous Cell Metaplasia and Interstitial Fibrosis in Mice Induced by NiNPs

Asthma is a complex, heterogeneous disease of the airways that develops in response to a combination of genetic and environmental exposures (87). In our study, we decided to analyze the effects of NiNPs on pre-existing chronic lung inflammation by utilizing mice deficient in the transcription factor TBX21 (T-bet). While the classic animal model of asthma is induce by allergen sensitization and challenge in mice, a transgenic mouse model of asthma would provide us with a better understanding of the gene environment that regulates asthma pathogenesis. T-bet is an important transcription factor for the differentiation of naïve, mature T helper cells into Th1 cells through the production of interferon (IFN)-γ (88). When absent, T helper cells preferentially differentiate into Th2 cells in response to GATA-3 transcription, the Th2 transcription factor (155). Interestingly, transgenic mice lacking the T-bet transcription factor were generated and found to spontaneously display a phenotype similar to allergic lung inflammation in humans (89). Moreover, the airways of asthmatics were discovered to have diminished T-bet expression that was often associated with severity of the disease providing further validation for the use of T-bet$^{-/-}$ mice as an *in vivo* model of chronic airway remodeling (107, 108). Researchers have recognized the benefit of using these mice to better understand the mechanisms regulating pathogen-induced exacerbations in genetically predisposed asthma (104, 105). However, to our knowledge, no one has

studied the effects of particle inhalation on T-bet deficient airway remodeling. Therefore, our study was the first, to our knowledge, to investigate mechanisms of nanoparticle exacerbation of allergic lung inflammation using the T-bet$^{-/-}$ mouse model.

Following oropharyngeal exposure of NiNPs, we evaluated hallmark pathological features associated with the exacerbation of asthma such as mucous cell metaplasia, inflammation, and airway fibrosis. We have demonstrated for that first time that NiNPs induced significantly greater mucous cell metaplasia in T-bet$^{-/-}$ mice compared to wild-type mice. In asthma, mucus hypersecretion leads to increased airflow obstruction by blocking approximately 98% of the airways and accounting for the majority of fatal asthma cases (50, 51). It is therefore beneficial to understand what exacerbating agents increase mucus production and the mechanisms controlling it in order to develop better therapeutic approaches. Production of the protein mucin within goblet cells of the epithelium was analyzed through the use of an Alcian blue/periodic acid-Schiff (AB/PAS) stain and found to be significantly increased in response to NiNP in T-bet$^{-/-}$ mice 21 days after the initial exposure. In combination with mucin protein expression, we also saw a similar trend in mucin mRNA expression for MUC5AC and MUC5B, the two most prominent mucins upregulated in the lung (50). They were both upregulated in T-bet$^{-/-}$ mice in response to NiNPs 21 days post-exposure. However, we did not see a significant increase in mucin production in the WT mice, suggesting that NiNP exposure either did not increase mucin production in these mice or that mucin production was not prolonged to the same extent that it was in the absence of T-bet. In support of our results, previous reports have determined that T-bet is protective against the development of goblet cell hyperplasia and mucous cell

metaplasia. Three separate studies showed that the overexpression of T-bet caused a decrease in ovalbumin (OVA)-induced goblet cell hyperplasia in addition to airway hyperreactivity (AHR), eosinophilic inflammation, and airway collagen (106, 109, 110). Collectively, all of these studies indicate that T-bet is protective in suppressing mucus production by various environmental stimuli, including NiNPs.

Inflammation, like excess mucus production, contributes to chronic airway remodeling associated with the pathogenesis of asthma and when exacerbated leads to airflow obstruction (55). We postulated that NiNPs would increase inflammation in both WT and T-bet$^{-/-}$ mice since previous studies have already determined that ultrafine nickel compounds (i.e. NiNPs) induce pulmonary inflammation (37, 39, 156). In addition, we expected to observe that NiNP-induced inflammation was exacerbated in the T-bet$^{-/-}$ mice. However, while we did observe a significant increase in inflammation in response to NiNPs 1 day post-exposure as predicted, we did not see a difference in inflammation between the two genotypes. As mentioned above, other researchers have demonstrated that overexpression of T-bet protected against OVA-induced eosinophilic inflammation (106, 109, 110). Similarly, we observed a decrease in eosinophil infiltration from the bronchoalveolar lavage fluid (BALF) of WT mice when compared to T-bet$^{-/-}$ mice in response to NiNP-induced inflammation. We found that T-bet$^{-/-}$ mice had elevated base levels of eosinophils that were exaggerated in response to NiNPs 1 day post-exposure. These data agree with a previous study by Finotto *et al*., which showed a spontaneous increase in eosinophilia in T-bet$^{-/-}$ mice (89). After 21 days, NiNPs also increased the amount of lymphocytes present in the BALF of T-bet$^{-/-}$ mice. However, NiNP-treated WT mice had a

different profile of inflammatory cells in BALF that consisted of macrophages and neutrophils. Interestingly, neutrophil-dominated inflammation is often indicative of Th17-mediated allergic airway remodeling, a more severe phenotype of asthma, that is regulated by IL-17 (157).

Airway fibrosis, due to increased deposition of subepithelial collagen by peribronchiolar myofibroblasts, functionally limits dilation of the airway and restricts airflow that is often irreversible (158). We have previously found that MWCNTs increase OVA-induced airway fibrosis upon inhalation and thought that it would be important to study the effects of NiNPs, the catalyst used in the fabrication of these specific MWCNTs (40). In order to evaluate the fibrotic response, we analyzed airway-associated collagen deposition. We found that NiNP exposure in both WT and T-bet$^{-/-}$ mice caused a similar increase in the amount of collagen produced. However, upon semi-quantitative scoring of trichrome stained lung sections, we observed a significant difference in the degree of interstitial fibrotic lesions at 21 days post NiNP exposure in T-bet$^{-/-}$ mice when compared to WT. Following oropharyngeal aspiration of NiNPs, T-bet$^{-/-}$ mice displayed more fibrosis in the parenchyma of the lungs and larger lesions that surrounded NiNP agglomerates. A previous study, using fibrosis resistant BALB/c mice, determined that T-bet deficiency causes exacerbation of bleomycin-induced interstitial fibrosis through a Th2-dominanted response (159). These results, in addition to our findings, support the idea that T-bet protects against the development of fibrosis.

Since we observed an overall increase in NiNP-induced airway fibrosis and interstitial fibrosis, we measured mRNA and protein expression for the profibrotic mediators

IL-13 and CCL2. IL-13 has been shown to potentiate pulmonary fibrosis by promoting recruitment of myofibroblasts that produce collagen through a TGF-β1 dependent mechanism (160). CCL2, or monocyte chemoattractant protein-1, also induces fibrogenesis through the chemotaxis of myofibroblasts as well as by recruiting a variety of other cells to the site of injury such as macrophages, eosinophils, T cells, and mast cells (146, 161). CCL2 has previously been established as contributory to the pathogenesis of fibrosis in mice. Moore *et. al.* determined that mice deficient in CCR2, the receptor for CCL2, were protected from bleomycin-induced pulmonary fibrosis, thereby establishing CCL2 as a potent profibrotic mediator (147). T-bet$^{-/-}$ mice have been shown to have a Th2-mediated phenotype that includes elevated levels of IL-13 without sensitization and challenge from an allergen. However, it had not been previously determined whether CCL2 was involved in regulating any of the characteristics associated with T-bet deficient airway remodeling. In this study, we did not observe a spontaneous increase in basal levels of the IL-13 protein in the BALF. However, we did find that NiNPs significantly increased IL-13 protein in T-bet$^{-/-}$ mice 1 day after exposure as well as the mRNA in both genotypes. Additionally, levels of CCL2 mRNA and protein were also elevated in response to NiNP exposure in WT mice after 1 day but significantly increased in T-bet$^{-/-}$ mice. Furthermore, expression of CCL2 protein was prolonged 21 days past the initial NiNP exposure in both genotypes and further exaggerated in T-bet$^{-/-}$ mice. These findings support results from previous studies that demonstrated that nickel oxide nanoparticles also caused increased CCL2 protein *in vivo* (156, 162). Our results suggest that CCL2 could be mediating interstitial fibrosis development that is protected when T-bet is present due to the similar trend that we see in both sets of results. Moreover, CCL2

might also play a role in promoting allergic lung inflammation and mucin expression as well as it has been found increased in the airways of asthmatics and implicated in regulating MUC5AC and MUC5B expression (137, 139).

Therefore, we decided that we wanted to further understand the mechanisms behind the exacerbation of mucin production and interstitial fibrosis seen in response to NiNP in T-bet$^{-/-}$ mice. We used a neutralizing antibody to block CCL2 from binding to its receptor, CCR2, before and after NiNP exposure to prevent it from signaling downstream. First, we evaluated mucin production and mucin gene expression in NiNP exposed T-bet$^{-/-}$ mice in mice treated with either anti-CCL2 or a control monoclonal antibody, IgG2B Isotype Control. We expected to find that NiNP exacerbation of these features would be diminished in response to anti-CCL2 therapy based on the results of previous studies. Research indicated that neutralization of CCL2 in allergen-induced models of asthma decreased AHR, inflammation, and macrophage infiltration (163, 164). Results from our study showed an increase in mucin production in response to anti-CCL2 treatment in NiNP exposed T-bet$^{-/-}$ mice 21 days post-exposure. Interestingly, other investigators have also shown that blocking CCL2 signaling through the use of CCR2$^{-/-}$ mice also enhanced goblet cell hyperplasia in response to allergen exposure or fungal infection, similar to our results (143, 144).

Additionally, we also evaluated the development of NiNP-induced interstitial fibrosis in response to the anti-CCL2 neutralizing antibody. Our results showed that an anti-CCL2 mAb did not cause a significant reduction in NiNP-induced interstitial lesions in T-bet$^{-/-}$ mice, suggesting that CCL2 might not play an important role in nickel-induced lung fibrosis. However, neither soluble collagen nor Col1A1 mRNA levels were increased by NiNPs in T-

bet$^{-/-}$ mice, indicating that the interstitial lesions not be fibrotic, but may represent chronic inflammation or pneumonitis. Overall, the results from the monoclonal antibody experiment did not support our hypothesis since it did not significantly prevent mucous cell metaplasia and interstitial pneumonitis as we had expected. An assessment of the monoclonal antibody's activity could be performed in order to determine if the antibody operated appropriately to blocked and neutralized CCL2 activity. Additionally, it is interesting to note that the receptor for CCL2, CCR2, can also be phosphorylated by other chemokines from the CCL family such as CCL3 and CCL5, as previously mentioned. Therefore, even if CCL2 is neutralized properly, other ligands could bind to the receptor to initial downstream activity. Future studies could be designed to investigate how CCR2 signaling modulates airway remodeling in T-bet-deficient mice in response to NiNP exposure in the lung.

To summarize, in Chapter 1, we discovered that NiNPs induce lung injury such as mucous cell metaplasia, inflammation, and pulmonary fibrosis. Furthermore, we determined that T-bet is a critical transcription factor for the protection of NiNP-induced mucin expression and interstitial fibrosis while CCL2 signaling contributes to fibrogenesis but protects against the production of mucin. In conclusion, results from our study suggest that asthmatic individuals deficient in T-bet could be at a greater risk of exacerbation when exposed to engineered nanomaterials such as NiNPs.

Chapter 2: NiNPs Enhance PDGF-Induced Chemokine Expression by Mesothelial Cells via Prolonged MAP Kinase Activation

In addition to affecting individuals with pre-existing pulmonary disease, there are also concerns that NiNPs could contribute to the progression of pleural disease, which includes both subpleural fibrosis and mesothelioma. We have previously shown that inhalation exposure to MWCNTs, containing residual nickel, causes subpleural fibrotic lesions beneath the mesothelium, as well as pleural inflammation, due to their ability to reach the pleura (17). Furthermore, other studies have demonstrated that NiNPs alone can also cause interstitial and pleural fibrosis *in vivo* (38, 153, 154). Therefore, our study was designed to better understand the cellular and molecular mechanisms that could be contributing to the development of NiNP-induced inflammation and fibrosis along the pleura.

We hypothesized that PDGF-BB, a key growth factor involved in mediating fibrogenesis, would modify NiNP-induced expression of CCL2, a profibrotic mediator, and CXCL10, an anti-fibrotic mediator indicative of injury, in cultured rat pleural mesothelial cells *in vitro*. During fibrogenesis, PDGF-BB expression is significantly increased in alveolar macrophages, which engulf MWCNTs and migrate to the pleura where they accumulate and communicate with mesothelial cells (17, 130). Additionally, pleural mesothelial cells are also a source of PDGF-BB as demonstrated in response to asbestos exposure and injury (150, 151). Therefore, in order to test this hypothesis, we used cultured rat pleural mesothelial cells to determine how PDGF-BB modifies the effects of NiNPs *in vitro* (165). Carbon black nanoparticles (CBNPs) served as a negative control throughout this study to demonstrate that

the results produced in response to NiNPs were not elicited primarily based on size of the particle.

According to the manufacturer, the NiNPs we purchased were composed of a nickel purity of 99.9%, spherical in shape, and had an average diameter size of 20 nm. A previous study verified that these NiNPs were a pure metal nanoparticle by characterizing them as having an oxidation state of zero (0) (166). We began by determining the cellular effects of NiNPs on rat pleural mesothelial cells (NRM2 cells) using transmission electron microscopy (TEM). TEM images revealed that NiNPs and CBNPs dispersed in a 0.1% pluronic solution formed agglomerates, even after sonication, and were taken up within membrane-bound vesicles of the cell. Additionally, both nanoparticles retained their spherical shape after phagocytosis. This observation, combined with the NiNPs' oxidation state, suggests that there is no dissolution of nickel ions that would cause any biological effects. Therefore, the results that we observed in this study are mostly likely because of the large surface area of the nanoparticle that increases reactivity when nickel is nanosized.

Expression of the chemokines CCL2 and CXCL10 were analyzed in response to the combination of PDGF-BB and NiNPs in NRM2 cells. CCL2 was measured due to the role it plays in the development of fibrosis. As previously mentioned, CCL2 can be produced by alveolar macrophages or pleural mesothelial cells in response to injury to begin generating extracellular matrix for wound healing (146). Overexpression or prolonged expression of CCL2 stimulates fibroblasts to increase collagen expression by induction and activation of TGF-β1 (146, 150, 167). Additionally, expression of CXCL10 was also analyzed even though it has been suggested to be protective against fibrogenesis (147). Although

researchers have found that transgenic mice lacking the ability to induce CXCL10 signaling have exaggerated pulmonary fibrosis, it is increased as a result of injury and inflammation (168, 169). CXCL10 is increased by mesothelial cells during inflammation and recruits inflammatory cells such as fibroblasts to the site of injury (170, 171). It is therefore important to understand how each of these chemokines are regulated since they have important functions in the development and resolution of pleural fibrosis.

In order to determine the appropriate dose of PDGF-BB and NiNPs, as well as the correct time point, a dose response and time course was determined for each by evaluating CCL2 levels and CXCL10 expression. Once established, NRM2 cells were treated with either 10 $\mu g/cm^2$ of NiNPs or CBNPs in the absence or presence of PDGF-BB at 50 ng/ml and collected at the appropriate time point that coincided with the specific assay. Our preliminary results revealed that PDGF caused a transient increase in CCL2 while NiNPs prolonged its expression. Interestingly, the combination of the two, PDGF and NiNPs, caused a significant synergistic increase in CCL2 mRNA and protein expression by 24 hours. Similar to CCL2, PDGF initially increased CXCL10 levels while NiNPs sustained expression. Additionally, CXCL10 mRNA and protein was synergistically increased in response to the combination of the two. Furthermore, CBNPs with or without PDGF-BB did not significantly increase either CCL2 or CXCL10 mRNA or protein suggesting that the results observed in response to NiNPs were not merely because of the size of the particle. Our findings indicate that there could be potentially important interaction between endogenous growth factors and environmental exposures for the progression of subpleural fibrosis or even other pulmonary diseases.

Once we found that PDGF and NiNPs synergistically increased CCL2 and CXCL10, we wanted to determine the signaling intermediates that was involved in mediating their expression. PDGF-BB binds to the extracellular domain and dimerizes PDGF-Rα and/or PDGF-Rβ to form the functional receptors, PDGF-Rαα, PDGF-Rββ, or PDGF-Rαβ (127). In our study, PDGF-BB induced phosphorylation of PDGF-Rβ and not PDGF-Rα. Furthermore, NiNPs did not alter phosphorylation of the receptor suggesting that it is involved in signaling mechanisms that occur downstream of PDGF-Rβ. Extracellular signal-related kinase (ERK1,2) is a classical mitogen-activated protein kinase (MAPK) that often signals downstream from PDGF in response to phosphorylation from the receptor's intracellular domains. ERK1,2 signaling is involved in regulating a wide variety of cellular activities including proliferation, differentiation, and survival, which are dependent on duration of the signal and cell type (172, 173). Therefore, we evaluated ERK1,2 phosphorylation in response to PDGF and NiNP exposure. Western blot analysis revealed that NiNPs prolonged PDGF-induced ERK1,2 phosphorylation suggesting that ERK1,2 stabilization was contributing to the synergistic expression of CCL2 and CXCL10.

In order to determine if sustained ERK1,2 phosphorylation was involved it regulating CCL2 and CXCL10 levels, we pre-treated the NRM2 cells with a MEK inhibitor, PD98059, to block ERK1,2 activity. Using a MEK inhibitor prevents phosphorylation of the MAP kinase cascade by binding to the inactive forms of MEK1,2 and inhibiting its activation. MEK1,2 is a MAPK kinase (MAPKK) signals upstream of ERK1,2 and activates it through phosphorylation (174). We found that blocking ERK1,2 from being phosphorylated in

NRM2 cells significantly inhibited PDGF plus NiNP-induced expression of both CCL2 and CXCL10, thereby validating the involvement of ERK1,2 in the signaling pathway.

Nanoparticles have been shown to increase the generation of reactive oxygen species (ROS) due to their small size and larger surface area reactivity. Furthermore, nano-sized metals are thought to generate additional ROS due to the presence of the metal on the surface of the particle (1). NiNPs, in addition to micron-sized nickel, have previously been shown to induce the generation of ROS, such as hydrogen peroxide and oxygen radicals (175, 176). In the cell, the presence of ROS often creates a hypoxic environment that leads to the stabilization of hypoxia-inducible factor (HIF)-1α, a biomarker of oxidative stress (177). We hypothesized that HIF-1α protein would be stabilized in response to NiNP exposure to further influence CCL2 and CXCL10 expression. Our results revealed a statistically significant effect from NiNP exposure on HIF-1α in NRM2 cells. Furthermore, the addition of PDGF to NiNP exposure significantly enhanced the expression of HIF-1α. Since NiNPs and PDGF also had a combined effect on ERK1,2 phosphorylation that lead to the synergistic increase of CCL2 and CXCL10, we wanted to determine if ERK1,2 was involved in HIF-1α stabilization. After treating the cells with the MEK1,2 inhibitor to block ERK1,2, we observed that the MEK1,2 inhibitor prevented PDGF from enhancing NiNP-induced HIF-1α expression but not induction of HIF-1α by NiNPs alone. Therefore, our results suggested that PDGF enhancement of NiNP-induced HIF-1α was ERK-dependent, while NiNP-induced expression of HIF-1α was ERK-independent. Additionally, our data support results from a previous study that also demonstrate that the stabilization of HIF-1α can be regulated by ROS-induced ERK phosphorylation in rat pleural mesothelial cells (178).

Although HIF-1α is indicative of oxidative stress, further analysis of NiNP-induced ROS mediated HIF-1α needed to be determined. Therefore, we decided to pretreat the NRM2 cells with an antioxidant, *N*-acetyl-*L*-cysteine (NAC), prior to exposure of NiNPs and PDGF in order to increase free radical scavengers that would decrease the generation of ROS production. Western blot analysis revealed that treatment with NAC significantly decreased HIF-1α protein levels after exposure to NiNPs alone or in combination with PDGF. ERK1,2 phosphorylation, as well as CCL2 protein levels induced by the combination of NiNPs and PDGF, were also significantly reduced in response to NAC treatment. However, due to the cytotoxicity of NAC past 24 hours, the effects of NiNPs and PDGF on the expression of CXCL10 could not be evaluated since it was analyzed at 48 hours post-exposure instead of 24 hours like CCL2. Pretreatment of NRM2 cells with NAC indicated that ROS is involved in mediating NiNP induction of HIF-1α while also contributing to PDGF plus NiNP phosphorylation of ERK1,2 and CCL2 expression. Moreover, NAC had no effect on PDGF-induced CCL2 and only partially reduced its expression after PDGF and NiNP exposure. Together our results indicate that ROS-dependent and independent signaling occurs to synergistically increase HIF-1α stabilization, ERK1,2 activation, and chemokine expression.

Our laboratory has previously determined that MWCNTs, containing residual nickel, induce subpleural fibrosis and inflammation after inhalation exposure (17). Additionally, we have also demonstrated that macrophages are a significant source of PDGF-BB in response to MWCNT exposure (40). Our present findings are highly relevant to both of our previous studies since we revealed that cultured mesothelial cells increased CCL2, a monocyte chemoattractant chemokine, in response to NiNP and PDGF exposure. Increased CCL2

levels from mesothelial cells could explain why there was an increase in MWCNT-containing macrophages migration and accumulation to the subpleura *in vivo*. Furthermore, while Ryman-Rasmussen *et. al.* observed inhaled MWCNTs in the subpleural wall after 14 weeks, there was a decrease in subpleural fibrosis compared to the response that was seen earlier from 2 to 6 weeks. In our study, in response to NiNPs and PDGF in cultured pleural mesothelial cells, we observed an increase in CXCL10, an anti-fibrotic chemokine that could contribute to the resolution of fibrosis. To summarize, our findings demonstrate how the combination of PDGF-BB, a pro-fibrotic growth factor, and NiNPs alters cellular signaling in rat pleural mesothelial cells. In response to injury by NiNPs, PDGF-BB acts as a critical co-activator to synergistically induce expression of chemokines involved in the development of pleural fibrosis through prolonged ERK phosphorylation and ROS generation.

General Conclusions

Both of these studies are important in order to better understand the mechanisms that regulate NiNP-induced exacerbation of pulmonary diseases such as allergic airway remodeling and pleural inflammation. While researchers have previously established nickel as an asthmagen, our study is the first to analyze the effects of nanosized nickel in pre-existing lung inflammation (152). Currently, there are approximately 170 million people being exposed to ambient ultrafine nickel particulates, however with the substantial growth of the nanotechnology industry that number is expected to increase dramatically over the next few years (26). Therefore, it is important to understand how NiNPs, as well as other engineered nanomaterials, affect susceptible populations in order to protect those at the

greatest risk. Additionally, there are concerns that NiNPs could cause idiopathic pulmonary fibrosis and pleural fibrosis upon inhalation due to the nanomaterial's unique physical and chemical properties as well as its high surface area per unit mass. However, because the nanotechnology industry is its early stages, there still is not any epidemiologic data showing that ENMs cause fibrogenic or carcinogenic effects in humans. Nevertheless, nanosized metals, such as NiNPs, represent a unique risk to human health since their micron-sized counterparts are known to induce lung disease (2, 38, 176). Therefore, precautionary measures should especially be taken into consideration when it comes to exposure of metal nanomaterials (2).

In summary, our *in vivo* study established that NiNP exposure in the lung could increase inflammation, fibrosis, and mucin production. Furthermore, it demonstrated that NiNPs exacerbate interstitial pulmonary fibrosis and mucous cell metaplasia in pre-existing, T-bet deficient, allergic airway inflammation implicating that the transcription factor, T-bet, is necessary to protect against NiNP-induced injury. Future studies could be designed to compare the effects of micron-sized nickel particles to NiNP in the lung in order to better assess the toxicity of the nanoparticles. Furthermore, analyzing studies for longer time points and exposing mice to NiNPs through inhalation rather than oropharyngeal aspiration could also be important to better understand lung diseases such as pleural fibrosis and mesothelioma. Additionally, *in vitro* experiments using established rat pleural mesothelial cells revealed that NiNPs act together with the pro-fibrotic growth factor, PDGF-BB, to synergistically increase CCL2 and CXCL10 chemokines through prolonged ERK1,2 phosphorylation and ROS-dependent HIF-1α stabilization. Additionally, further analysis of

the role that HIF-1α plays should be analyzed in order to better understand how it alone can also regulate CCL2 and CXCL10 production. These results suggest that PDGF-BB is a critical co-activator that potentiates NiNP-induced cellular mechanisms that could contribute to the development of pleural fibrosis. All together, we have established critical regulatory cell signaling mechanisms involved in the exacerbation of allergic airway inflammation and pleural fibrosis induced by NiNP injury. The research is important for understanding the relative risk of NiNPs, compared to other nanoparticles, to guide regulatory agencies in making decisions regarding the safe production and use of NiNPs to prevent occupational, environmental or consumer exposures. Furthermore, identifying key features involved in the progression of these diseases is vital for the development of effective therapies. Overall, we are hopeful that our research will help to better understand the extent in which ENMs can cause harm in order to prevent future exposures that could induce disease.

GENERAL REFERENCES

1. Nel, A., T. Xia, L. Mädler, and N. Li. 2006. Toxic potential of materials at the nanolevel. *Science* 311: 622–627.

2. Bonner, J. C. 2010. Nanoparticles as a Potential Cause of Pleural and Interstitial Lung Disease. *Proceedings of the American Thoracic Society* 7: 138–141.

3. Buzea, C., I. I. Pacheco, and K. Robbie. 2007. Nanomaterials and nanoparticles: sources and toxicity. *Biointerphases* 2: MR17–71.

4. Card, J. W., D. C. Zeldin, J. C. Bonner, and E. R. Nestmann. 2008. Pulmonary applications and toxicity of engineered nanoparticles. *AJP: Lung Cellular and Molecular Physiology* 295: L400–L411.

5. Tiede, K., A. B. A. Boxall, S. P. Tear, J. Lewis, H. David, and M. Hassellov. 2008. Detection and characterization of engineered nanoparticles in food and the environment. *Food Addit Contam Part A Chem Anal Control Expo Risk Assess* 25: 795–821.

6. Wang, X., Q. Li, J. Xie, Z. Jin, J. Wang, Y. Li, K. Jiang, and S. Fan. 2009. Fabrication of ultralong and electrically uniform single-walled carbon nanotubes on clean substrates. *Nano Lett.* 9: 3137–3141.

7. Donaldson, K., F. A. Murphy, R. Duffin, and C. A. Poland. 2010. Asbestos, carbon nanotubes and the pleural mesothelium: a review of the hypothesis regarding the role of long fibre retention in the parietal pleura, inflammation and mesothelioma. *Part Fibre Toxicol* 7: 5.

8. Jaurand, M.-C. F., A. Renier, and J. Daubriac. 2009. Mesothelioma: Do asbestos and carbon nanotubes pose the same health risk? *Part Fibre Toxicol* 6: 16.

9. Donaldson, K., and C. A. Poland. 2009. Nanotoxicology: New insights into nanotubes. *Nature Nanotechnology* 1–2.

10. Lam, C.-W., J. T. James, R. McCluskey, and R. L. Hunter. 2004. Pulmonary toxicity of single-wall carbon nanotubes in mice 7 and 90 days after intratracheal instillation. *Toxicol. Sci.* 77: 126–134.

11. Shvedova, A. A., E. R. Kisin, R. Mercer, A. R. Murray, V. J. Johnson, A. I. Potapovich, Y. Y. Tyurina, O. Gorelik, S. Arepalli, D. Schwegler-Berry, A. F. Hubbs, J. Antonini, D. E. Evans, B.-K. Ku, D. Ramsey, A. Maynard, V. E. Kagan, V. Castranova, and P. Baron. 2005. Unusual inflammatory and fibrogenic pulmonary responses to single-walled carbon nanotubes in mice. *Am. J. Physiol. Lung Cell Mol. Physiol.* 289: L698–708.

12. Mangum, J. B., E. A. Turpin, A. Antao-Menezes, M. F. Cesta, E. Bermudez, and J. C. Bonner. 2006. Single-Walled Carbon Nanotube (SWCNT)-induced interstitial fibrosis in the lungs of rats is associated with increased levels of PDGF mRNA and the formation of uniue intercellular carbon structures that bridge alveolar macrophages *In Situ*. *Part Fibre Toxicol* 3: 15.

13. Muller, J., F. Huaux, N. Moreau, P. Misson, J.-F. Heilier, M. Delos, M. Arras, A. Fonseca, J. B. Nagy, and D. Lison. 2005. Respiratory toxicity of multi-wall carbon nanotubes. *Toxicology and Applied Pharmacology* 207: 221–231.

14. Li, J.-G., W.-X. Li, J.-Y. Xu, X.-Q. Cai, R.-L. Liu, Y.-J. Li, Q.-F. Zhao, and Q.-N. Li. 2007. Comparative study of pathological lesions induced by multiwalled carbon nanotubes in lungs of mice by intratracheal instillation and inhalation. *Environ. Toxicol.* 22: 415–421.

15. Mitchell, L. A., J. Gao, R. V. Wal, A. Gigliotti, S. W. Burchiel, and J. D. McDonald. 2007. Pulmonary and systemic immune response to inhaled multiwalled carbon nanotubes. *Toxicol. Sci.* 100: 203–214.

16. Poland, C. A., R. Duffin, I. Kinloch, A. Maynard, W. A. H. Wallace, A. Seaton, V. Stone, S. Brown, W. MacNee, and K. Donaldson. 2008. Carbon nanotubes introduced into the abdominal cavity of mice show asbestos-like pathogenicity in a pilot study. *Nature Nanotechnology* 3: 423–428.

17. Ryman-Rasmussen, J. P., M. F. Cesta, A. R. Brody, J. K. Shipley-Phillips, J. I. Everitt, E. W. Tewksbury, O. R. Moss, B. A. Wong, D. E. Dodd, M. E. Andersen, and J. C. Bonner. 2009. Inhaled carbon nanotubes reach the subpleural tissue in mice. *Nature Nanotechnology* 4: 747–751.

18. Brown, D. M., I. A. Kinloch, U. Bangert, A. H. Windle, D. M. Walter, G. S. Walker, C. A. Scotchford, K. Donaldson, and V. Stone. 2007. An in vitro study of the potential of carbon nanotubes and nanofibres to induce inflammatory mediators and frustrated phagocytosis. *Carbon* 45: 1743–1756.

19. Mitchell, L. A., F. T. Lauer, S. W. Burchiel, and J. D. McDonald. 2009. Mechanisms for how inhaled multiwalled carbon nanotubes suppress systemic immune function in mice. *Nature Nanotechnology* 4: 451–456.

20. Erdely, A., T. Hulderman, R. Salmen, A. Liston, P. C. Zeidler-Erdely, D. Schwegler-Berry, V. Castranova, S. Koyama, Y.-A. Kim, M. Endo, and P. P. Simeonova. 2009. Cross-talk between lung and systemic circulation during carbon nanotube respiratory exposure. Potential biomarkers. *Nano Lett.* 9: 36–43.

21. Sanchez, V. C., J. R. Pietruska, N. R. Miselis, R. H. Hurt, and A. B. Kane. 2009.

Biopersistence and potential adverse health impacts of fibrous nanomaterials: what have we learned from asbestos? *Wiley Interdiscip Rev Nanomed Nanobiotechnol* 1: 511–529.

22. Gwinn, M. R., and V. Vallyathan. 2006. Nanoparticles: health effects--pros and cons. *Environ Health Perspect* 114: 1818–1825.

23. Donaldson, K., D. Brown, A. Clouter, R. Duffin, W. MacNee, L. Renwick, L. Tran, and V. Stone. 2002. The pulmonary toxicology of ultrafine particles. *J Aerosol Med* 15: 213–220.

24. Oberdörster, G., J. Ferin, and B. E. Lehnert. 1994. Correlation between particle size, in vivo particle persistence, and lung injury. *Environ Health Perspect* 102 Suppl 5: 173–179.

25. Oberdörster, G., J. Ferin, R. Gelein, S. C. Soderholm, and J. Finkelstein. 1992. Role of the alveolar macrophage in lung injury: studies with ultrafine particles. *Environ Health Perspect* 97: 193–199.

26. Leikauf, G. D. 2002. Hazardous air pollutants and asthma. *Environ Health Perspect* 110 Suppl 4: 505–526.

27. Hinds, W. C. 2012. *Aerosol Technology*. Wiley-Interscience.

28. Oberdörster, G. 2000. Pulmonary effects of inhaled ultrafine particles. *International archives of occupational and environmental health* 74: 1–8.

29. Andujar, P., S. Lanone, P. Brochard, and J. Boczkowski. 2011. Respiratory effects of manufactured nanoparticles. *Revue des Maladies Respiratoires* 28: e66–e75.

30. Park, S., Y. K. Lee, M. Jung, K. H. Kim, N. Chung, E.-K. Ahn, Y. Lim, and K.-H. Lee. 2007. Cellular toxicity of various inhalable metal nanoparticles on human alveolar epithelial cells. *Inhalation Toxicology* 19 Suppl 1: 59–65.

31. Duffin, R., L. Tran, D. Brown, V. Stone, and K. Donaldson. 2007. Proinflammogenic effects of low-toxicity and metal nanoparticles in vivo and in vitro: highlighting the role of particle surface area and surface reactivity. *Inhalation Toxicology* 19: 849–856.

32. Pumera, M. 2007. Carbon nanotubes contain residual metal catalyst nanoparticles even after washing with nitric acid at elevated temperature because these metal nanoparticles are sheathed by several graphene sheets. *Langmuir* 23: 6453–6458.

33. Bonner, J. C. 2010. Mesenchymal cell survival in airway and interstitial pulmonary fibrosis. *Fibrogenesis Tissue Repair* 3: 15.

34. Wittczak, T., W. Dudek, J. Walusiak-Skorupa, D. Świerczyńska-Machura, W. Cader, M.

Kowalczyk, and C. Pałczyński. 2012. Metal-induced asthma and chest X-ray changes in welders. *Int J Occup Med Environ Health* 25: 242–250.

35. Fernández-Nieto, M., S. Quirce, and J. Sastre. 2006. Occupational asthma in industry. *Allergol Immunopathol (Madr)* 34: 212–223.

36. Kasprzak, K., F. Sunderman, and K. Salnikow. 2003. Nickel carcinogenesis. *Mutation Research* 533: 67–97.

37. Magaye, R., and J. Zhao. 2012. Recent progress in studies of metallic nickel and nickel-based nanoparticles' genotoxicity and carcinogenicity. *Environ. Toxicol. Pharmacol.*

38. Ogami, A., Y. Morimoto, T. Myojo, T. Oyabu, M. Murakami, M. Todoroki, K. Nishi, C. Kadoya, M. Yamamoto, and I. Tanaka. 2009. Pathological features of different sizes of nickel oxide following intratracheal instillation in rats. *Inhalation Toxicology* 21: 812–818.

39. Zhang, Q., Y. Kusaka, X. Zhu, K. Sato, Y. Mo, T. Kluz, and K. Donaldson. 2003. Comparative toxicity of standard nickel and ultrafine nickel in lung after intratracheal instillation. *J Occup Health* 45: 23–30.

40. Ryman-Rasmussen, J. P., E. W. Tewksbury, O. R. Moss, M. F. Cesta, B. A. Wong, and J. C. Bonner. 2008. Inhaled Multiwalled Carbon Nanotubes Potentiate Airway Fibrosis in Murine Allergic Asthma. *American Journal of Respiratory Cell and Molecular Biology* 40: 349–358.

41. Centers for Disease Control and Prevention (CDC). 2011. Vital signs: asthma prevalence, disease characteristics, and self-management education: United States, 2001--2009. *MMWR Morb. Mortal. Wkly. Rep.* 60: 547–552.

42. Cruz, A. A. 2007. Global surveillance, prevention and control of chronic respiratory diseases: a comprehensive approach.

43. Medoff, B. D., S. Y. Thomas, and A. D. Luster. 2008. T Cell Trafficking in Allergic Asthma: The Ins and Outs. *Annu. Rev. Immunol.* 26: 205–232.

44. 1998. Worldwide variation in prevalence of symptoms of asthma, allergic rhinoconjunctivitis, and atopic eczema: ISAAC. The International Study of Asthma and Allergies in Childhood (ISAAC) Steering Committee. *Lancet* 351: 1225–1232.

45. Gold, D. R., and R. Wright. 2005. Population disparities in asthma. *Annu Rev Public Health* 26: 89–113.

46. March, M. E., P. M. Sleiman, and H. Hakonarson. 2013. Genetic polymorphisms and

associated susceptibility to asthma. *Int J Gen Med* 6: 253–265.

47. British Thoracic Society Scottish Intercollegiate Guidelines Network. 2008. British Guideline on the Management of Asthma. *Thorax* 63 Suppl 4: iv1–121.

48. Kaminska, M., S. Foley, K. Maghni, C. Storness-Bliss, H. Coxson, H. Ghezzo, C. Lemière, R. Olivenstein, P. Ernst, and Q. Hamid. 2009. Airway remodeling in subjects with severe asthma with or without chronic persistent airflow obstruction. *J. Allergy Clin. Immunol.* 124: 45–51. e4.

49. Murphy, D. M., and P. M. O'Byrne. 2010. Recent advances in the pathophysiology of asthma. *Chest* 137: 1417–1426.

50. Evans, C. M., K. Kim, M. J. Tuvim, and B. F. Dickey. 2009. Mucus hypersecretion in asthma: causes and effects. *Curr Opin Pulm Med* 15: 4–11.

51. Kuyper, L. M., P. D. Paré, J. C. Hogg, R. K. Lambert, D. Ionescu, R. Woods, and T. R. Bai. 2003. Characterization of airway plugging in fatal asthma. *Am. J. Med.* 115: 6–11.

52. Yawn, B. P. 2008. Factors accounting for asthma variability: achieving optimal symptom control for individual patients. *Prim Care Respir J* 17: 138–147.

53. Ying, S., Q. Meng, K. Zeibecoglou, D. S. Robinson, A. Macfarlane, M. Humbert, and A. B. Kay. 1999. Eosinophil chemotactic chemokines (eotaxin, eotaxin-2, RANTES, monocyte chemoattractant protein-3 (MCP-3), and MCP-4), and C-C chemokine receptor 3 expression in bronchial biopsies from atopic and nonatopic (Intrinsic) asthmatics. *J. Immunol.* 163: 6321–6329.

54. Singh, A. M., and W. W. Busse. 2006. Asthma exacerbations. 2: aetiology. *Thorax* 61: 809–816.

55. Wark, P. A. B., and P. G. Gibson. 2006. Asthma exacerbations . 3: Pathogenesis. *Thorax* 61: 909–915.

56. McDonald, V. M., and P. G. Gibson. 2012. Exacerbations of severe asthma. *Clin. Exp. Allergy* 42: 670–677.

57. BOUSQUET, J., P. K. JEFFERY, W. W. BUSSE, M. JOHNSON, and A. M. VIGNOLA. Asthma. *http://dx.doi.org.prox.lib.ncsu.edu/10.1164/ajrccm.161.5.9903102*.

58. Jinfang Zhu, W. E. P. 2008. CD4 T cells: fates, functions, and faults. *Blood* 112: 1557–1569.

59. Vock, C., H.-P. Hauber, and M. Wegmann. 2010. The other T helper cells in asthma pathogenesis. *J Allergy (Cairo)* 2010: 519298.

60. Luckheeram, R. V., R. Zhou, A. D. Verma, and B. Xia. 2012. CD4+T Cells: Differentiation and Functions. *Clinical and Developmental Immunology* 2012: 1–12.

61. Cohn, L., R. J. Homer, N. Niu, and K. Bottomly. 1999. T helper 1 cells and interferon gamma regulate allergic airway inflammation and mucus production. *J. Exp. Med.* 190: 1309–1318.

62. Hansen, G., G. Berry, R. H. DeKruyff, and D. T. Umetsu. 1999. Allergen-specific Th1 cells fail to counterbalance Th2 cell-induced airway hyperreactivity but cause severe airway inflammation. *J. Clin. Invest.* 103: 175–183.

63. Van Oosterhout, A., and A. C. Motta. 2005. Th1/Th2 paradigm: not seeing the forest for the trees? *Eur. Respir. J.* 25: 591–593.

64. Robinson, D. S., Q. Hamid, S. Ying, A. Tsicopoulos, J. Barkans, A. M. Bentley, C. Corrigan, S. R. Durham, and A. B. Kay. 1992. Predominant TH2-like bronchoalveolar T-lymphocyte population in atopic asthma. *N. Engl. J. Med.* 326: 298–304.

65. Kaplan, M. H., U. Schindler, S. T. Smiley, and M. J. Grusby. 1996. Stat6 is required for mediating responses to IL-4 and for development of Th2 cells. *Immunity* 4: 313–319.

66. Zhu, J., H. Yamane, J. Cote-Sierra, L. Guo, and W. E. Paul. 2006. GATA-3 promotes Th2 responses through three different mechanisms: induction of Th2 cytokine production, selective growth of Th2 cells and inhibition of Th1 cell-specific factors. *Cell Res.* 16: 3–10.

67. Finkelman, F. D., S. P. Hogan, G. K. K. Hershey, M. E. Rothenberg, and M. Wills-Karp. 2010. Importance of cytokines in murine allergic airway disease and human asthma. *The Journal of Immunology* 184: 1663–1674.

68. Barnes, P. J. 2008. The cytokine network in asthma and chronic obstructive pulmonary disease. *J. Clin. Invest.* 118: 3546–3556.

69. Grünig, G., M. Warnock, A. E. Wakil, R. Venkayya, F. Brombacher, D. M. Rennick, D. Sheppard, M. Mohrs, D. D. Donaldson, R. M. Locksley, and D. B. Corry. 1998. Requirement for IL-13 independently of IL-4 in experimental asthma. *Science* 282: 2261–2263.

70. Kuperman, D. A., X. Huang, L. L. Koth, G. H. Chang, G. M. Dolganov, Z. Zhu, J. A. Elias, D. Sheppard, and D. J. Erle. 2002. Direct effects of interleukin-13 on epithelial cells cause airway hyperreactivity and mucus overproduction in asthma. *Nat Med* 8: 885–889.

71. Yang, G., L. Li, A. Volk, E. Emmell, T. Petley, J. Giles-Komar, P. Rafferty, M. Lakshminarayanan, D. E. Griswold, P. J. Bugelski, and A. M. Das. 2005. Therapeutic dosing with anti-interleukin-13 monoclonal antibody inhibits asthma progression in mice. *J. Pharmacol. Exp. Ther.* 313: 8–15.

72. Bree, A., F. J. Schlerman, M. Wadanoli, L. Tchistiakova, K. Marquette, X.-Y. Tan, B. A. Jacobson, A. Widom, T. A. Cook, N. Wood, S. Vunnum, R. Krykbaev, X. Xu, D. D. Donaldson, S. J. Goldman, J. Sypek, and M. T. Kasaian. 2007. IL-13 blockade reduces lung inflammation after Ascaris suum challenge in cynomolgus monkeys. *J. Allergy Clin. Immunol.* 119: 1251–1257.

73. Catley, M. C., J. Coote, M. Bari, and K. L. Tomlinson. 2011. Monoclonal antibodies for the treatment of asthma. *Pharmacology and Therapeutics* 132: 333–351.

74. McKinley, L., J. F. Alcorn, A. Peterson, R. B. Dupont, S. Kapadia, A. Logar, A. Henry, C. G. Irvin, J. D. Piganelli, A. Ray, and J. K. Kolls. 2008. TH17 cells mediate steroid-resistant airway inflammation and airway hyperresponsiveness in mice. *The Journal of Immunology* 181: 4089–4097.

75. Bullens, D. M. A., E. Truyen, L. Coteur, E. Dilissen, P. W. Hellings, L. J. Dupont, and J. L. Ceuppens. 2006. IL-17 mRNA in sputum of asthmatic patients: linking T cell driven inflammation and granulocytic influx? *Respir Res* 7: 135.

76. Deenick, E. K., and S. G. Tangye. 2007. Autoimmunity: IL-21: a new player in Th17-cell differentiation. *Immunol. Cell Biol.* 85: 503–505.

77. Laan, M., Z. H. Cui, H. Hoshino, J. Lötvall, M. Sjöstrand, D. C. Gruenert, B. E. Skoogh, and A. Lindén. 1999. Neutrophil recruitment by human IL-17 via C-X-C chemokine release in the airways. *J. Immunol.* 162: 2347–2352.

78. Aujla, S. J., and J. F. Alcorn. 2011. T(H)17 cells in asthma and inflammation. *Biochim. Biophys. Acta* 1810: 1066–1079.

79. Chen, Y., P. Thai, Y.-H. Zhao, Y.-S. Ho, M. M. DeSouza, and R. Wu. 2003. Stimulation of airway mucin gene expression by interleukin (IL)-17 through IL-6 paracrine/autocrine loop. *J. Biol. Chem.* 278: 17036–17043.

80. Fujisawa, T., S. Velichko, P. Thai, L.-Y. Hung, F. Huang, and R. Wu. 2009. Regulation of airway MUC5AC expression by IL-1beta and IL-17A; the NF-kappaB paradigm. *The Journal of Immunology* 183: 6236–6243.

81. Meiler, F., M. Zimmermann, K. Blaser, C. A. Akdis, and M. Akdis. 2006. T-cell subsets in the pathogenesis of human asthma. *Curr Allergy Asthma Rep* 6: 91–96.

82. Broide, D. H. 2008. Immunologic and inflammatory mechanisms that drive asthma progression to remodeling. *J. Allergy Clin. Immunol.* 121: 560–70; quiz 571–2.

83. Lloyd, C. M., and E. M. Hessel. 2010. Functions of T cells in asthma: more than just T(H)2 cells. *Nat Rev Immunol* 10: 838–848.

84. Nials, A. T., and S. Uddin. 2008. Mouse models of allergic asthma: acute and chronic allergen challenge. *Disease Models and Mechanisms* 1: 213–220.

85. Bates, J. H. T., M. Rincon, and C. G. Irvin. 2009. Animal models of asthma. *AJP: Lung Cellular and Molecular Physiology* 297: L401–10.

86. Herrick, C. A., L. Xu, A. V. Wisnewski, J. Das, C. A. Redlich, and K. Bottomly. 2002. A novel mouse model of diisocyanate-induced asthma showing allergic-type inflammation in the lung after inhaled antigen challenge. *J. Allergy Clin. Immunol.* 109: 873–878.

87. Mukherjee, A. B., and Z. Zhang. 2011. Allergic asthma: influence of genetic and environmental factors. *Journal of Biological Chemistry* 286: 32883–32889.

88. Szabo, S. J., B. M. Sullivan, C. Stemmann, A. R. Satoskar, B. P. Sleckman, and L. H. Glimcher. 2002. Distinct effects of T-bet in TH1 lineage commitment and IFN-gamma production in CD4 and CD8 T cells. *Science* 295: 338–342.

89. Finotto, S., M. F. Neurath, J. N. Glickman, S. Qin, H. A. Lehr, F. H. Y. Green, K. Ackerman, K. Haley, P. R. Galle, S. J. Szabo, J. M. Drazen, G. T. De Sanctis, and L. H. Glimcher. 2002. Development of spontaneous airway changes consistent with human asthma in mice lacking T-bet. *Science* 295: 336–338.

90. Szabo, S. J., S. T. Kim, G. L. Costa, X. Zhang, C. G. Fathman, and L. H. Glimcher. 2000. A novel transcription factor, T-bet, directs Th1 lineage commitment. *Cell* 100: 655–669.

91. Liu, N., N. Ohnishi, L. Ni, S. Akira, and K. B. Bacon. 2003. CpG directly induces T-bet expression and inhibits IgG1 and IgE switching in B cells. *Nat. Immunol.* 4: 687–693.

92. Garrett, W. S., G. M. Lord, S. Punit, G. Lugo-Villarino, S. K. Mazmanian, S. Ito, J. N. Glickman, and L. H. Glimcher. 2007. Communicable ulcerative colitis induced by T-bet deficiency in the innate immune system. *Cell* 131: 33–45.

93. Koch, M. A., G. Tucker-Heard, N. R. Perdue, J. R. Killebrew, K. B. Urdahl, and D. J. Campbell. 2009. The transcription factor T-bet controls regulatory T cell homeostasis and function during type 1 inflammation. *Nature Publishing Group* 10: 595–602.

94. Lu, Y., S. Bocca, S. Anderson, H. Wang, C. Manhua, H. Beydoun, and S. Oehninger.

2013. Modulation of the Expression of the Transcription Factors T-Bet and GATA-3 in Immortalized Human Endometrial Stromal Cells (HESCs) by Sex Steroid Hormones and cAMP. *Reprod Sci* 20: 699–709.

95. Afkarian, M., J. R. Sedy, J. Yang, N. G. Jacobson, N. Cereb, S. Y. Yang, T. L. Murphy, and K. M. Murphy. 2002. T-bet is a STAT1-induced regulator of IL-12R expression in naïve CD4+ T cells. *Nat. Immunol.* 3: 549–557.

96. Mullen, A. C., F. A. High, A. S. Hutchins, H. W. Lee, A. V. Villarino, D. M. Livingston, A. L. Kung, N. Cereb, T. P. Yao, S. Y. Yang, and S. L. Reiner. 2001. Role of T-bet in commitment of TH1 cells before IL-12-dependent selection. *Science* 292: 1907–1910.

97. Peng, X. H. 2006. Cross-talk between Epidermal Growth Factor Receptor and Hypoxia-inducible Factor-1 Signal Pathways Increases Resistance to Apoptosis by Up-regulating Survivin Gene Expression. *Journal of Biological Chemistry* 281: 25903–25914.

98. Oestreich, K. J., and A. S. Weinmann. 2012. T-bet employs diverse regulatory mechanisms to repress transcription. *Trends in Immunology* 33: 78–83.

99. Hwang, E.-S., S. J. Szabo, P. L. Schwartzberg, and L. H. Glimcher. 2005. T helper cell fate specified by kinase-mediated interaction of T-bet with GATA-3. *Science* 307: 430–433.

100. Lazarevic, V., X. Chen, J.-H. Shim, E.-S. Hwang, E. Jang, A. N. Bolm, M. Oukka, V. K. Kuchroo, and L. H. Glimcher. 2010. T-bet represses TH17 differentiation by preventing Runx1-mediated activation of the gene encoding ROR [gamma] t. *Nat. Immunol.* 12: 96–104.

101. Finotto, S., M. Hausding, A. Doganci, J. H. Maxeiner, H. A. Lehr, C. Luft, P. R. Galle, and L. H. Glimcher. 2005. Asthmatic changes in mice lacking T-bet are mediated by IL-13. *Int. Immunol.* 17: 993–1007.

102. Durrant, D. M., S. L. Gaffen, E. P. Riesenfeld, C. G. Irvin, and D. W. Metzger. 2009. Development of Allergen-Induced Airway Inflammation in the Absence of T-bet Regulation Is Dependent on IL-17. *The Journal of Immunology* 183: 5293–5300.

103. Fujiwara, M., K. Hirose, S.-I. Kagami, H. Takatori, H. Wakashin, T. Tamachi, N. Watanabe, Y. Saito, I. Iwamoto, and H. Nakajima. 2007. T-bet inhibits both TH2 cell-mediated eosinophil recruitment and TH17 cell-mediated neutrophil recruitment into the airways. *J. Allergy Clin. Immunol.* 119: 662–670.

104. Sullivan, B. M., O. Jobe, V. Lazarevic, K. Vasquez, R. Bronson, L. H. Glimcher, and I. Kramnik. 2005. Increased susceptibility of mice lacking T-bet to infection with Mycobacterium tuberculosis correlates with increased IL-10 and decreased IFN-gamma production. *J. Immunol.* 175: 4593–4602.

105. Bakshi, C. S., M. Malik, P. M. Carrico, and T. J. Sellati. 2006. T-bet deficiency facilitates airway colonization by Mycoplasma pulmonis in a murine model of asthma. *J. Immunol.* 177: 1786–1795.

106. Park, J. W., H. J. Min, J. H. Sohn, J. Y. Kim, J. H. Hong, K. S. Sigrist, L. H. Glimcher, and E.-S. Hwang. 2009. Restoration of T-box–containing protein expressed in T cells protects against allergen-induced asthma. *J. Allergy Clin. Immunol.* 123: 479–485.e6.

107. Raby, B. A., E.-S. Hwang, K. Van Steen, K. Tantisira, S. Peng, A. Litonjua, R. Lazarus, C. Giallourakis, J. D. Rioux, D. Sparrow, E. K. Silverman, L. H. Glimcher, and S. T. Weiss. 2006. T-bet polymorphisms are associated with asthma and airway hyperresponsiveness. *Am. J. Respir. Crit. Care Med.* 173: 64–70.

108. Tantisira, K. G., E.-S. Hwang, B. A. Raby, E. S. Silverman, S. L. Lake, B. G. Richter, S. L. Peng, J. M. Drazen, L. H. Glimcher, and S. T. Weiss. 2004. TBX21: a functional variant predicts improvement in asthma with the use of inhaled corticosteroids. *Proc. Natl. Acad. Sci. U.S.A.* 101: 18099–18104.

109. Kiwamoto, T., Y. Ishii, Y. Morishima, K. Yoh, A. Maeda, K. Ishizaki, T. Iizuka, A. E. Hegab, Y. Matsuno, S. Homma, A. Nomura, T. Sakamoto, S. Takahashi, and K. Sekizawa. 2006. Transcription factors T-bet and GATA-3 regulate development of airway remodeling. *Am. J. Respir. Crit. Care Med.* 174: 142–151.

110. Wang, S. Y., M. Yang, X. P. Xu, G. F. Qiu, J. Ma, S. J. Wang, X. X. Huang, and H. X. Xu. 2008. Intranasal delivery of T-bet modulates the profile of helper T cell immune responses in experimental asthma. *J Investig Allergol Clin Immunol* 18: 357–365.

111. Wang, N.-S. 1998. ANATOMY OF THE PLEURA. *Clinics in Chest Medicine* 19: 229–240.

112. Antony, V. B. 2003. Immunological mechanisms in pleural disease. *Eur. Respir. J.* 21: 539–544.

113. Mutsaers, S. E. 2002. Mesothelial cells: their structure, function and role in serosal repair. *Respirology* 7: 171–191.

114. Mutsaers, S. E., C. M. Prele, A. R. Brody, and S. Idell. 2004. Pathogenesis of pleural fibrosis. *Respirology* 9: 428–440.

115. Medford, A. R., A. Medford, and N. Maskell. 2005. Pleural effusion. *Postgrad Med J* 81: 702–710.

116. Manning, C. B., V. Vallyathan, and B. T. Mossman. 2002. Diseases caused by asbestos:

mechanisms of injury and disease development. *International Immunopharmacology* 2: 191–200.

117. Hillerdal, G. 1994. Pleural plaques and risk for bronchial carcinoma and mesothelioma. A prospective study. *Chest* 105: 144–150.

118. Huggins, J. T., and S. A. Sahn. 2004. Causes and management of pleural fibrosis. *Respirology* 9: 441–447.

119. Antony, V. B., J. W. Hott, S. L. Kunkel, S. W. Godbey, M. D. Burdick, and R. M. Strieter. 1995. Pleural mesothelial cell expression of C-C (monocyte chemotactic peptide) and C-X-C (interleukin 8) chemokines.

120. Li, F. K., A. Davenport, R. L. Robson, P. Loetscher, R. Rothlein, J. D. Williams, and N. Topley. 1998. Leukocyte migration across human peritoneal mesothelial cells is dependent on directed chemokine secretion and ICAM-1 expression. *Kidney Int.* 54: 2170–2183.

121. Idell, S. 2003. Coagulation, fibrinolysis, and fibrin deposition in acute lung injury. *Crit. Care Med.* 31: S213–20.

122. Leask, A., and D. J. Abraham. 2004. TGF-beta signaling and the fibrotic response. *The FASEB Journal* 18: 816–827.

123. Ingram, J. L., and J. C. Bonner. 2006. EGF and PDGF receptor tyrosine kinases as therapeutic targets for chronic lung diseases. *Curr. Mol. Med.* 6: 409–421.

124. Mutsaers, S. E., R. J. McAnulty, G. J. Laurent, M. A. Versnel, D. Whitaker, and J. M. Papadimitriou. 1997. Cytokine regulation of mesothelial cell proliferation in vitro and in vivo. *Eur. J. Cell Biol.* 72: 24–29.

125. Seppä, H., G. Grotendorst, S. Seppä, E. Schiffmann, and G. R. Martin. 1982. Platelet-derived growth factor in chemotactic for fibroblasts. *J. Cell Biol.* 92: 584–588.

126. Li, W., J. Fan, M. Chen, S. Guan, D. Sawcer, G. M. Bokoch, and D. T. Woodley. 2004. Mechanism of human dermal fibroblast migration driven by type I collagen and platelet-derived growth factor-BB. *Mol. Biol. Cell* 15: 294–309.

127. Bonner, J. C. 2004. Regulation of PDGF and its receptors in fibrotic diseases. *Cytokine & Growth Factor Reviews* 15: 255–273.

128. Versnel, M. A., A. Hagemeijer, M. J. Bouts, T. H. van der Kwast, and H. C. Hoogsteden. 1988. Expression of c-sis (PDGF B-chain) and PDGF A-chain genes in ten human malignant mesothelioma cell lines derived from primary and metastatic tumors.

Oncogene 2: 601–605.

129. Martinet, Y., P. B. Bitterman, J. F. Mornex, G. R. Grotendorst, G. R. Martin, and R. G. Crystal. 1986. Activated human monocytes express the c-sis proto-oncogene and release a mediator showing PDGF-like activity. *Nature* 319: 158–160.

130. Nagaoka, I., B. C. Trapnell, and R. G. Crystal. 1990. Upregulation of platelet-derived growth factor-A and -B gene expression in alveolar macrophages of individuals with idiopathic pulmonary fibrosis. *J. Clin. Invest.* 85: 2023–2027.

131. Rose, C. E., S.-S. J. Sung, and S. M. Fu. 2003. Significant involvement of CCL2 (MCP-1) in inflammatory disorders of the lung. *Microcirculation* 10: 273–288.

132. Yadav, A., V. Saini, and S. Arora. 2010. MCP-1: chemoattractant with a role beyond immunity: a review. *Clin. Chim. Acta* 411: 1570–1579.

133. Charo, I. F., S. J. Myers, A. Herman, C. Franci, A. J. Connolly, and S. R. Coughlin. 1994. Molecular cloning and functional expression of two monocyte chemoattractant protein 1 receptors reveals alternative splicing of the carboxyl-terminal tails. *Proc. Natl. Acad. Sci. U.S.A.* 91: 2752–2756.

134. Deshmane, S. L., S. Kremlev, S. Amini, and B. E. Sawaya. 2009. Monocyte chemoattractant protein-1 (MCP-1): an overview. *J. Interferon Cytokine Res.* 29: 313–326.

135. Sousa, A. R., S. J. Lane, J. A. Nakhosteen, T. Yoshimura, T. H. Lee, and R. N. Poston. 1994. Increased expression of the monocyte chemoattractant protein-1 in bronchial tissue from asthmatic subjects. *American Journal of Respiratory Cell and Molecular Biology* 10: 142–147.

136. Holgate, S. T., K. S. Bodey, A. Janezic, A. J. Frew, A. P. Kaplan, and L. M. Teran. 1997. Release of RANTES, MIP-1 alpha, and MCP-1 into asthmatic airways following endobronchial allergen challenge. *Am. J. Respir. Crit. Care Med.* 156: 1377–1383.

137. Alam, R., J. York, M. Boyars, S. Stafford, J. A. Grant, J. Lee, P. Forsythe, T. Sim, and N. Ida. 1996. Increased MCP-1, RANTES, and MIP-1alpha in bronchoalveolar lavage fluid of allergic asthmatic patients. *Am. J. Respir. Crit. Care Med.* 153: 1398–1404.

138. Baay-Guzman, G. J., I. G. Bebenek, M. Zeidler, R. Hernandez-Pando, M. I. Vega, E. A. Garcia-Zepeda, G. Antonio-Andres, B. Bonavida, M. Riedl, E. Kleerup, D. P. Tashkin, O. Hankinson, and S. Huerta-Yepez. 2012. HIF-1 expression is associated with CCL2 chemokine expression in airway inflammatory cells: implications in allergic airway inflammation. *Respir Res* 13: 60.

139. Monzon, M. E., R. M. Forteza, and S. M. Casalino-Matsuda. 2011. MCP-1/CCR2B-dependent loop upregulates MUC5AC and MUC5B in human airway epithelium. *AJP: Lung Cellular and Molecular Physiology* 300: L204–15.

140. Karpus, W. J., N. W. Lukacs, K. J. Kennedy, W. S. Smith, S. D. Hurst, and T. A. Barrett. 1997. Differential CC chemokine-induced enhancement of T helper cell cytokine production. *J. Immunol.* 158: 4129–4136.

141. Zhu, Z., B. Ma, T. Zheng, R. J. Homer, C. G. Lee, I. F. Charo, P. Noble, and J. A. Elias. 2002. IL-13-induced chemokine responses in the lung: role of CCR2 in the pathogenesis of IL-13-induced inflammation and remodeling. *J. Immunol.* 168: 2953–2962.

142. Campbell, E. M., I. F. Charo, S. L. Kunkel, R. M. Strieter, L. Boring, J. Gosling, and N. W. Lukacs. 1999. Monocyte chemoattractant protein-1 mediates cockroach allergen-induced bronchial hyperreactivity in normal but not CCR2-/- mice: the role of mast cells. *J. Immunol.* 163: 2160–2167.

143. Blease, K., B. Mehrad, T. J. Standiford, N. W. Lukacs, J. Gosling, L. Boring, I. F. Charo, S. L. Kunkel, and C. M. Hogaboam. 2000. Enhanced pulmonary allergic responses to Aspergillus in CCR2−/− mice. *J. Immunol.* 165: 2603–2611.

144. Kim, Y., Sung Ss, W. A. Kuziel, S. Feldman, S. M. Fu, and C. E. Rose. 2001. Enhanced airway Th2 response after allergen challenge in mice deficient in CC chemokine receptor-2 (CCR2). *J. Immunol.* 166: 5183–5192.

145. Car, B. D., F. Meloni, M. Luisetti, G. Semenzato, G. Gialdroni-Grassi, and A. Walz. 1994. Elevated IL-8 and MCP-1 in the bronchoalveolar lavage fluid of patients with idiopathic pulmonary fibrosis and pulmonary sarcoidosis. *Am. J. Respir. Crit. Care Med.* 149: 655–659.

146. Gharaee-Kermani, M., E. M. Denholm, and S. H. Phan. 1996. Costimulation of fibroblast collagen and transforming growth factor beta1 gene expression by monocyte chemoattractant protein-1 via specific receptors. *J. Biol. Chem.* 271: 17779–17784.

147. Moore, B. B., R. Paine, P. J. Christensen, T. A. Moore, S. Sitterding, R. Ngan, C. A. Wilke, W. A. Kuziel, and G. B. Toews. 2001. Protection from pulmonary fibrosis in the absence of CCR2 signaling. *J. Immunol.* 167: 4368–4377.

148. Gharaee-Kermani, M. 2003. CC-chemokine receptor 2 required for bleomycin-induced pulmonary fibrosis. *Cytokine* 24: 266–276.

149. Inoshima, I., K. Kuwano, N. Hamada, N. Hagimoto, M. Yoshimi, T. Maeyama, A. Takeshita, S. Kitamoto, K. Egashira, and N. Hara. 2004. Anti-monocyte chemoattractant

protein-1 gene therapy attenuates pulmonary fibrosis in mice. *Am. J. Physiol. Lung Cell Mol. Physiol.* 286: L1038–44.

150. Hill, G. D., J. B. Mangum, O. R. Moss, and J. I. Everitt. 2003. Soluble ICAM-1, MCP-1, and MIP-2 protein secretion by rat pleural mesothelial cells following exposure to amosite asbestos. *Exp. Lung Res.* 29: 277–290.

151. Tanaka, S., N. Choe, A. Iwagaki, D. R. Hemenway, and E. Kagan. 2000. Asbestos exposure induces MCP-1 secretion by pleural mesothelial cells. *Exp. Lung Res.* 26: 241–255.

152. Arrandale, V. H., G. M. Liss, S. M. Tarlo, M. D. Pratt, D. Sasseville, I. Kudla, and D. L. Holness. 2012. Occupational contact allergens: are they also associated with occupational asthma? *Am. J. Ind. Med.* 55: 353–360.

153. Kane, A. B. 2006. Animal models of malignant mesothelioma. *Inhalation Toxicology* 18: 1001–1004.

154. Zhang, Q., Y. Kusaka, K. Sato, K. Nakakuki, N. Kohyama, and K. Donaldson. 1998. Differences in the extent of inflammation caused by intratracheal exposure to three ultrafine metals: role of free radicals. *J. Toxicol. Environ. Health Part A* 53: 423–438.

155. Zheng, W., and R. A. Flavell. 1997. The transcription factor GATA-3 is necessary and sufficient for Th2 cytokine gene expression in CD4 T cells. *Cell* 89: 587–596.

156. Gillespie, P. A., G. S. Kang, A. Elder, R. Gelein, L. Chen, A. L. Moreira, J. Koberstein, K.-M. Tchou-Wong, T. Gordon, and L. C. Chen. 2010. Pulmonary response after exposure to inhaled nickel hydroxide nanoparticles: short and long-term studies in mice. *Nanotoxicology* 4: 106–119.

157. Fossiez, F., O. Djossou, P. Chomarat, L. Flores-Romo, S. Ait-Yahia, C. Maat, J. J. Pin, P. Garrone, E. Garcia, S. Saeland, D. Blanchard, C. Gaillard, B. Das Mahapatra, E. Rouvier, P. Golstein, J. Banchereau, and S. Lebecque. 1996. T cell interleukin-17 induces stromal cells to produce proinflammatory and hematopoietic cytokines. *J. Exp. Med.* 183: 2593–2603.

158. Shifren, A., C. Witt, C. Christie, and M. Castro. 2012. Mechanisms of remodeling in asthmatic airways. *J Allergy (Cairo)* 2012: 316049.

159. Xu, J., A. L. Mora, J. LaVoy, K. L. Brigham, and M. Rojas. 2006. Increased bleomycin-induced lung injury in mice deficient in the transcription factor T-bet. *Am. J. Physiol. Lung Cell Mol. Physiol.* 291: L658–67.

160. Lee, C. G., R. J. Homer, Z. Zhu, S. Lanone, X. Wang, V. Koteliansky, J. M. Shipley, P.

Gotwals, P. Noble, Q. Chen, R. M. Senior, and J. A. Elias. 2001. Interleukin-13 induces tissue fibrosis by selectively stimulating and activating transforming growth factor beta(1). *J. Exp. Med.* 194: 809–821.

161. Romagnani, S. 2002. Cytokines and chemoattractants in allergic inflammation. *Mol. Immunol.* 38: 881–885.

162. Cho, W.-S., R. Duffin, M. Bradley, I. L. Megson, W. Macnee, S. E. M. Howie, and K. Donaldson. 2012. NiO and Co3O4 nanoparticles induce lung DTH-like responses and alveolar lipoproteinosis. *European Respiratory Journal* 39: 546–557.

163. Chensue, S. W., K. S. Warmington, J. H. Ruth, P. S. Sanghi, P. Lincoln, and S. L. Kunkel. 1996. Role of monocyte chemoattractant protein-1 (MCP-1) in Th1 (mycobacterial) and Th2 (schistosomal) antigen-induced granuloma formation: relationship to local inflammation, Th cell expression, and IL-12 production. *J. Immunol.* 157: 4602–4608.

164. Gonzalo, J.-A., C. M. Lloyd, D. Wen, J. P. Albar, T. N. C. Wells, A. Proudfoot, C. Martinez-A, M. Dorf, T. Bjerke, A. J. Coyle, and J.-C. Gutierrez-Ramos. 1998. The coordinated action of CC chemokines in the lung orchestrates allergic inflammation and airway hyperresponsiveness. *J. Exp. Med.* 188: 157–167.

165. Bermudez, E., B. Libbus, and J. B. Mangum. 1998. Rat pleural mesothelial cells adapted to serum-free medium as a model for the study of growth factor effects. *Cell Biol. Toxicol.* 14: 243–251.

166. Choquette, K. A., D. V. Sadasivam, and R. A. Flowers II. 2011. Catalytic Ni(II) in Reactions of SmI 2: Sm(II)- or Ni(0)-Based Chemistry? *J. Am. Chem. Soc.* 133: 10655–10661.

167. Fine, A., and R. H. Goldstein. 1987. The effect of transforming growth factor-beta on cell proliferation and collagen formation by lung fibroblasts. *J. Biol. Chem.* 262: 3897–3902.

168. Keane, M. P., J. A. Belperio, D. A. Arenberg, M. D. Burdick, Z. J. Xu, Y. Y. Xue, and R. M. Strieter. 1999. IFN-gamma-inducible protein-10 attenuates bleomycin-induced pulmonary fibrosis via inhibition of angiogenesis. *J. Immunol.* 163: 5686–5692.

169. Jiang, D., and P. Noble. 2004. Regulation of pulmonary fibrosis by chemokine receptor CXCR3. *J. Clin. Invest.* 114: 291–299.

170. Visser, C. E., J. Tekstra, J. J. Brouwer-Steenbergen, C. W. Tuk, D. M. Boorsma, S. C. Sampat-Sardjoepersad, S. Meijer, R. T. Krediet, and R. H. Beelen. 1998. Chemokines produced by mesothelial cells: huGRO-alpha, IP-10, MCP-1 and RANTES. *Clinical & Experimental Immunology* 112: 270–275.

171. Tager, A., A. Luster, and R. Kradin. 1999. T-cell chemokines interferon-inducible protein-10 and monokine induced by interferon-gamma are upregulated in bleomycin-induced lung injury. *Chest* 116: 90S.

172. Jurek, A., K. Amagasaki, A. Gembarska, C.-H. Heldin, and J. Lennartsson. 2009. Negative and positive regulation of MAPK phosphatase 3 controls platelet-derived growth factor-induced Erk activation. *J. Biol. Chem.* 284: 4626–4634.

173. MURPHY, L., and J. BLENIS. 2006. MAPK signal specificity: the right place at the right time. *Trends in Biochemical Sciences* 31: 268–275.

174. Crews, C. M., A. Alessandrini, and R. L. Erikson. 1992. The primary structure of MEK, a protein kinase that phosphorylates the ERK gene product. *Science* 258: 478–480.

175. Huang, X., K. Frenkel, C. B. Klein, and M. Costa. 1993. Nickel induces increased oxidants in intact cultured mammalian cells as detected by dichlorofluorescein fluorescence. *Toxicology and Applied Pharmacology* 120: 29–36.

176. Pietruska, J. R., X. Liu, A. Smith, K. McNeil, P. Weston, A. Zhitkovich, R. Hurt, and A. B. Kane. 2011. Bioavailability, intracellular mobilization of nickel, and HIF-1α activation in human lung epithelial cells exposed to metallic nickel and nickel oxide nanoparticles. *Toxicological Sciences* 124: 138–148.

177. Andrew, A. S., L. R. Klei, and A. Barchowsky. 2001. Nickel requires hypoxia-inducible factor-1 alpha, not redox signaling, to induce plasminogen activator inhibitor-1. *Am. J. Physiol. Lung Cell Mol. Physiol.* 281: L607–15.

178. Jimenez, L. A., C. Zanella, H. Fung, Y. M. Janssen, P. Vacek, C. Charland, J. Goldberg, and B. T. Mossman. 1997. Role of extracellular signal-regulated protein kinases in apoptosis by asbestos and H2O2. *Am. J. Physiol.* 273: L1029–35.